Aus der Klinik für Neurochirurgie
der Medizinischen Fakultät Charité – Universitätsmedizin Berlin

DISSERTATION

Characterization of cancer treatment-related neurotoxicity in patients with malignant glioma

-

Charakterisierung behandlungsbedingter Neurotoxizität bei Patienten mit malignen Gliomen

zur Erlangung des akademischen Grades
Medical Doctor - Doctor of Philosophy (MD/PhD)

vorgelegt der Medizinischen Fakultät
Charité – Universitätsmedizin Berlin

von

Sebastian Friedrich Winter
aus Dallas, Texas, USA

Datum der Promotion: 26.06.2022

In loving memory of my father,
Stefan F. Winter, M.D. Ph.D.

Table of Contents

List of Figures and Tables

List of Figures

List of Tables

List of Abbreviations

Abbreviation	Explanation
AA	Anaplastic astrocytoma
AED	Antiepileptic drugs
AOD	Anaplastic oligodendroglioma
AMS	Altered mental status
ASA	Acetylsalicylic acid
CBF	Cerebral blood flow
CBV	Cerebral blood volume
CNS	Central nervous system
CTP	Computed tomography perfusion
DWI	Diffusion-weighted imaging
Dx	Diagnosis
EBRT	External beam radiation therapy
EEG	Electroencephalography
F	Female
FBG	Foreign body granuloma
FLAIR	Fluid-attenuated inversion recovery
GBM	Glioblastoma multiforme
Gy	Gray
HGG	High grade glioma
IDH1	Isocitrate dehydrogenase 1
KPS	Karnofsky performance status
LITT	Laser interstitial thermal therapy
M	Male
MGMT	O^6-methylguanine DNA methyltransferase
mo	months
MRI	Magnetic resonance imaging
MRP	Magnetic resonance perfusion-weighted imaging
MRS	Magnetic resonance spectroscopy
Mx	Management
PD	Progressive disease

PET	Positron emission tomography
PP	Pseudoprogression
QoL	Quality of life
RANO	Response Assessment in Neuro-Oncology
RBE	Relative biological effectiveness
RCT	Randomized controlled trial
ROI	Region of interest
RT	Radiation therapy
Rx	Radiation
SCLC	Small cell lung cancer
SMART	Stroke-like migraine attacks after radiation therapy
SOC	Standard of care
s/p	Status post
Sx	Symptoms
T1+C	T1-weighted contrast-enhanced sequence
TMZ	Temozolomide
TN	Treatment-induced necrosis
WBRT	Whole brain radiation therapy
WHO	World Health Organization
y	years

Abstract

Objective

To improve the understanding, diagnosis, and management of treatment-related adverse effects that mimic progressive disease (PD) in patients with malignant glioma, including pseudoprogression (PP), treatment-induced necrosis (TN), and stroke-like migraine attacks after radiation therapy (SMART) syndrome.

Background

Treatment-related neurotoxicity is a major challenge in neuro-oncology. Central neurologic sequelae from cranial radiation therapy (RT), chemotherapy, and/or novel antineoplastic agents can be therapy-limiting, severely disabling, and difficult to diagnose and manage. Conditions such as TN, PP, and SMART are typically indistinguishable from PD and remain insufficiently characterized and defined. Invasive tissue biopsy is frequently necessary to guide management. Misdiagnosis can have deleterious consequences and compromise response assessment in neuro-oncology.

Patients and Methods

A comprehensive analysis of relevant clinical literature (n=101 studies) was performed to delineate the diagnostic and therapeutic status quo in the management of TN and develop actionable strategies directed at clinical gaps and research barriers in the field (*Publication 1*). Using an institutional database, patients with glioma and confirmed PP or TN were retrospectively identified and characterized based on analysis of clinical, radiographic, and histopathological data (*Publication 2*). Individual PP/TN lesions (regions of interest [ROIs]) were longitudinally evaluated by serial imaging. Analogously, patients diagnosed with SMART were retrospectively identified and characterized by analysis of clinical and radiographic data (*Publication 3*).

Results

Although multiple diagnostic and therapeutic strategies for TN have been proposed, no standard of care presently exists. Identifiable clinical and systemic factors (n=12) have challenged progress in the field but appear addressable by six proposed research pillars

(*Publication 1*). Informed by this research framework, characteristics of 60 glioma patients with PP (n=27) and/or TN (n=37), comprising 137 ROIs in total, were analyzed and compared (*Publication 2*). PP and TN differ uniquely in clinical course, spatiotemporal radiographic lesion pattern, and histopathological features, and likely represent distinct conditions encountered in specific patient populations. Identified PP/TN ROIs universally developed in the main prior radiation field. Both conditions may be associated with above-average survival. Finally, analysis of patients with SMART (n=7) identified typical clinical features, pathognomonic MR imaging abnormalities, and impaired cerebral autoregulation as an implicated pathomechanism (*Publication 3*).

Discussion

Taken together, the presented thesis offers new insights into the growing spectrum of disease-mimicking treatment-related effects in neuro-oncology and demonstrates that rigorous characterization of these conditions is feasible and paramount to improve the management of patients with brain cancer.

Abstract (German)

Zielsetzung

Verbesserung des Verständnisses, der Diagnose und Therapie tumorimitierender Behandlungseffekte bei Patienten mit malignen Gliomen, einschließlich Pseudoprogression (PP), Strahlennekrose (TN) und Stroke-like migraine attacks after radiation therapy (SMART)-Syndrom.

Hintergrund

Behandlungsbedingte Neurotoxizität bleibt eine Herausforderung der Neuroonkologie. Zentrale neurologische Folgeerscheinungen nach kranialer Strahlentherapie (RT), Chemotherapie und/oder neuen antineoplastischen Wirkstoffen sind oftmals therapiebegrenzend, klinisch einschränkend und schwer diagnostizier- und behandelbar. Zustände wie TN, PP und SMART sind nicht eindeutig von Tumorprogress differenzierbar und bleiben unzureichend charakterisiert. Diagnosestellung und Beurteilung des Therapieansprechens erfordern daher häufig eine invasive Gewebebiopsie.

Patienten und Methodik

Anhand umfassender Analyse relevanter klinischer Literatur (n=101 Studien) wurde der diagnostische sowie therapeutische Status quo in der Behandlung von TN ermittelt und Strategien zur Überwindung klinischer Lücken und Forschungsbarrieren entwickelt (*Publikation 1*). Mithilfe einer institutionellen Datenbank wurden Gliompatienten mit bestätigter PP oder TN retrospektiv identifiziert und anhand Analyse klinischer, radiologischer und histopathologischer Daten charakterisiert (*Publikation 2*). Einzelne PP/TN-Läsionen (regions of interest [ROIs]) wurden durch serielle Bildgebung longitudinal ausgewertet. Analog dazu erfolgte die Charakterisierung von Patienten mit SMART mittels retrospektiver Analyse klinischer und radiologischer Daten (*Publikation 3*).

Ergebnisse

Trotz diagnostischer und therapeutischer Ansätze existiert bisher kein optimaler Behandlungsstandard für TN. Vorhandene klinische und systemische Barrieren (n=12) sind durch Anwendung von sechs Forschungssäulen potenziell überwindbar (*Publikation 1*). Basierend auf diesem Forschungskonzept wurden die Charakteristika von 60 Gliompatienten

mit PP (n=27) und/oder TN (n=37), und insgesamt 137 ROIs, analysiert und verglichen (*Publikation 2*). PP und TN weisen im klinischen Verlauf, im räumlich-zeitlichen radiologischen Läsionsmuster und histopathologisch signifikante Unterschiede auf, und stellen offenbar unterschiedliche Entitäten mit Auftreten in spezifischen Patientenpopulationen dar. Identifizierte PP/TN ROIs entwickelten sich durchgängig im Hauptfeld der vorherigen Bestrahlung. Beide Entitäten korrelieren potenziell mit überdurchschnittlichem Überleben. Die Analyse von Patienten mit SMART (n=7) zeigte typische klinische Merkmale und pathognomonische MR-Bildgebungsanomalien sowie pathophysiologisch eine gestörte zerebrale Autoregulation (*Publikation 3*).

Diskussion

Zusammenfassend ermöglicht die vorliegende Arbeit neue Einblicke in das wachsende Spektrum tumorimitierender Behandlungseffekte in der Neuroonkologie und zeigt auf, dass eine rigorose Charakterisierung dieser Entitäten für die Verbesserung der Versorgung von Hirntumorpatienten wegweisend ist.

I. Synopsis

Preface

The following dissertation constitutes a cumulative synopsis of the research activities conducted as part of the MD/PhD doctoral research track at the Charité - Universitätsmedizin Berlin. As such, the conceptual ideas, research methodology and results presented and discussed in this synopsis are based largely on numerous previously published peer-reviewed articles, the manuscripts of which I have drafted as first author. The respective published research works (*Publications 1 – 3*) have been referenced throughout the text, whenever applicable, and their print versions are appended to this synopsis (see section *III. Selected Publications*).

1. Introduction

1.1 Background

Neurotoxicity from anticancer treatment is a widely recognized issue in clinical oncology (Dietrich, 2020; Santomasso, 2020). In particular, central nervous system (CNS) toxicity can be treatment-limiting, severely disabling, and often results in major diagnostic and therapeutic challenges (Dietrich et al., 2019). Damage to healthy brain parenchyma may occur in the setting of conventional cytotoxic therapies, like systemic chemotherapy (Dietrich, 2010; Huehnchen et al., 2020) and cranial radiation therapy (RT) (Tofilon and Fike, 2000), as well as novel antineoplastic agents including targeted therapies, antiangiogenics, immunotherapies, or combinations thereof (Chukwueke et al., 2020, 2019; Dietrich et al., 2008; Wick et al., 2016; Winter et al., 2021c, 2020a). In addition, neurosurgical brain tumor removal may result in late surgery-related sequelae such as intracranial foreign body granuloma (FBG), a rare but likely underrecognized inflammatory reaction to retained (hemostatic) foreign material resembling tumor progression on imaging (Winter et al., 2021a).

As such, treatment-related CNS toxicity is an especially frequent complication in neuro-oncological patients, who commonly receive several of the aforementioned treatments as part of a multimodal therapeutic regimen (Dietrich et al., 2019; Winter et al., 2019). For instance, the standard of care (SOC) for patients with glioblastoma multiforme (GBM; WHO grade IV) consists of maximal safe surgical resection, followed by RT with temozolomide (TMZ)-based concomitant (chemo-RT) and adjuvant chemotherapy (Stupp et al., 2005). Consequently, a significant number of patients with malignant brain tumors may develop a range of functional and structural treatment-related neurologic sequelae (Dietrich et al., 2019). These include, most commonly, neurocognitive impairment, progressive brain atrophy, leukoencephalopathy, pseudoprogression, and treatment-induced brain tissue necrosis (Dietrich et al., 2019). Moreover, cranial RT is known to increase the risk of cerebrovascular complications, including stroke and intracranial hemorrhage (Campen et al., 2012; Dietrich et al., 2019), and unique forms of RT-related neurovascular toxicity such as cerebral microbleeds (Roongpiboonsopit et al., 2017) and stroke-like migraine attacks after radiation therapy (SMART) syndrome (Black et al., 2006; Winter et al., 2021b) have been documented in (neuro-)oncological patients.

In addition to the unique therapeutic difficulties related to managing affected patients, several of these treatment-related conditions can be indistinguishable from progressive disease (PD)

on conventional imaging (Dietrich et al., 2017). At present, this diagnostic conundrum cannot be reliably resolved by non-invasive neuroimaging modalities and is a frequent limitation to appropriate radiographic response assessment in neuro-oncology (Huang et al., 2015).

Overall, the prevalence of treatment-related CNS toxicity is expected to rise as gradual therapeutic improvements lead to more durable anti-tumor responses that translate to prolonged patient survival (Dietrich, 2020; Dietrich et al., 2019). In addition, widespread clinical adoption of novel antineoplastic agents has resulted in a range of newly emerging adverse events, including hitherto unseen forms of CNS toxicity (Wick et al., 2016). In particular, CNS immunotoxicity from emerging cancer immunotherapies constitutes a rapidly growing field of investigation that is adding further complexity to the current spectrum of treatment-related neurotoxic syndromes (Chukwueke et al., 2020; Winter et al., 2021c, 2020a). These developments have reinforced an existing unmet need to better understand and thoroughly characterize cancer treatment-related effects on the CNS – a prerequisite to foster clinical awareness, improve diagnostic principles and response assessment criteria, and identify best management practices in affected patients.

1.2 Pseudoprogression and treatment-induced necrosis

Pseudoprogression (PP) and treatment-induced brain tissue necrosis (TN; aka "radiation necrosis") represent some of the most frequent yet challenging types of treatment-related effects encountered in patients with malignant glioma (Dietrich et al., 2017). Occurring months to years following (chemo-)RT (**Figure 1**) (Winter et al., 2019), PP and TN are typically indistinguishable from PD on conventional imaging, making them prone to misdiagnosis and inadequate or delayed clinical management (Dietrich et al., 2017). Many patients ultimately require tissue biopsy to establish a definite diagnosis and guide clinical management, resulting in potentially unnecessary surgical procedures in a significant number of patients (Winter et al., 2019). Moreover, diagnostic misclassification of either condition as PD may adversely affect clinical trial enrollment and potentially compromise appropriate evaluation of investigational antineoplastic agents (Winter et al., 2019). This is especially problematic in cases where treatment-related effects manifest beyond the temporal cutoff point stipulated by the Response Assessment in Neuro-Oncology (RANO) criteria, which currently limit clinical

trial enrollment to patients with radiographic evidence of PD in whom contrast enhancing lesions (on T1+C MRI) appear at or beyond 12 weeks post-RT (Winter et al., 2019).

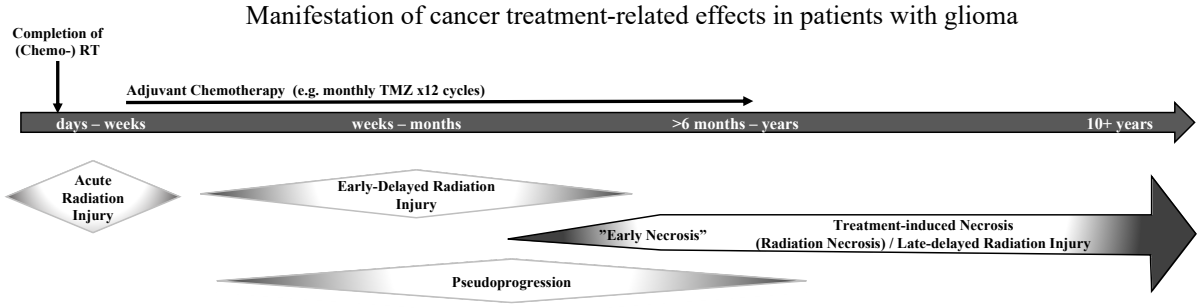

Figure 1. Timeline schematic of treatment-related effects.
Timeline schematic illustrating the temporal manifestation pattern and clinical course of relevant cancer treatment-related effects, including pseudoprogression and treatment-induced necrosis. Adapted from *Publication 1, Figure 3* (Winter et al., 2019). Abbreviations: RT, radiation therapy; TMZ, temozolomide.

The reported incidences for both conditions (9 – 30 % for PP (Thust et al., 2018), 5 – 50% for TN (Rahmathulla et al., 2013)) vary widely, depending on brain tumor type, treatment regimen, data acquisition parameters, and clinical definitions (Winter et al., 2019). Despite their relatively frequent manifestations, PP and TN remain insufficiently characterized and the exact pathomechanisms driving either condition are incompletely understood (Perry and Schmidt, 2006; Rahmathulla et al., 2013). At present, both clinical terms are arbitrarily defined and occasionally used interchangeably in the clinical literature (Kruser et al., 2013). While the distinction between both entities is the subject of an active clinical debate, existing clinical definitions have focused primarily on delineating differences between the temporal manifestation patterns of these entities following anticancer treatment (Winter et al., 2019). As such, TN commonly occurs 6 months to several years following (chemo-)RT (Giglio and Gilbert, 2003; Tofilon and Fike, 2000; Winter et al., 2020b), can take an irreversible and progressive clinical course, and is frequently associated with significant patient morbidity and occasionally even mortality (**Figure 2**) (Winter et al., 2019). By contrast, PP appears to occur within the first few months of temozolomide (TMZ)-based chemo-RT initiation as a transient clinical scenario predominantly observed in patients with high-grade gliomas (HGGs; World Health Organization [WHO] grades III–IV) (Brandsma et al., 2008; Dietrich et al., 2017; Kucharczyk et al., 2017; Taal et al., 2008; Winter et al., 2020b). Importantly, the term "pseudoprogression" has also been used to denote the purely radiological phenomenon of any imaging findings mimicking PD, i.e. irrespective of the underling type of treatment-related condition, which has contributed to existing semantic inconsistencies surrounding the

definition of PP (Winter et al., 2019). Moreover, recent studies have observed that "early brain tissue necrosis" (TN onset <5 months from RT completion) can increasingly occur in patients receiving TMZ-based chemo-RT, suggesting that TMZ may act as a radiosensitizing agent and potentially accelerate the onset of TN (Chamberlain et al., 2007; Winter et al., 2020b, 2019). As such, PP and TN can overlap in clinical practice causing further diagnostic ambiguities (**Figure 1**) (Winter et al., 2019). At the same time, histopathological criteria specific to either condition have not yet been established, such that histopathological findings in biopsied patients are commonly summarized under the generic term "treatment effect" (Winter et al., 2020b, 2019).

While tissue biopsy remains the diagnostic gold standard, recent efforts have investigated the use of advanced functional imaging modalities for improved noninvasive differentiation of both conditions from PD (Jain et al., 2010; Verma et al., 2013; Yang and Aghi, 2009). Positron emission tomography (PET) with novel amino acid tracers (e.g., fluoro-ethyl-tyrosine–PET), computed tomography perfusion (CTP) studies, multivoxel magnetic resonance spectroscopy (MRS), and combined MR-PET are among the more promising imaging-based strategies increasingly employed to augment diagnostic certainty in cases where findings on conventional (MR) imaging appear equivocal (Alexiou et al., 2009; Jain et al., 2010; Langen et al., 2017; Verma et al., 2013; Winter et al., 2020b, 2019; Yang and Aghi, 2009). A comprehensive overview of existing systematic reviews evaluating the diagnostic performance of different advanced imaging modalities in the setting of treatment-related effects is provided in *Publication 1, Table 1, pages 66 - 68*.

The symptoms associated with PP and TN are highly variable but often mimic those of PD. As such, approximately 50% of affected patients may present with signs of raised intracranial pressure, such as headache and nausea/vomiting, as well as progressive cognitive decline, seizures, and diffuse or focal neurological deficits (Chi et al., 2008; Winter et al., 2019). Clinical management includes corticosteroids and/or surgical resection; bevacizumab, anticoagulant drugs, and hyperbaric oxygen therapy are additional therapeutic strategies but remain experimental (Winter et al., 2020b). More recently, laser interstitial thermal therapy (LITT) has been investigated as a suitable minimally invasive alternative for lesions that are surgically inaccessible or located in eloquent brain regions (Ahluwalia et al., 2018; Winter et al., 2019). For a comprehensive overview and critical evaluation of relevant therapeutic strategies see *Publication 1, Supplementary Table 1, pages 72 - 77*.

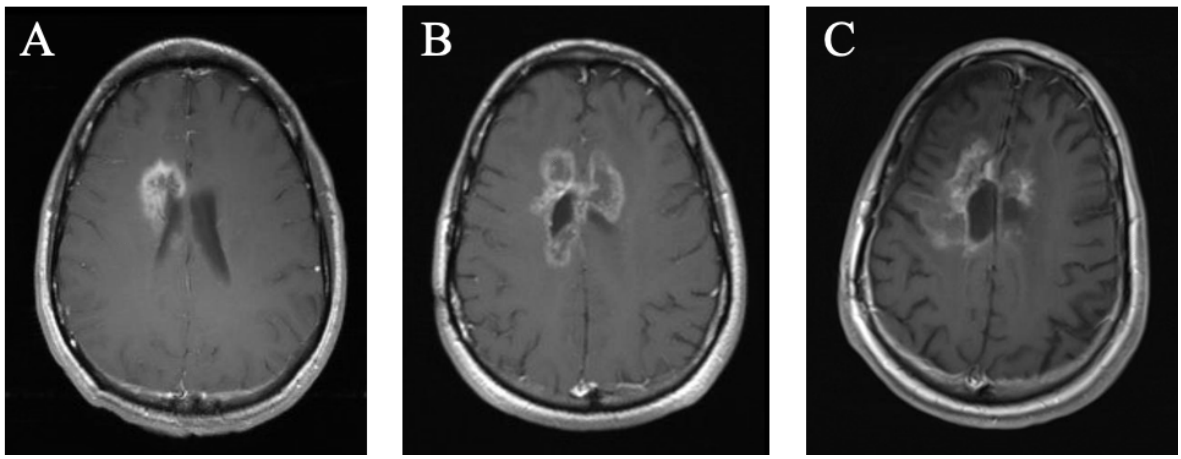

Figure 2. Case example of treatment-induced necrosis.
A case of biopsy-confirmed TN in a 35-year-old patient s/p surgical resection and TMZ-based concurrent/adjuvant chemo-RT for a WHO grade II astrocytoma diagnosis. Briefly, symptomatic TN developed 8 months post-RT and progressed over the course of 2.5 years with gradual neurologic deterioration and ultimately fatal outcome. T1-weighted gadolinium-enhanced axial MRI sequences **(A – C)** demonstrate the lesion at different timepoints. The illustrated case is adapted from and described in more detail in *Publication 1, Figure 2* (Winter et al., 2019). Abbreviations: MRI, magnetic resonance imaging; TMZ, temozolomide; TN, treatment-induced necrosis.

1.3 Stroke-like migraine attacks after radiation therapy syndrome

Stroke-like migraine attacks after radiation therapy (SMART) syndrome constitutes a rare but serious and likely underdiagnosed cancer treatment-related neurologic complication encountered many years to decades following cranial RT (Black et al., 2006; Shuper et al., 1995). Less than 50 cases of SMART have been reported in the literature and the pathomechanisms driving the condition remain largely unknown (Biju et al., 2020). A set of early diagnostic criteria has been proposed, which include a remote history of cranial RT, clinical presentation with migraine-like headaches, stroke-like deficits, and/or seizures, as well as pathognomonic MRI findings in previously irradiated brain regions (Black et al., 2013, 2006; Fan et al., 2018; Kerklaan et al., 2011). While most SMART episodes are transient and manageable with supportive therapy, several cases with persistent clinical and imaging sequelae have been reported (Black et al., 2013; Winter et al., 2021b). A diagnosis of exclusion, SMART can radiographically mimic PD (including local tumor progression or leptomeningeal disease), infection, and ischemic events (Winter et al., 2021b). To avoid misdiagnosis with potentially deleterious consequences, this challenging clinical entity requires careful patient work-up and occasionally tissue-biopsy to guide management (Black et al., 2013). Better characterization of the distinctive clinico-radiographic features and novel insights into putative

pathomechanisms of SMART is warranted to improve the diagnosis and management of this rare but serious treatment-related condition in oncology (Winter et al., 2021b).

2. Aims of the Study

The overall aims of the presented studies (*Publications 1 – 3*) were as follows:

1. To delineate the current diagnostic and therapeutic status quo in the management of treatment-related effects (most notably treatment-induced necrosis; TN) that mimic recurrent disease in patients with malignant glioma, based on identification of the most important existing clinical pitfalls and systemic research barriers. As a second step, to propose a research framework that addresses relevant identified core issues and may serve as a valuable guideline for future clinical investigations in this field.

2. To identify distinctive demographic, clinical, radiographic, and histopathological characteristics of two of the most relevant and diagnostically challenging, yet poorly described treatment-related conditions in neuro-oncology: pseudoprogression (PP) and treatment-induced necrosis (TN).

The generated results shall serve to

(a) increase clinical understanding and familiarity with the distinct clinico-radiographic features of PP and TN and the specific clinical settings in which these conditions are commonly encountered.

(b) facilitate noninvasive diagnosis of PP and TN, including increased utilization of radiotherapy dose distribution curves for the interpretation of diagnostically ambivalent MR imaging findings

(c) help establish consensus definitions for PP and TN and improve response assessment criteria for outcome interpretation in neuro-oncology

3. To holistically characterize SMART syndrome, a rare but serious and underrecognized treatment-related neurologic condition in (neuro-)oncological patients, based on identification of distinctive demographic, clinical, imaging features as well as effective management strategies.

3. Patients and Methods

3.1 Identification of research barriers and opportunities in the field

An extensive search (including index databases PubMed/MEDLINE, EMBASE, Google Scholar, and the clinical trial registries WHO ICTRP and ClinicalTrials.gov) of relevant published clinical literature and clinical trials (n= 101 included studies) was performed to 1) systematically evaluate the current diagnostic and therapeutic status quo, 2) identify, analyze, and contextualize the most important clinical pitfalls and research barriers, and 3) propose a holistic research framework directed at addressing identified challenges to advance the field of treatment-related effects in neuro-oncology, with a focus on TN. The results, including analysis and interpretation of gathered information, are summarized in section *4.1*. and have been published in a comprehensive review article (*Publication 1*; (Winter et al., 2019)). Moreover, parts of the proposed research framework served as a guideline to inform the research concept and design employed in subsequent studies directed at holistic characterization of PP and TN (*Publication 2*; (Winter et al., 2020b)) as well as SMART syndrome (*Publication 3*; (Winter et al., 2021b)) in neuro-oncological patients.

3.2 Characterization of pseudoprogression and treatment-induced necrosis

The following segments constitute a summary of previously published research methodology used to characterize clinico-radiographic features of PP and TN in patients with malignant glioma. For reference and greater detail please see *Publication 2, Materials and Methods, Pages 83 - 85* (Winter et al., 2020b).

3.2.1 Study design and patient eligibility

The characterization of treatment-related effects was based on a retrospective analysis, whereby demographic, clinical, radiographic, and histopathological data were collected from 60 brain tumor patients diagnosed with either PP or TN following glioma therapy at the Massachusetts General Hospital (MGH) between 1997 – 2015 (Winter et al., 2020b). Patient data were obtained from an MGH institutional database and institutional review board approval was granted for all activities (Winter et al., 2020b). Patients were selected based on the following eligibility criteria (Winter et al., 2020b):

(a) tissue-based diagnosis of glioma (WHO grades I–IV)

(b) antineoplastic treatment, i.e., RT with or without chemotherapy

(c) biopsy-proven or clinico-radiographically established diagnosis of treatment-related effects based on serial imaging.

3.2.2 Classification of treatment-related effects

Based on current literature consensus (Dietrich et al., 2017; Giglio and Gilbert, 2003; Tofilon and Fike, 2000), classification of treatment-related effects was primarily based on the time of radiographic appearance of each lesion (=region of interest; ROI) following RT, whereby a temporal cutoff point at 5 months post-RT was used as a proxy to differentiate between PP (ROI appearance <5 months post-RT) and TN (ROI appearance ≥5 months post-RT) (Winter et al., 2020b). Patients were accordingly categorized into either PP or TN groups for further comparison of clinical and imaging characteristics (Winter et al., 2020b). Notably, 4/60 patients were found to have biopsy-proven treatment-related effects both before and after the stipulated cutoff point and were therefore included in both groups, yielding a total of 64 cases of treatment-related effects in this cohort of 60 patients (Winter et al., 2020b). For further details on classification of treatment-related effects see *Publication 2, Materials and Methods, Page 83.*

3.2.3 Variables of interest

A series of variables were collected for each patient, including demographic, clinical, therapeutic, and outcome parameters (Winter et al., 2020b). Briefly, variables specific to the initial manifestation of treatment-related effects (=first ROI) were collected and included, whenever available, characteristics of radiographic onset, presence of new neurologic symptoms, treatments rendered for PP/TN, advanced diagnostic imaging results, histopathological features, and total number of ROIs developed over the course of the condition (Winter et al., 2020b). Whenever available, additional variables of interest were collected for each individual ROI, including longitudinal evaluation of a range of spatiotemporal radiographic patterns, the degree of radiation dose exposure, and histopathological characteristics (Winter et al., 2020b). For further details on collected variables of interest see *Publication 2, Materials and Methods, Pages 83 - 84.*

3.2.4 Radiographic analysis

Briefly, radiographic analysis of individual ROIs in each patient was based on T1-weighted gadolinium enhanced MR imaging (T1+C MRI) sequences from relevant MRI scans using standard clinical imaging software (Winter et al., 2020b). The time of appearance of the first ROI was determined retrospectively and approximated based on the first MRI demonstrating de novo enhancement on T1+C in the ROI's respective anatomical location (Winter et al., 2020b). Longitudinal tracing of each ROI with analysis of spatiotemporal radiographic pattern was carried out based on imaging data from follow-up MRI scans (Winter et al., 2020b). Accordingly, the radiographic duration of each ROI was defined as the time of first appearance on MRI until complete radiographic resolution or last available MRI (Winter et al., 2020b). Further radiographic measurements for each ROI included maximum ROI area (cm^2), the shortest ROI-to-resection cavity margin distance (mm), and the extent of radiation dose exposure (based on correlation of the patient's RT dose distribution to ROI anatomical location) (Winter et al., 2020b). Whenever available, diagnostic results from MR perfusion (MRP) and diffusion weighted imaging (DWI) were analyzed to characterize functional imaging characteristics of individual ROIs (Winter et al., 2020b). For further details on the radiographic analysis see *Publication 2, Materials and Methods, Pages 82 - 83.*

3.2.5 Statistical analysis

The statistical analysis has been previously summarized in *Publication 2* as follows: "Descriptive statistics were used to analyze clinical and radiographic features for both groups. For associations between groups, p values were determined using chi-square and Fisher's exact tests for categorical variables and a Wilcoxon rank-sum test for continuous variables. All reported p values were adjusted for multiple hypothesis testing by false discovery rate; statistical significance was considered as $p < .05$. The Kaplan-Meier (KM) method was used to calculate median overall survival (OS); median follow-up time was calculated based on the reverse KM estimator approach." (Winter et al., 2020b). Furthermore, a univariate generalized estimating equation model was employed to compare characteristics of individual ROIs between patient groups (Winter et al., 2020b), the details of which can be found in *Publication 2, Materials and Methods, Page 83.*

3.3 Characterization of stroke-like migraine attacks after radiation therapy syndrome

3.3.1 Study design and patient eligibility

The study was designed as a retrospective analysis of clinical and imaging data in patients diagnosed with SMART syndrome at the Massachusetts General Hospital, Brigham and Women's Hospital, and the Dana-Farber Cancer Institute between 2013 – 2020 (Winter et al., 2021b). Patient data were obtained from the respective clinical databases and institutional review board approval was granted for all activities (Winter et al., 2021b). Patients were selected based on the following inclusion criteria:

a) remote history of cranial RT for malignancy

b) Diagnosis of SMART syndrome, established by longitudinal clinico-radiographic follow-up

c) adult patients (≥ 18 years at diagnosis of SMART syndrome)

3.3.2 Variables of interest

A series of variables were collected for each patient, including demographic (age at diagnosis, gender), clinical (relevant past medical history, type of malignancy, RT type, interval from RT, presenting clinical signs and symptoms, recurrent episodes of SMART), therapeutic (type of pharmacologic management), and outcome (clinical course, time to complete/incomplete clinical recovery) parameters.

Radiographic features of SMART syndrome were analyzed and interpreted based on T1+C and T2/FLAIR sequences from relevant MRI scans, using standard imaging software. Results of diagnostic functional imaging, including DWI and MRP, were included in the analysis, whenever available. Radiographic variables of interest with respect to identified lesions included anatomic location, correlation with RT dose distribution, appearance/behavior on T1+C, T2/FLAIR, DWI, and MRP, as well as time to radiographic improvement.

4. Results

4.1. Treatment effects in neuro-oncology: research challenges and opportunities

4.1.1 Identified clinical and systemic challenges

Our observations and those of others (Brandsma et al., 2008; Chamberlain et al., 2007; Dietrich et al., 2017; Verma et al., 2013) suggest that, over the past decades, the study of pseudoprogression and treatment-induced necrosis has been complicated by a set of at least 12 identifiable clinical and systemic factors, summarized in **Table 1** (Winter et al., 2019).

Table 1. Identified clinical and systemic challenges.

Clinical factors	***Identified core issues***
Risk factor profile	• Insufficient characterization; likely complex dynamic interplay between unknown predisposing *intrinsic* factors (patient clinical status, inherent genetic susceptibility, tumor entity & molecular-genetic factors) and partly identified *extrinsic* factors (treatment regimen).
Complex pathomechanisms	• Incomplete understanding of causal sequence of events and key targetable pathways/molecules driving & sustaining TN (Furuse et al., 2015; Rahmathulla et al., 2013).
Spatiotemporal radiographic pattern	• Incoherent terminology / arbitrary temporal distinction between PP, vs early-delayed radiation injury vs "early necrosis" vs TN. • Lack of spatial analyses correlating anatomical location of TN lesions with therapeutic radiation dose distribution and respective Rx dose exposure.
Mixed lesions	• Frequent manifestation of lesions containing both TN and residual or recurrent tumor and/or tumor necrosis (Dequesada et al., 2008; Kumar et al., 2000). • Inability to distinguish between mixed entities on conventional MRI → pitfall for identifying correct biopsy targets, affecting diagnostic yield.
Diagnostic ambiguity	
Radiographic	• Inability to distinguish TN from PD on conventional MRI → no optimal advanced imaging modality → lack of robust imaging biomarkers → no consensus on preferred non-invasive diagnostic algorithm (Dietrich and Klein, 2014; Eisele and Dietrich, 2015; Kumar et al., 2000). • Concomitant treatment with glucocorticoids, anti-angiogenics, or immune/targeted therapies may further complicate image interpretation with conventional MRI (Ellingson et al., 2017; Fink et al., 2012; Huang et al., 2015).
Clinical	• The clinical picture of TN frequently mimics that of PD (Eisele and Dietrich, 2015).
Histopathological	• No established histopathological classification criteria for TN or PP → final pathologic diagnosis largely depends on pathologist's experience and subjective impression. • Radiation induced cellular atypia in non-neoplastic cells may mimic intra-lesional infiltration by scattered tumor cells and these can be virtually indistinguishable.(Perry and Schmidt, 2006)
Clinical course	• Heterogenous, difficult to predict. • Symptomatic cases may further progress or deteriorate despite medical intervention, occasionally requiring surgery to prevent fatal outcome.(Dietrich and Klein, 2014; Eisele and Dietrich, 2015) • Lack of level I or II clinical evidence for currently available treatment options.

Summary of identified clinical and systemic factors challenging the study of treatment-related effects in neuro-oncology, with a focus on TN. Adapted from *Publication 1, Figure 1* (Winter et al., 2019). Abbreviations: Dx, diagnosis; MRI, magnetic resonance imaging; PD, progressive disease; PP, pseudoprogression; Rx, radiation; TN, treatment-induced necrosis.

Table 1, continued.

Systemic factors	***Identified core issues***
Prospective biopsy-controlled studies	• There is a paucity of both prospective and biopsy-controlled studies that assess the predictive value of advanced diagnostic imaging methods for TN (Alexiou et al., 2009). • Conversely, routine biopsy of diagnostically ambiguous cases carries surgical risk, may curtail patients' QoL, and is associated with increased costs.
Focused randomized controlled clinical trials (RCTs)	• Lack of RCTs with endpoints devoted to characterizing treatment effects. • Potential "treatment effect confounders" are insufficiently controlled for in past and ongoing clinical trials → pitfall to interpretation of efficacy of experimental anti-neoplastic agents (Chamberlain et al., 2007; Huang et al., 2015; Sanghera et al., 2012).
Functional imaging performance assessment	• Poor inter-study comparability of diagnostic performance of functional imaging modalities due to associated image-acquisition/processing standardization issues (Jain et al., 2010).
Clinical feasibility of functional imaging	• No comprehensive availability of advanced imaging modalities in standard medical care facilities (Verma et al., 2013). • Increased operating cost of scanners/equipment, lack of insurance coverage for advanced diagnostic procedures (Verma et al., 2013). • Frequent diagnostic need to combine different modalities → increased cost and time
Response assessment criteria	• Insufficiency of current criteria in accounting for potential radiographic correlates of treatment effects in follow-up treatment response monitoring
Current diagnostic approach	• Risk of over-emphasis on radiologic findings → pitfall of excluding potentially important risk factors, antecedent events and clinical aspects that may corroborate or challenge a Dx of TN.

Summary of identified clinical and systemic factors challenging the study of treatment-related effects in neuro-oncology, with a focus on TN. Adapted from *Publication 1, Figure 1* (Winter et al., 2019). Abbreviations: Dx, diagnosis; QoL, quality of life; TN, treatment-induced necrosis.

4.1.2 Proposed research framework to advance the field

Following contextualization of identified research barriers with current and expectable future clinical needs, we proposed a comprehensive research framework based on six eminent research pillars (**Figure 3**) directed at advancing clinical understanding, diagnosis, and management of cancer treatment-related effects in neuro-oncology. For greater detail see *Publication 1, Future Perspectives: Mapping the Field, pages 67 - 68* (Winter et al., 2019).

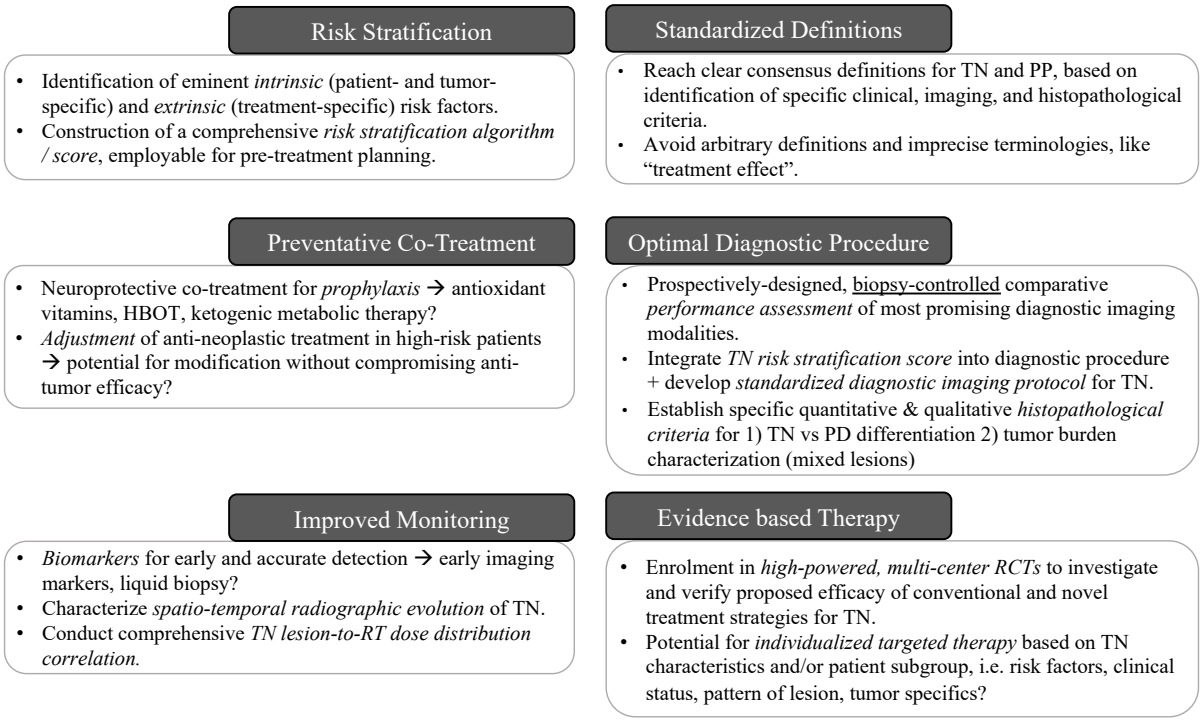

Figure 3. Proposed research framework.
Schematic illustrating six eminent research pillars to advance understanding and management of treatment-related effects such as TN and PP in neuro-oncology. Modified and adapted from *Publication 1, Figure 4* (Winter et al., 2019). Abbreviations: HBOT, hyperbaric oxygen therapy; PD, progressive disease; PP, pseudoprogression; RCT, randomized controlled trial; RT, radiation therapy; TN, treatment-induced necrosis.

4.2. Characterization of pseudoprogression and treatment-induced necrosis

The following segments summarize our previously published results on distinctive clinico-radiographic features of PP and TN in patients with malignant glioma. For reference and greater detail please see *Publication 2, Results, Pages 85 - 90* (Winter et al., 2020b).

Analysis included a total of 64 cases of treatment-related effects classified as either PP (n=27) or TN (n=37), diagnosis of which was predominantly confirmed by tissue biopsy (80%) (Winter et al., 2020b). The clinical characteristics, treatment specifics, and outcome parameters identified in this cohort are summarized in **Table 2**. Briefly, all 60 patients (median age 53 years) had a history of prior RT (most with concurrent and sequential TMZ-based chemotherapy), predominantly in the setting of HGG diagnosis (87.5%) (Winter et al., 2020b). Clinically, Karnofsky performance status (KPS) post initial surgery was high (median score 90/100). Nearly two-thirds of the cohort (64.1%) were found to have underlying vascular comorbidities, a potential risk factor of treatment-related effects. Overall, incidence of disease recurrence was 60% and median OS was 6.25 (95% confidence interval, 0.94–11.56) years (Winter et al., 2020b).

To identify putative differences in clinical parameters and radiographic spatiotemporal pattern between patients with PP versus those with TN, an in-depth comparative analysis between groups was performed (Winter et al., 2020b). The results of this analysis are summarized in sections *4.2.1 – 3*.

4.2.1 Differences in clinical parameters

Comparative analysis identified significant intergroup differences in patient characteristics, treatment specifics, and outcome parameters, summarized in **Table 2**.

Table 2. Summary of patient characteristics, treatment specifics, and clinical outcome.

Patient characteristics	*Value total cohort*	*Value PP group*	*Value TN group*	*p value* for difference between groups*
Demographics				
% sex ratio (m/f)	56 / 44	67 / 33	49 / 51	0.29456
Median Age at diagnosis (yrs)	53	55	47	0.08752
Tumor specifics				
Tumor burden				
% single lesion / multifocal disease	75 / 25	67 / 33	81 / 19	0.33091
Intracranial Location				
% left / right / central or mixed	42 / 50 / 8	59 / 41 / 0	30 / 57 / 13	0.05799
WHO Grade % (N)				**0.02750**
I	1.5 (1)	0 (0)	2.7 (1)	
II	10.9 (7)	0 (0)	18.9 (7)	
III	29.7 (19)	18.5 (5)	37.8 (14)	
IV	57.8 (37)	81.5 (22)	40.5 (15)	
Molecular-genetic profile				
% IDH1 mutated (N)	41.5 (17/41)	11.1 (2/18)	65.2 (15/23)	**0.00548**
% MGMT methylated (N)	58.8 (20/34)	52.6 (10/19)	66.6 (10/15)	0.61115
Clinical status				
% w/ cardiovascular comorbidities	64.1	70.4	59.5	0.56611
Earliest KPS (median) post initial surgery	90	90	90	0.87992
Treatment specifics				
Extent of surgical resection (N)				0.64589
GTR	18	8	10	
NTR	11	6	5	
STR	20	9	11	
PR	6	4	2	
Biopsy only	5	0	5	
Regimen				
Proton / photon RT (N)	5 / 59	1 / 26	4 / 33	-
% w/ (modified) TMZ-based standard chemo-RT	68.8	88.9	54.1	**0.01534**
% w/ concurrent Ctx	76.6	92.6	64.9	**0.04579**
% Steroid use (N)	70.1 (44/62)	81.5 (22/27)	62.9 (22/35)	0.24848
% Bevacizumab use (N)	58.1 (36/62)	63 (17/27)	54.3 (19/35)	0.67511
Clinical outcome				
Median OS in years (95% CI)	6.25 (0.94 – 11.56)	3.0 (2.08 – 3.92)	not reached; last observation censored at 24.9 yrs (OS estimate at 62%)	**<0.0001**
% w/ recurrence (N)	59.6 (34/57)	83.3 (20/24)	42.4 (14/33)	**0.03062**

** FDR-adjusted for multiple hypothesis testing.*

Summary of patient characteristics, treatment specifics, and clinical outcome. Adapted from *Publication 2, Table 1* (Winter et al., 2020b). Abbreviations: chemo-RT, chemoradiation; CI, confidence interval; Ctx, chemotherapy; f, female; FDR, false discovery rate; GTR, gross-total resection; KPS, Karnofsky performance status; m, male; NTR, near-total resection; OS, overall survival; PP, pseudoprogression; PR, partial resection; RT, radiotherapy; TMZ, temozolomide; TN, treatment-induced brain tissue necrosis; STR, subtotal resection; WHO, World Health Organization.

Briefly, the PP group was found to have twice as many GBM cases (81.5 vs. 40.5%; $p < .002$), with significant differences in tumor molecular-genetic profile, i.e. fewer IDH1 mutations (11.1 vs. 65.2%; $p < .006$) and a lower incidence of MGMT promoter methylation (52.6 vs. 66.6%), as compared with the TN group (Winter et al., 2020b). These differences in underlying diagnosis were also reflected by significant differences in systemic antineoplastic- and supportive treatments rendered, as well as differences in clinical outcome (**Table 2**) (Winter et al., 2020b). Accordingly, median follow-up times for PP and TN groups were 5.6 and 10.7 years, respectively, with significant differences in 5-year survival (26% vs. 82%) and median OS (3.25 years vs. not reached; 62% survival estimate, last observation censored at 24.5 years; $p < .0001$) rates between both groups (**Figure 4**) (Winter et al., 2020b).

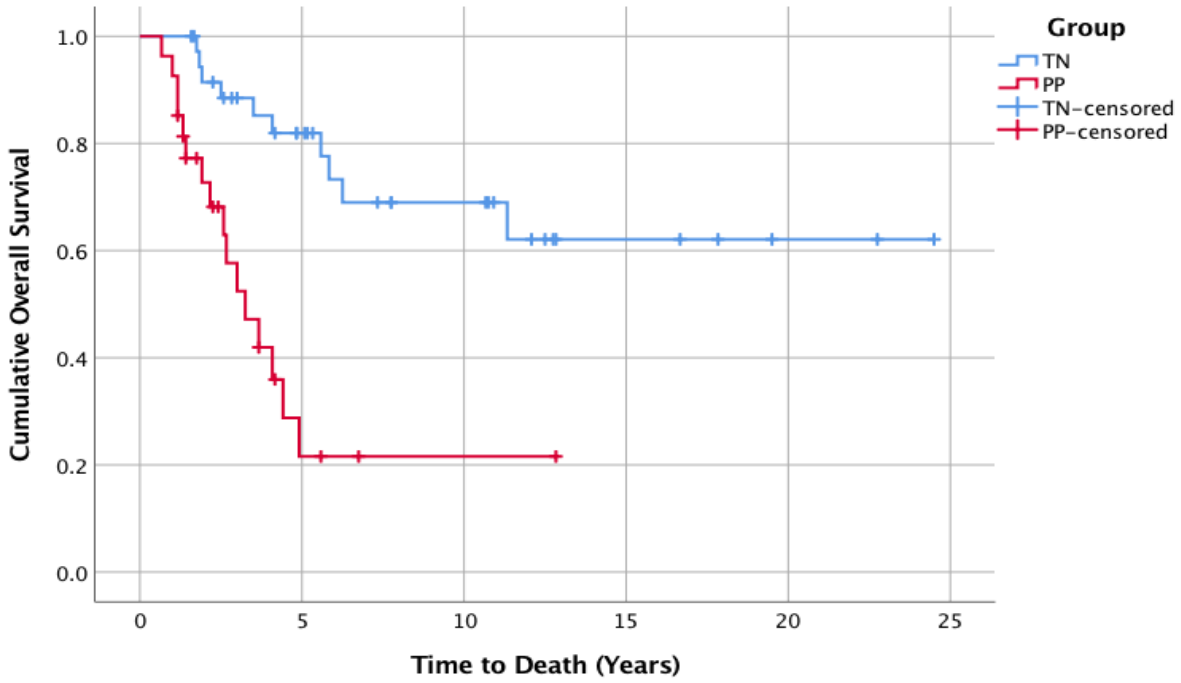

Figure 4. Kaplan-Meier survival analysis of PP and TN cohorts.
Kaplan-Meier survival analysis depicting PP (red line; 16 progression events; 11 censored. Median OS, 3.25 years [95% confidence interval, 2.16–4.9]) and TN (blue line; 10 progression events; 27 censored. Median OS not reached; last observation censored at 24.5 years; survival estimate 62%) groups. For comparison, $p < .0001$. Adapted from *Publication 2, Figure 1* (Winter et al., 2020b). Abbreviations: OS, overall survival; PP, pseudoprogression; TN, treatment-induced necrosis.

4.2.2 Differences in initial presentation

To characterize putative differences in initial presentation between PP and TN, the radiographic and histopathological features of the first appearing lesion ("first ROI") in each patient were analyzed and compared between groups (**Table 3**).

Table 3. Characteristics of first ROI identified as treatment effect.

Characteristics of first ROI	*Value total cohort*	*Value PP group*	*Value TN group*	*p value* for difference between groups*
Spatiotemporal Radiographic Features				
Median onset (mos) post-RT completion (range)	6.5 (0– 239)	1.0 (0 – 4)	11.0 (3– 239)	**<0.00001**
% periventricular location	48.4	33.3	59.5	0.09098
% ring-like enhancement around RC	37.5	70.4	13.5	**0.00009**
Functional Imaging Features				
% w/ functional imaging (N)	77.4 (48/62)	92.0 (23/25)	67.6 (25/37)	0.07587
% elevated rCBV in MRP	75.0 (30/40)	88.8 (16/18)	63.6 (14/22)	0.19976
% restricted diffusion in DWI	54.1 (20/37)	57.7 (8/14)	52.2 (12/23)	0.75603
Clinical Features				
% onset during active treatment	54.7	85.2	32.4	**0.00044**
Median amount of Ctx received (mos) prior to onset	3.0 (IQR=1 – 9)	1.0 (IQR=1 – 3)	7.5 (IQR=2 – 12)	**0.00574**
% w/ concurrent new symptoms (N)	65.6 (40/61)	69.2 (18/26)	62.9 (22/35)	0.82835
% of symptoms related to ROI	60.0 (24/40)	59.1 (13/22)	61.1 (11/18)	0.61115
% receiving any treatment for ROI	78.1	88.9	70.2	0.20967
% receiving steroids	54.7	74.1	40.5	**0.03592**
% receiving bevacizumab	18.8	11.1	24.3	0.29698
% receiving surgical debulking	35.9	51.9	24.3	0.07991
Histopathological features				**0.03592**
% treatment effect only (N)	16.0 (8/50)	0.0 (0/24)	30.8 (8/26)	
% treatment effect w/ rare atypical cells (N)	62.0 (31/50)	70.8 (17/24)	53.8 (14/26)	
% treatment effect w/ foci of solid tumor (N)	22.0 (11/50)	29.2 (7/24)	15.4 (4/26)	

** FDR-adjusted for multiple hypothesis testing.*

Characteristics of first ROI identified as treatment effect. Adapted from *Publication 2, Table 2* (Winter et al., 2020b). Abbreviations: Ctx, chemotherapy; DWI, diffusion weighted imaging; FDR, false discovery rate; IQR, interquartile range; MRP, magnetic resonance perfusion; PP, pseudoprogression; RC, resection cavity; rCBV, relative cerebral blood volume; ROI, region of interest; RT, radiotherapy; TN, treatment-induced brain tissue necrosis.

In summary, intergroup comparison identified specific temporal incidence peaks for PP and TN (Winter et al., 2020b). While group allocation per se was based on temporal stratification using a 5-month cutoff point, development of PP and TN peaked at distinct timepoints, whereby PP mostly occurred at or within 1 month and TN mostly between 7 and 12 (median, 11) months post-RT completion (**Figure 5**) (Winter et al., 2020b). As such, PP manifestation peaked during active antineoplastic treatment (85 vs. 32%; $p < .0005$), while TN mostly developed during imaging surveillance periods (Winter et al., 2020b). In addition, late-delayed TN (>5 years) was identified in a subset of patients, including 2 cases manifesting decades after RT (**Figure 5**).

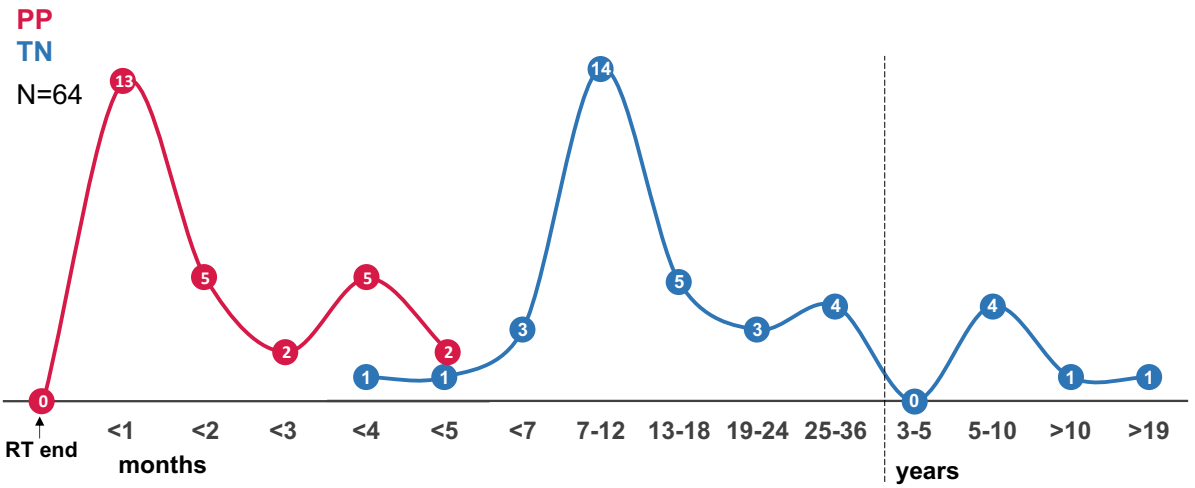

Figure 5. Temporal distribution of first ROI manifestation.
Temporal distribution of first region of interest (ROI) manifestation on MRI post-RT completion. Adapted from *Publication 2, Figure 2 A* (Winter et al., 2020b). Abbreviations: PP= pseudoprogression; RT, radiation therapy; TN, treatment-induced necrosis.

Beyond temporal differences, PP and TN were found to exhibit unique radiographic features (**Figure 6**). As such, most PP lesions were non-nodular, ring-like enhancing structures that developed around the tumor resection cavity (RC) margin (70.4 vs. 13.5%; $p < .0001$; **Figure 6 D – F**), whereas TN typically manifested as multiple small nodular lesions with a predilection for the periventricular white matter (**Figure 6 A – C**) (Winter et al., 2020b).

In both groups, initial manifestation of treatment-related effects was associated with new neurologic symptoms in the majority of cases (60%), although patients with PP received significantly more steroid-based (74.1 vs. 40.5%; $p < .04$) or surgical (51.9 vs. 24.3%) interventions (**Table 3**) (Winter et al., 2020b). Interestingly, results of advanced diagnostic

imaging such as DWI and MRP (more frequently conducted in the PP group), were frequently suggestive of recurrent disease rather than treatment effect (**Table 3**) (Winter et al., 2020b). Finally, histopathological analysis of biopsied/resected initial ROIs revealed intergroup differences in the content of malignant elements, whereby PP specimens more frequently contained mixed lesions, i.e. treatment effects with rare atypical cells or foci of solid tumor ($p < .04$; **Table 3**) (Winter et al., 2020b).

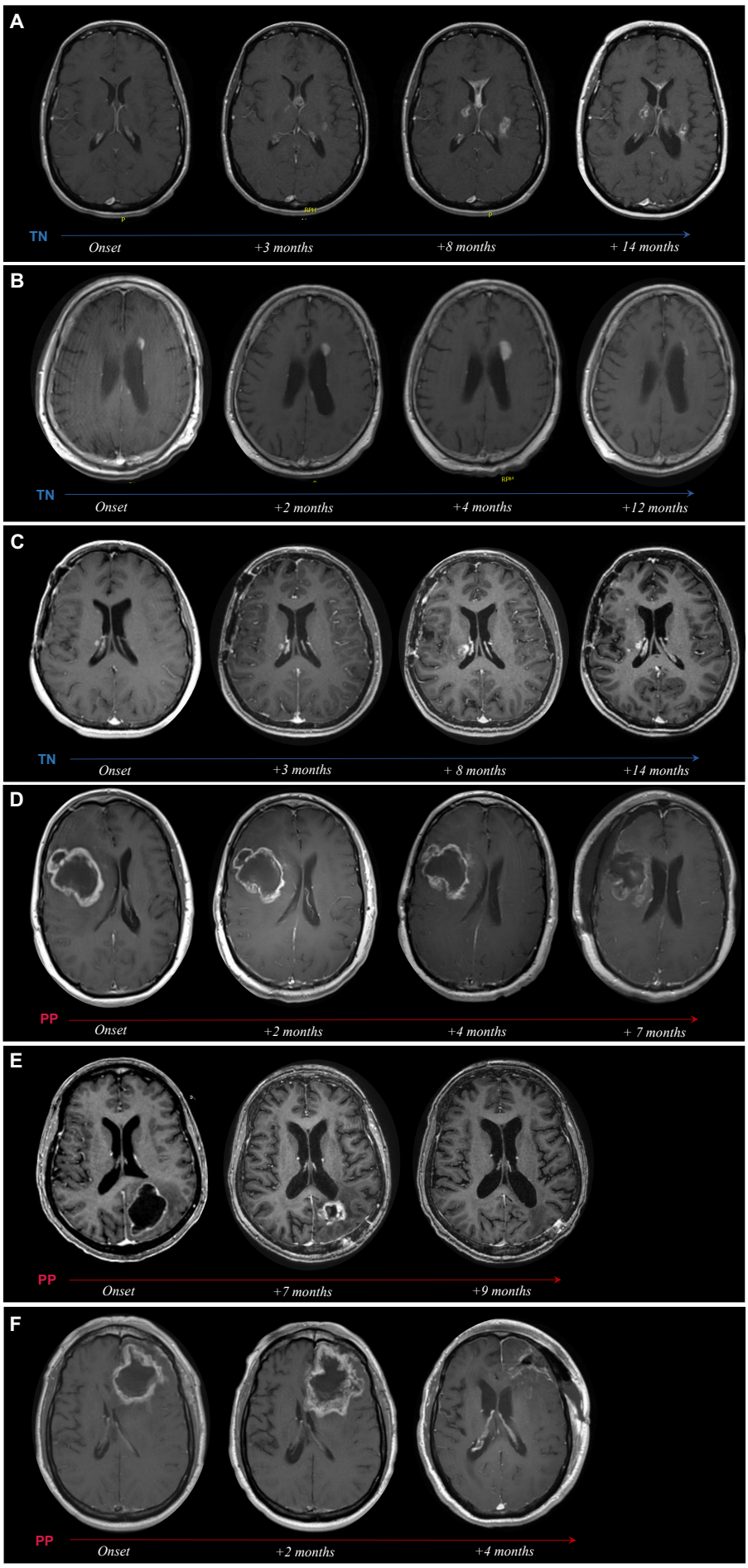

Figure 6. Radiographic evolution of TN and PP over time.

T1+C axial MRI scans from representative patients with TN **(A–C)** and PP **(D–F)** depicting radio-graphic evolution of treatment-related changes over time. Adapted from *Publication 1, Figure 3*, where detailed descriptions of the illustrated cases can be found (Winter et al., 2020b). Abbreviations: MRI, magnetic resonance imaging; PP, pseudoprogression; TN, treatment-induced necrosis.

4.2.3 Differences in spatiotemporal radiographic lesion pattern

Longitudinal radiographic evaluation of the 64 PP and TN cases identified a total of 137 treatment-related ROIs (n = 62 biopsied; n = 75 clinico-radiographic diagnosis) classified as either PP or TN lesions (Winter et al., 2020b). Intergroup comparison at the level of individual ROIs revealed distinct spatiotemporal radiographic features and histopathological differences, summarized in **Table 4** (Winter et al., 2020b).

Briefly, most PP-related ROIs (n = 30) were unifocal (81.4%) and, unlike TN-related ROIs, located at the tumor RC margin as non-nodular entities with ring-like enhancement (63.3 vs. 5.6%; $p < .0001$; **Figure 7 B**) (Winter et al., 2020b). Conversely, TN-related ROIs (n = 107) were typically nodular, more numerous (median, 2 vs. 1 ROIs; $p = .01$), located in deep-seated brain regions such as the periventricular white matter ($p = .0001$) with highly variable distances from the tumor RC (median, 21.5 mm; range, 0–78 mm; **Figure 7 B**), and contained fewer malignant elements upon biopsy ($p = .008$) (Winter et al., 2020b). As such, TN mostly evolved into multiple small nodular lesions over time, whereby a quarter of TN-related ROIs developed later than 3 years post-RT completion (**Figure 7 C**) (Winter et al., 2020b).

Furthermore, the "fate" of each individual PP- or TN-related ROI was characterized via longitudinal radiographic tracing, i.e. from onset until either surgical resection, antiangiogenic treatment, radiographic resolution, or last available MRI scan, as exemplified in **Figure 6**. In summary, the vast majority of PP-related ROIs (80%) were surgically resected and/or treated by antiangiogenics a few (median, 4) months after lesion onset (Winter et al., 2020b). Conversely, only about one-third of TN-related ROIs were treated (median interval, 8 months), whereas the untreated majority either resolved radiographically (36%; median time to resolution, 11.5 months) or persisted until the last available MRI scan (29%; median interval, 15 months) (Winter et al., 2020b).

Finally, individual ROIs were correlated anatomically to available RT dose distribution curves, as exemplified in **Figure 8**. Based on this analysis, 98.9% (n = 87/88) of ROIs were located in the main radiation field, nearly half of which (46%) were spatially correlated to areas of supratherapeutic radiation maxima (**Table 4**)) (Winter et al., 2020b).

Table 4. ROI spatiotemporal radiographic and histopathological characteristics.

ROI Characteristics	*Value total cohort*	*Value PP group*	*Value TN group*	*P value (estimate)**
Number of analyzed ROIs	137	30	107	
N biopsied	62	26	36	
% needle biopsy / open resection / autopsy	40.3 / 53.2 / 7.7	19.2 / 80.8 / 0.0	55.6 / 33.3 / 11.1	0.3580 (-0.7338)
N not biopsied, but spatiotemporal radiographic pattern similar to a biopsied ROI in same patient	45	1	44	
N clinico-radiographic diagnosis only	30	3	27	
Spatiotemporal Radiographic Features				
Median onset (mos) post-RT completion (IQR)	11 (5 – 28)	0 (0 – 2)	16 (10 – 36)	**0.0010 (2.4756)**
% deep-seated- / lobar- / both locations	33.6 / 57.7 / 8.8	6.7 / 73.3 / 20.0	41.1 / 53.3 / 5.6	**0.0001 (-1.4993)**
% periventricular location	40.2	30.0	43.0	0.2600 (0.5651)
% ring-like enhancement around RC	18.3	63.3	5.6	**<.0001 (-3.3699)**
Max. size in cm^2 (median; IQR)	0.99 (0.16 – 4.42)	3.70 (1.08 – 7.50)	0.55 (0.15 – 3.36)	0.1672 (-0.0341)
Shortest distance (mm) from RC (median; IQR)	16.5 (0.0 – 27.0)	0.0 (0.0 – 12.0)	21.5 (10.0 – 31.0)	**0.0011 (0.0902)**
Correlation to RT dose distribution				
% located in main radiation field	98.9 (87/88)	100 (25/25)	98.4 (62/63)	
% receiving less than / equal to / more than max. therapeutic radiation dose	11.5 / 42.3 / 46.2	8.3 / 29.2 / 62.5	13.0/ 48.1 / 38.9	
Histopathological features				**0.0084 (-1.4779)**
% treatment effect only (N)	24.2 (15/62)	0.0 (0/26)	41.7 (15/36)	
% treatment effect w/ rare atypical cells (N)	56.5 (35/62)	73.1 (19/26)	44.4 (16/36)	
% treatment effect w/ foci of solid tumor (N)	19.4 (12/62)	26.9 (7/26)	13.9 (5/36)	

**Based on a generalized estimating equation model, adjusted for multiple observations per patient, and applied to eight preselected variables of interest.*

Adapted from *Publication 2, Table 3* (Winter et al., 2020b). Abbreviations: IQR, interquartile range; PP, pseudoprogression; RC, resection cavity; ROI, region of interest; RT, radiotherapy; TN, treatment- induced brain tissue necrosis.

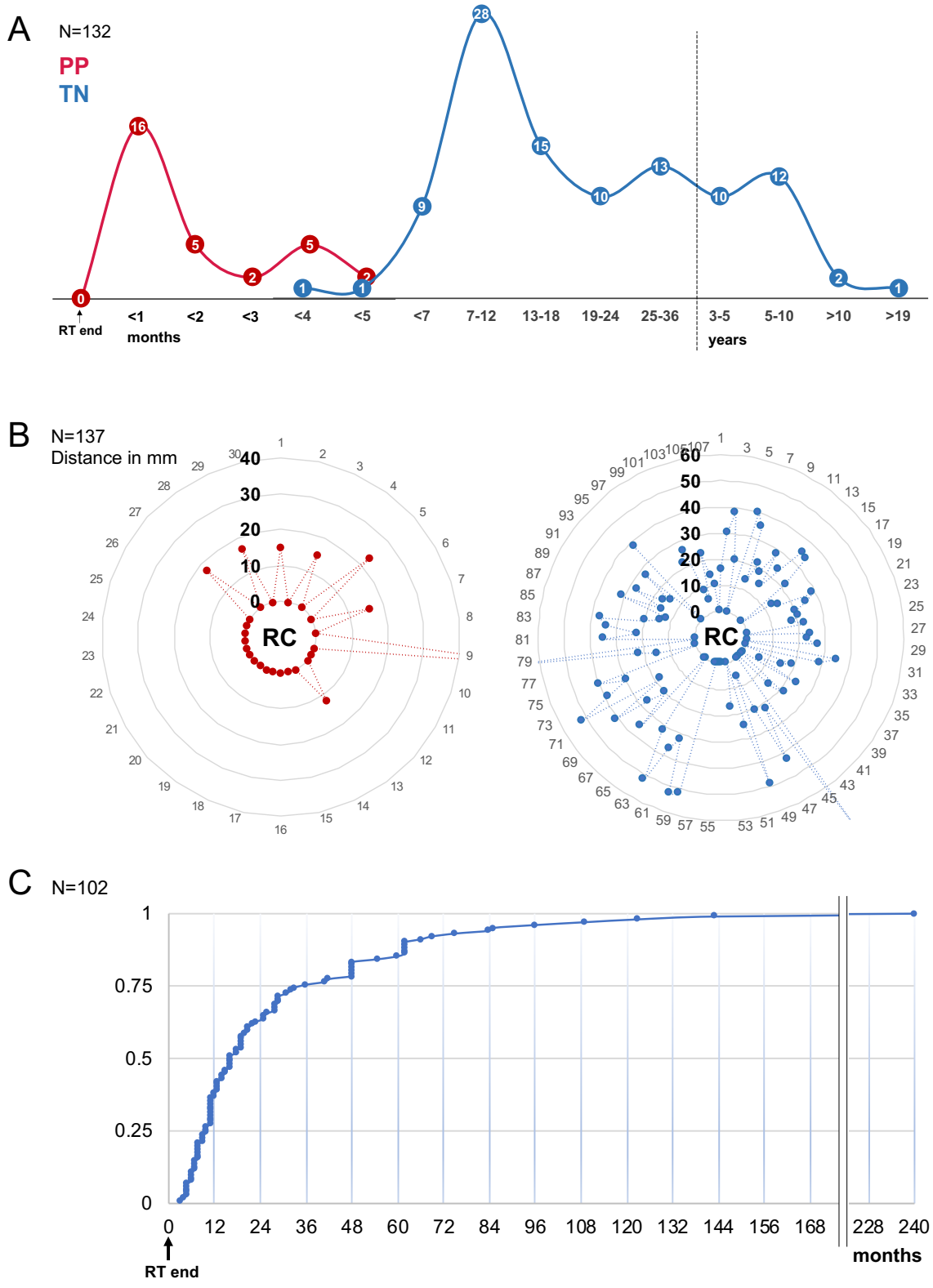

Figure 7. Spatiotemporal radiographic characteristics of PP and TN.
(A) Temporal distribution of overall ROI manifestation on MRI post-RT completion. (**B**) Spatial distribution of ROIs relative to the tumor resection cavity (RC), illustrating the shortest ROI-to-RC distance for each ROI. (**C**) Cumulative frequency of TN group ROI onset latency from RT completion. Adapted from *Publication 2, Figure 2 B – D* (Winter et al., 2020b). Abbreviations: PP, pseudoprogression; RC, resection cavity; ROI, region of interest; RT, radiation therapy; TN, treatment-induced necrosis.

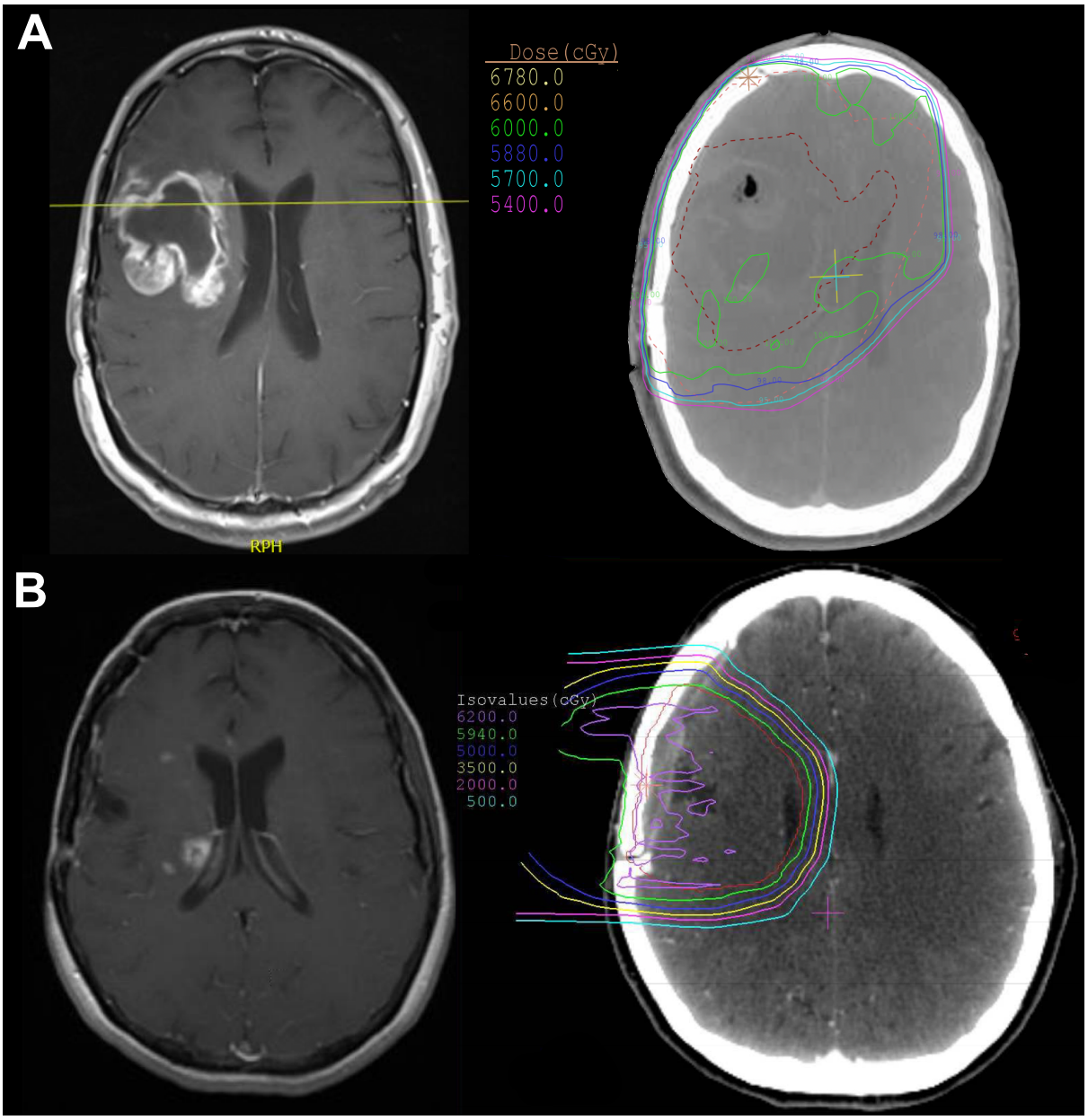

Figure 8. Typical radiographic features of PP and TN.
Typical radiographic features of PP **(A)** and TN **(B)** observed on axial T1+C MRI scans (left panels), with corresponding radiotherapy dose distribution overlay on axial computed tomography (right panels) demonstrating prior exposure of these enhancing ROIs to the main radiation field. Adapted from *Publication 2, Figure 4* (Winter et al., 2020b). Abbreviations: MRI, magnetic resonance imaging; PP, pseudoprogression; RT, radiation therapy; TN, treatment-induced necrosis.

4.3 Characterization of stroke-like migraine attacks after radiation therapy syndrome

The following segments summarize our previously published results on distinctive clinico-radiographic features of SMART syndrome in (neuro-)oncological patients. For reference and greater detail please see *Publication 3, Case Series, Pages 100 – 101* (Winter et al., 2021b).

4.3.1 Clinical presentation, evolution, and management

In this retrospective multicenter study, a total of 7 consecutive patients with diagnosis of SMART syndrome were identified an analyzed. Of note, portions of 2 patient cases included in this series were previously published elsewhere (Olsen et al., 2016). Relevant demographic and clinical characteristics are summarized in **Table 5**.

Briefly, all 7 patients (6 males and 1 female, aged 49 – 68 [mean, 58] years) had received partial (71%) or whole brain RT (29%) (dose range, 36 – 60Gy [n=5/7]), including proton RT in 2 cases (Winter et al., 2021b). The RT-to-SMART time interval was highly variable, (range, <1.5 to 28 years [mean, 11.8 years]) and the most common presenting signs and symptoms included migraine-type headaches (71%), aphasia (71%), and seizures (57%) (**Table 5**). 57% of patients experienced multiple (range, 2 – 4) SMART episodes, generally affecting the same cerebral region (Winter et al., 2021b). Observed clinical symptoms were universally accompanied by pathognomonic MR imaging changes (see section *4.3.2 Radiographic features*). All patients received supportive therapy, including antiepileptics (86%), nonsteroidal anti-inflammatory drugs (NSAIDs) (57%), and steroids (43%), und which all achieved radiographic improvement with full (71%) or partial (29%) neurologic recovery (Winter et al., 2021b).

Table 5. Clinical characteristics in SMART syndrome.

Patient	*Gender*	*Age, y*	*RT indication*	*RT type (dose)*	*Interval from RT, y*	*Migraine history*	*Clinical symptoms*				*Recurrent episodes*	*Clinical Mx*	*Time to full clinical recovery*
							Seizures	*Headache*	*Aphasia*	*Other*			
1	M	49	Secondary CNS lymphoma	WBRT	16	-	+	+	+	AMS	-	Levetiracetam, Lacosamide	1mo
2	M	55	AA (left occipital)	Protons (59.4Gy(RBE))	<1.5	-	- (abnormal EEG)	+	-	Visual oscillations	-	Levetiracetam, ASA	10mo
3	M	68	SCLC (prophylactic)	WBRT (36Gy)	28	-	+	-	+	Hemiparesis	+	Levetiracetam, Lacosamide, Magnesium	1mo
4	F	59	Osteosarcoma affecting the skull base	EBRT	14	-	+	+	-	Hemiparesis and visual field deficits	+	AED, Methylprednisolone	1mo
5	M	62	AOD (left temporo-parietal)	Protons (59.4 Gy(RBE))	4	+	-	+	+	AMS	+	Levetiracetam, Lacosamide, ASA, Atorvastatin	Partial recovery; >3y of fluctuating neurologic sx
6	M	59	GBM (left temporal)	Photons (60Gy)	10	-	+	-	+	Hemiparesis and AMS, fever	-	Levetiracetam, Dexamethasone, Prednisone, ASA	1mo
7	M	56	GBM (left occipital)	Photons (60Gy)	9	+	-	+	+	-	+	Methylprednisolone, Verapamil, Fioricet, Galcanezumab, Celecoxib	Partial recovery; episode ongoing

Abbreviations: AA, anaplastic astrocytoma (WHO III); AED, antiepileptic drugs; AOD, anaplastic oligodendroglioma (WHO III); AMS, altered mental status; ASA, acetylsalicylic acid; Dx, diagnosis; EBRT, external beam radiation therapy; F, female; GBM, glioblastoma multiforme (WHO IV); Gy, gray; M, male; mo= months; Mx, management; RBE, relative biological effectiveness; RT, radiation therapy; SCLC, small cell lung cancer; Sx, symptoms; WBRT, whole brain radiation therapy; y, years

Demographic, clinical, and management characteristics identified in patients with SMART syndrome. Adapted from *Publication 3, Table 1* (Winter et al., 2021b).

4.3.2 Radiographic features

In all 7 patients, cranial MRI demonstrated characteristic imaging abnormalities during SMART episodes, summarized in **Table 6.**

Briefly, MR imaging findings were strictly unilateral, located in previously irradiated brain regions, and characterized by cortical gyriform enhancement (100%) with associated T2/FLAIR signal hyperintensity (86%) and inconsistent diffusion restriction (43%) (Winter et al., 2021b). In most instances, radiographic resolution occurred over the course of 1 – 10 months and was accompanied by recovery of neurologic function (**Figure 9 A & B**). In all patients who underwent advanced functional imaging by MRP (n=3/3), corresponding regional hyperperfusion (as per elevations in cerebral blood flow [CBF] and/or -volume [CBV]) was noted, suggestive of vascular dysfunction (**Figure 9 C**) (Winter et al., 2021b).

Table 6. MR imaging characteristics in SMART syndrome.

Patient	*Laterality (L/R)*	*In radiation field*	*Cortical gyriform enhancement (location)*	*T2/FLAIR signal hyperintensity*	*DWI diffusion restriction*	*MR perfusion*	*Time to radiographic improvement*
1	L	+	Temporal, parietal, occipital	+	+ (mild)	↑CBF	<1mo
2	L	+	Occipital, parietal	+	+ (foci)	N/A	10mo
3	L	+	Entire hemisphere	+	-	↑CBF, ↑CBV	1mo
4	L	+	Occipital, parietal	+	-	↑CBV	>5y (gradual resolution w/ intermittent worsening)
5	L	+	Temporal	+	-	N/A	3mo
6	L	+	Entire hemisphere	-	-	N/A	1mo
7	L	+	Parietal, occipital	+	+	N/A	N/A; episode ongoing

MR imaging characteristics identified in patients with SMART syndrome. Adapted from *Publication 3, Table 2* (Winter et al., 2021b). Abbreviations: CBF, cerebral blood flow; CBV, cerebral blood volume; DWI, diffusion-weighted imaging; L, left; mo, months; N/A, not applicable; R, right; w/, with; y, years.

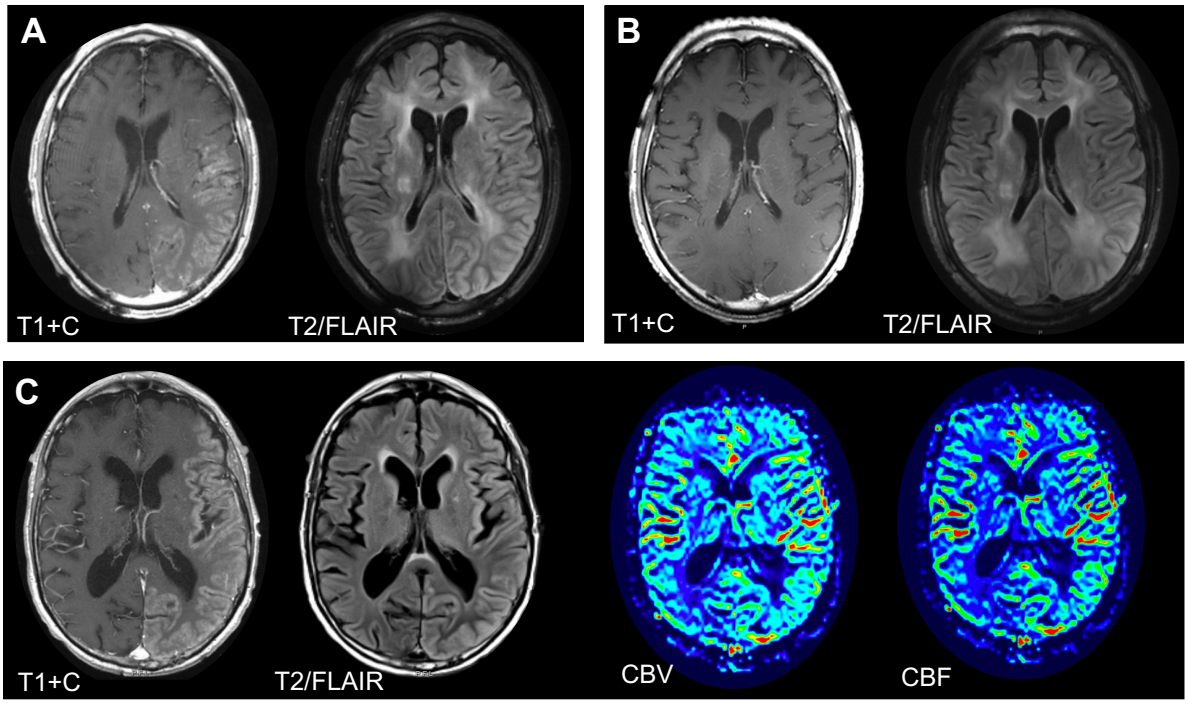

Figure 9. Examples of imaging characteristics identified in SMART syndrome.
(A & B) Patient 1. Brain MRI (hospital day 6) taken after an episode of non-convulsive status epilepticus in a patient who presented with aphasia, confusion, and headache 16 years post-WBRT. Findings demonstrate new cortical gyriform enhancement in the left temporo-parieto-occipital region, associated T2/FLAIR signal hyperintensity, and extensive post-radiation white matter changes which are unchanged from previous scans **(A)**. Follow-up MRI (+3 weeks) with interval resolution of cortical enhancement and persistent but decreased T2 hyperintense gyral swelling **(B)**.
(C) Patient 3. Brain MRI (hospital day 4), taken after seizure development in a patient who presented with sudden right hemiparesis and aphasia 28 years after prophylactic WBRT (36Gy). Findings demonstrate extensive cortical gyriform enhancement with associated diffuse T2/FLAIR signal hyperintensity involving large portions of the left cerebral hemisphere; there are corresponding regional elevations in cerebral blood volume (CBV) and -flow (CBF) on perfusion MRI.
Adapted and modified from *Publication 3, Figure 1* (Winter et al., 2021b). Abbreviations: CBF, cerebral blood flow; CBV, cerebral blood volume.

5. Discussion

Cancer treatment-related neurotoxicity remains a major challenge in the therapeutic management of (neuro-)oncological patients (Dietrich et al., 2019). Our in-depth analysis of the current state of research in the field of treatment-related effects that mimic progressive disease (i.e. TN and PP) (*Publication 1*) suggests that, although a multiplicity of diagnostic imaging modalities and numerous treatment strategies for TN and PP have been put forward, no diagnostic or therapeutic SOC has yet been established (Winter et al., 2019). Based on the existing clinical literature, we identified a set of major clinical and systemic factors that have challenged the development of best management practices for these conditions (Winter et al., 2019). To address these existing barriers, we developed a comprehensive research framework (**Figure 3**) as a potential blueprint to help improve the direction and design of clinical investigations in this field (Winter et al., 2019). Numerous aspects of this framework (including elements of the research pillars *Optimal Diagnostic Procedure*, *Evidence-based Therapy*, *Standardized Definitions*, *Improved Monitoring*, and *Risk Stratification*) served to inform the design of our subsequent study, in which we aimed to address relevant unanswered questions by holistic analysis of the clinical and imaging characteristics of 60 glioma patients diagnosed with either PP or TN as a consequence of brain tumor therapy (*Publication 2*) (Winter et al., 2020b). Using a similar approach, we aimed to characterize distinctive clinico-radiographic features in 7 (neuro-)oncological patients with SMART syndrome (*Publication 3*). Like PP and TN, this rare treatment-related condition can be radiographically indistinguishable from PD and remains difficult to diagnose and manage.

The following sections provide a brief critical discussion of the methods and results from *Publications 2 and 3*, with a focus on clinical implications and contextualization with relevant clinical literature. For the respective in-depth discussions of these studies, see *Publication 2, Discussion, Pages 90 – 92* and *Publication 3, Discussion, Pages 102 - 103*.

5.1 Pseudoprogression and treatment-induced necrosis

Our results are consistent with the clinical literature on treatment-related effects in neuro-oncology and offer several important new findings. In line with observations by others, we found that treatment-related effects largely occurred in HGG patients, especially following (TMZ-based) chemo-RT (Brandsma et al., 2008; Chamberlain et al., 2007). Radiographic onset

post-RT was either early or late (classified in this study as PP or TN) (Dietrich et al., 2017; Giglio and Gilbert, 2003; Tofilon and Fike, 2000), frequently symptomatic (Chi et al., 2008; Minniti et al., 2011), and typically managed by steroids, antiangiogenics, and/or surgery (Lubelski et al., 2013; McPherson and Warnick, 2004; Shaw and Bates, 1984; Winter et al., 2020b). Moreover, the presence of either type of treatment-related effects appeared to be associated with above-average overall survival (Winter et al., 2020b).

Our comparative analysis by temporal stratification of treatment-related effects identified unique differences between PP and TN, especially with regards to clinical course, spatiotemporal radiographic lesion pattern, histopathological features, characteristics of affected patient populations (including tumor molecular-genetic profile), and clinical outcome – discussed in more detail in *Publication 2, Discussion, Pages 90 – 92* (Winter et al., 2020b). Taken together, our observations suggest that PP and TN represent distinct conditions that occur in specific neuro-oncological patient populations and most likely differ in underlying pathophysiology (Winter et al., 2020b). These findings provide evidence for the necessity to establish separate clinical definitions for both conditions and thereby improve the quality of – and comparability between – future clinical investigations in this field (Winter et al., 2019). In addition, a clear consensus must be reached regarding the terminology attributed to early versus late treatment-related effects (here termed PP and TN). This includes resolution of semantic inconsistencies surrounding the term “pseudoprogression”, which is sometimes used in the literature to denote a purely radiographic phenomenon. Instead, PP likely represents a distinct clinical condition predominantly encountered in patients with GBM in the weeks to months after TMZ-based chemo-RT treatment, as we and others have described (Brandsma et al., 2008; Dietrich et al., 2017; Taal et al., 2008).

Our longitudinal radiographic analysis at the level of individual ROIs corroborates previous descriptions of the spatiotemporal imaging characteristics of PP (Brandsma et al., 2008; Taal et al., 2008) and TN (Kumar et al., 2000; van West et al., 2017), including the finding that the periventricular white matter appears to be a predilection site for TN development (Brandsma et al., 2008; Kumar et al., 2000; van West et al., 2017). Notably, we observed significant heterogeneity in the behavior of TN ROIs traced over time, suggesting the existence of different lesion subpopulations within the spectrum of TN (Winter et al., 2020b). As such, some TN lesions are transient and may spontaneously resolve without therapeutic intervention

(van West et al., 2017; Winter et al., 2020b). By contrast, other, more aggressive forms of TN require therapeutic intervention and/or continue to progress over time in an irreversible manner (Winter et al., 2020b, 2019). The reasons for these different behaviors remain unclear and warrant further clinical investigation.

Our correlative spatial analysis using RT dose distribution curves revealed that PP and TN lesions reliably developed in the main field of prior radiation and, as such, predominantly in areas of therapeutic radiation maxima and in supratherapeutic radiation "hot spots" (Winter et al., 2020b). This finding underscores the diagnostic utility of RT dose distribution curves in the interpretation of newly enhancing lesions on MRI (Winter et al., 2020b). Making use of this valuable noninvasive tool may facilitate diagnosis in the setting of equivocal findings on structural or even functional neuroimaging. Notably, analysis of PP/TN lesions by DWI and/or MRP imaging reports in our study was frequently suggestive of PD and most patients eventually underwent tissue biopsy to resolve imaging ambiguities (Winter et al., 2020b). This finding demonstrates the current limitations of advanced imaging modalities in reliably differentiating PP/TN from true PD and the continued importance of tissue-biopsy to resolve diagnostic ambiguities and guide management (Winter et al., 2020b).

Our study has several strengths and limitations:
While patient selection and data collection were carried out retrospectively, our study is, to our knowledge, the first in which a majority (80%) of analyzed cases of treatment-related effects in neuro-oncological patients were diagnostically confirmed by tissue biopsy (Winter et al., 2020b). Patient stratification into PP and TN diagnosis groups was based on a defined temporal cutoff point in accordance with the typical manifestation ranges reported for both conditions in the literature (Brandsma et al., 2008; Dietrich et al., 2019; Eisele and Dietrich, 2015; Giglio and Gilbert, 2003; Tofilon and Fike, 2000; Winter et al., 2019). Potential diagnostic inaccuracies caused by this approach cannot be fully ruled out, although we carefully reviewed each allocated diagnosis post-hoc, taking into account all available clinical and radiographic information (Winter et al., 2020b). Qualitative histopathological characterization of biopsied lesions was limited as no standardized histopathological criteria for PP/TN presently exist and available pathology reports commonly summarized findings as "treatment effect" (Winter et al., 2020b). Nevertheless, we found that biopsied TN lesions contained comparably fewer malignant elements, while foci of "mixed pathology" were present in 25% of biopsied PP

lesions (Winter et al., 2020b). This finding is reflective of the spatiotemporal characteristics seen in PP, including preferential location around the tumor RC and early manifestation during active antineoplastic treatment, and supports the hypothesis that PP and TN differ in underlying pathophysiology, as discussed in more detail in *Publication 2, Discussion, Pages 90 – 92* (Winter et al., 2020b). Future studies with qualitative histopathological analysis of PP and TN are warranted to 1) establish robust histopathological criteria and 2) identify implicated pathomechanisms that may translate to effective therapeutic applications (Winter et al., 2020b). Lastly, our observations and those of others suggest an association between the development of treatment-related effects and improved clinical outcome, possibly due to a more durable treatment response seen in patients with PP/TN (Brandes et al., 2008; Chamberlain et al., 2007; Winter et al., 2020b; Yang and Aghi, 2009). However, this finding should be interpreted with caution as survival analyses in selected patient populations with (late-delayed) treatment-related effects are prone to an implicit time bias (van West et al., 2017; Winter et al., 2019). Further studies with matched controls are thus warranted to assess whether PP/TN might constitute a potential biomarker for improved outcome in glioma patients (Winter et al., 2020b). Moreover, the co-occurrence of other independent positive prognostic biomarkers, including IDH1 mutation (Loebel et al., 2017; Nobusawa et al., 2009; Sanson et al., 2009) and MGMT promoter methylation (Gerstner et al., 2009; Rivera et al., 2010; Wick et al., 2013) must be factored in, as these mutations may be enriched in in tumors of patients with treatment-related effects (Li et al., 2016; Motegi et al., 2013; Winter et al., 2020b).

5.2 Stroke-like migraine attacks after radiation therapy syndrome

Our findings support previous descriptions of SMART (Black et al., 2013, 2006; Fan et al., 2018; Kerklaan et al., 2011) and offer several new insights into the clinico-radiographic manifestation of this rare and underrecognized treatment-related condition (Winter et al., 2021b). Consistent with the literature, all our patients had a remote history of cranial RT, were predominantly older men, presented with typical clinical signs and symptoms (including migraine-like headaches, seizures, and/or neurologic deficits), and demonstrated pathognomonic MR imaging abnormalities strictly confined to previously irradiated brain regions (**Figure 9**) (Winter et al., 2021b). Notably, we found that left cerebral hemispheres were universally affected; whether right hemispheric involvement is clinically less pronounced

– and therefore potentially underrepresented in patients with SMART – remains unknown (Winter et al., 2021b). Although SMART manifestation post-RT in adults generally occurs after many years to decades (Black et al., 2013; Fan et al., 2018), our study identified two cases of "early-onset" SMART (<4 years and <14 months, respectively). Interestingly, these patients had underlying vascular comorbidities, a potential risk factor for SMART (Olsen et al., 2016), and, in addition, had received proton RT. Since RT dose has been proposed as a risk factor for SMART development (Kerklaan et al., 2011), it is conceivable that specific radiation modalities like proton RT may play a contributory role (Winter et al., 2021b), as has been observed with other types of treatment-related effects (Dworkin et al., 2019). The pathophysiology of SMART is complex, and several mechanisms have been proposed, as discussed in more detail in *Publication 3, Discussion, Pages 101 - 102* (Winter et al., 2021b). Briefly, our findings point to radiation-induced impaired cerebral arterial autoregulation (with resultant regional hyperperfusion) as a putative mechanism driving the characteristic imaging abnormalities – and preceding seizure development – in SMART (Winter et al., 2021b). Consistent with previous studies (Black et al., 2013; Fan et al., 2018), SMART episodes frequently recurred and in a subset of patients neurologic recovery was incomplete (Winter et al., 2021b). Our findings support the notion that a prior migraine history may predispose to a complicated clinical course, though future investigations are necessary to corroborate this hypothesis (Winter et al., 2021b). Limitations of our study include a descriptive and retrospective design, as well as a lack of tissue-based diagnosis of SMART, although current diagnostic criteria for SMART are solely clinico-radiographic and both the safety and utility of biopsy in the setting of SMART have been questioned (Black et al., 2013; Winter et al., 2021b).

In addition to providing new insights into the clinical dynamics and potential pathomechanisms underlying SMART development, several clinical implications can be derived from our study. In all patients, SMART was considered a diagnosis of exclusion and, as such, it remains pivotal that other more common differential diagnoses (e.g., local tumor progression, leptomeningeal disease, infection, and ischemic events) are ruled out during diagnostic work-up (Winter et al., 2021b). Moreover, by virtue of the mostly transient nature of SMART, it appears feasible to allocate sufficient time for careful clinico-radiographic observation prior to consideration of salvage antineoplastic treatment (Winter et al., 2021b). Finally, our study adds to previous descriptions of SMART as a unique late-delayed radiation-related syndrome with typical clinical presentation and pathognomonic MR imaging findings, recognition of which is

paramount in (neuro-)oncological patients with a remote history of prior cranial RT (Winter et al., 2021b).

5.3 Future perspectives

The incidence and spectrum of treatment-related neurotoxicity are expected to increase in the setting of a growing armamentarium of novel antineoplastic therapies and continual improvements in patient survivorship (Dietrich, 2020; Dietrich et al., 2017). Timely and focused research strategies are pivotal to address current and future clinical demands related to effective diagnosis and management of these conditions in neuro-oncological patients (Winter et al., 2019). At the same time, more emphasis must be placed on rigorous documentation, characterization, and integrated analysis of treatment-related effects across the neuro-oncological care trajectory, not least to ensure sufficient availability of dependable clinical data (Winter et al., 2019). Our analyses in neuro-oncological patients with PP, TN, and SMART demonstrate that holistic characterization of these challenging conditions is feasible, of significant clinical utility, and paramount to constructively inform future work in the field.

In the case of PP and TN, further biopsy-controlled studies are warranted to address important questions pertaining to the identification of robust histopathological criteria and targetable pathomechanisms for either condition (Winter et al., 2020b). Additionally, greater knowledge of putative risk factors may enable identification of “high risk” patients and/or clinical scenarios that predispose to PP/TN development (Winter et al., 2019). Similarly, in patients with TN, identification of biomarkers predictive of a progressive versus transient lesion behavior would greatly facilitate decision-making regarding therapeutic intervention. Future work should also evaluate the prognostic significance of PP and TN development in neuro-oncological patients (Winter et al., 2020b). Finally, recognition of PP and TN as distinct treatment-related conditions and classification based on evidence-based clinical definitions should be considered. In addition, greater knowledge of the unique radiographic features of PP and TN lesions may help refine current response assessment (RANO) criteria to foster accuracy in clinical trial enrolment and outcome interpretation in neuro-oncology (Winter et al., 2020b, 2019).

In the case of SMART, there remains a paucity of dependable clinical information (less than 50 published cases) given the nature of this relatively rare, diagnostically challenging, and likely underrecognized treatment-related condition (Winter et al., 2021b). Our findings in 7 patients with SMART support previous descriptions of the condition and identified a typical clinical presentation with universal presence of pathognomonic imaging abnormalities in affected patients. Additionally, we found that impaired cerebral autoregulation with resultant region cerebral hyperperfusion appears to be a putative pathomechanism driving SMART development (Winter et al., 2021b). Further research into the unique abnormalities observed on structural and functional neuroimaging is warranted to improve differentiation from other, more common pathologies, without the need for tissue biopsy. In addition, a better understanding of implicated, targetable pathomechanisms is expected to improve both clinical management and outcome in patients with SMART.

Beyond the disease-mimicking forms of treatment-related conditions addressed in this thesis, other areas in need of further research include emerging forms of neurotoxicity related to novel cancer immunotherapies (Winter et al., 2020a), antineoplastic agents (Brandes et al., 2015; Jeyaretna et al., 2011; Vaios et al., 2020) and targeted therapies (Chukwueke et al., 2019; Wick et al., 2016). In particular, combinations of these novel therapies with conventional antineoplastic treatment may further complicate accurate imaging-based response assessment and aggravate neurotoxic effects, with potentially unforeseen neurologic complications (Huang et al., 2015; Winter et al., 2021c).

6. References

Ahluwalia, M., Barnett, G.H., Deng, D., Tatter, S.B., Laxton, A.W., Mohammadi, A.M., Leuthardt, E., Chamoun, R., Judy, K., Asher, A., Essig, M., Dietrich, J., Chiang, V.L., 2018. Laser ablation after stereotactic radiosurgery: a multicenter prospective study in patients with metastatic brain tumors and radiation necrosis. J. Neurosurg. 1–8.

Alexiou, G.A., Tsiouris, S., Kyritsis, A.P., Voulgaris, S., Argyropoulou, M.I., Fotopoulos, A.D., 2009. Glioma recurrence versus radiation necrosis: accuracy of current imaging modalities. J. Neurooncol. 95, 1–11.

Biju, R.D., Dower, A., Moon, B.G., Gan, P., 2020. Smart (Stroke-like migraine attacks after radiation therapy) syndrome: A case study with imaging supporting the theory of vascular dysfunction. Am. J. Case Rep. 21, e921795-1.

Black, D.F., Bartleson, J.D., Bell, M.L., Lachance, D.H., 2006. SMART: Stroke-like migraine attacks after radiation therapy. Cephalalgia 26, 1137–1142.

Black, D.F., Morris, J.M., Lindell, E.P., Krecke, K.N., Worrell, G.A., Bartleson, J.D., Lachance, D.H., 2013. Stroke-like migraine attacks after radiation therapy (SMART) syndrome is not always completely reversible: A case series. Am. J. Neuroradiol. 34, 2298–2303.

Brandes, A.A., Bartolotti, M., Tosoni, A., Poggi, R., Franceschi, E., 2015. Practical management of bevacizumab-related toxicities in glioblastoma. Oncologist 20, 166–75.

Brandes, A.A., Franceschi, E., Tosoni, A., Blatt, V., Pession, A., Tallini, G., Bertorelle, R., Bartolini, S., Calbucci, F., Andreoli, A., Frezza, G., Leonardi, M., Spagnolli, F., Ermani, M., 2008. *MGMT* Promoter Methylation Status Can Predict the Incidence and Outcome of Pseudoprogression After Concomitant Radiochemotherapy in Newly Diagnosed Glioblastoma Patients. J. Clin. Oncol. 26, 2192–2197.

Brandsma, D., Stalpers, L., Taal, W., Sminia, P., van den Bent, M.J., 2008. Clinical features, mechanisms, and management of pseudoprogression in malignant gliomas. Lancet. Oncol. 9, 453–61.

Campen, C.J., Kranick, S.M., Kasner, S.E., Kessler, S.K., Zimmerman, R.A., Lustig, R., Phillips, P.C., Storm, P.B., Smith, S.E., Ichord, R., Fisher, M.J., 2012. Cranial irradiation increases risk of stroke in pediatric brain tumor survivors. Stroke 43, 3035–3040.

Chamberlain, M.C., Glantz, M.J., Chalmers, L., Van Horn, A., Sloan, A.E., 2007. Early necrosis following concurrent Temodar and radiotherapy in patients with glioblastoma. J. Neurooncol. 82, 81–83.

Chi, D., Behin, A., Delattre, J.-Y., 2008. Neurologic complications of radiation therapy. In: Schiff, D., Kesari, S., Wen, P. (Eds.), Cancer Neurology in Clinical Practice. Humana Press; New Jersey, pp. 259–286.

Chukwueke, U.N., Lee, E.Q., Wen, P.Y., 2019. Neurological complications of targeted therapies. In: Central Nervous System Metastases. Springer International Publishing, pp.

341–363.

Chukwueke, U.N., Lee, E.Q., Wen, P.Y., 2020. Neurological Complications of Immune-Based Therapies. In: Ahluwalia, M., Metellus, P., Soffietti, R. (Eds.), Central Nervous System Metastases. Springer International Publishing, Cham, pp. 365–372.

Dequesada, I.M., Quisling, R.G., Yachnis, A., Friedman, W.A., 2008. Can standard magnetic resonance imaging reliably distinguish recurrent tumor from radiation necrosis after radiosurgery for brain metastases? A radiographic-pathological study. Neurosurgery 63, 898–904.

Dietrich, J., 2010. Chemotherapy associated central nervous system damage. Adv. Exp. Med. Biol. 678, 77–85.

Dietrich, J., 2020. Neurotoxicity of Cancer Therapies. Contin. Lifelong Learn. Neurol. 26, 1646–1672.

Dietrich, J., Klein, J.P., 2014. Imaging of Cancer Therapy–Induced Central Nervous System Toxicity. Neurol. Clin. 32, 147–157.

Dietrich, J., Norden, A.D., Wen, P.Y., 2008. Emerging antiangiogenic treatments for gliomas - efficacy and safety issues. Curr. Opin. Neurol. 21, 736–44.

Dietrich, J., Winter, S.F., Klein, J., 2017. Neuroimaging of Brain Tumors: Pseudoprogression, Pseudoresponse, and Delayed Effects of Chemotherapy and Radiation. Semin. Neurol. 37, 589–596.

Dietrich, J., Winter, S.F., Parsons, M.W., 2019. Delayed Neurologic Complications of Brain Tumor Therapy. In: Tonn, J.-C., Reardon, D.A., Rutka, J.T., Westphal, M. (Eds.), Oncology of CNS Tumors. Springer International Publishing, Cham, pp. 751–767.

Dworkin, M., Mehan, W., Niemierko, A., Kamran, S.C., Lamba, N., Dietrich, J., Martinez-Lage, M., Oh, K.S., Batchelor, T.T., Wen, P.Y., Loeffler, J.S., Shih, H.A., 2019. Increase of pseudoprogression and other treatment related effects in low-grade glioma patients treated with proton radiation and temozolomide. J. Neurooncol. 142, 69–77.

Eisele, S.C., Dietrich, J., 2015. Cerebral radiation necrosis: diagnostic challenge and clinical management. Rev. Neurol. 61, 225–32.

Ellingson, B.M., Chung, C., Pope, W.B., Boxerman, J.L., Kaufmann, T.J., 2017. Pseudoprogression, radionecrosis, inflammation or true tumor progression? challenges associated with glioblastoma response assessment in an evolving therapeutic landscape. J. Neurooncol.

Fan, E.P., Heiber, G., Gerard, E.E., Schuele, S., 2018. Stroke-like migraine attacks after radiation therapy: A misnomer? Epilepsia 59, 259–268.

Fink, J., Born, D., Chamberlain, M.C., 2012. Radiation Necrosis: Relevance with Respect to Treatment of Primary and Secondary Brain Tumors. Curr. Neurol. Neurosci. Rep. 12, 276–285.

Furuse, M., Nonoguchi, N., Kawabata, S., Miyatake, S.-I., Kuroiwa, T., 2015. Delayed brain

radiation necrosis: pathological review and new molecular targets for treatment. Med. Mol. Morphol. 48, 183–190.

Gerstner, E.R., Yip, S., Wang, D.L., Louis, D.N., Iafrate, A.J., Batchelor, T.T., 2009. MGMT methylation is a prognostic biomarker in elderly patients with newly diagnosed glioblastoma. Neurology.

Giglio, P., Gilbert, M.R., 2003. Cerebral Radiation Necrosis. Neurologist 9, 180–188.

Huang, R.Y., Neagu, M.R., Reardon, D.A., Wen, P.Y., 2015. Pitfalls in the neuroimaging of glioblastoma in the era of antiangiogenic and immuno/targeted therapy - detecting illusive disease, defining response. Front. Neurol.

Huehnchen, P., Van Kampen, A., Boehmerle, W., Endres, M., 2020. Cognitive impairment after cytotoxic chemotherapy. Neuro-Oncology Pract. 7, 11–21.

Jain, R., Narang, J., Sundgren, P.M., Hearshen, D., Saksena, S., Rock, J.P., Gutierrez, J., Mikkelsen, T., 2010. Treatment induced necrosis versus recurrent/progressing brain tumor: going beyond the boundaries of conventional morphologic imaging. J. Neurooncol. 100, 17–29.

Jeyaretna, D.S., Curry, W.T., Batchelor, T.T., Stemmer-Rachamimov, A., Plotkin, S.R., 2011. Exacerbation of cerebral radiation necrosis by bevacizumab. J. Clin. Oncol. 29, e159-62.

Kerklaan, J.P., Lycklama Á Nijeholt, G.J., Wiggenraad, R.G.J., Berghuis, B., Postma, T.J., Taphoorn, M.J.B., 2011. SMART syndrome: A late reversible complication after radiation therapy for brain tumours. J. Neurol. 258, 1098–1104.

Kruser, T.J., Mehta, M.P., Robins, H.I., 2013. Pseudoprogression after glioma therapy: a comprehensive review. Expert Rev. Neurother. 13.

Kucharczyk, M.J., Parpia, S., Whitton, A., Greenspoon, J.N., 2017. Evaluation of pseudoprogression in patients with glioblastoma. Neuro-Oncology Pract. 4, 128–134.

Kumar, A.J., Leeds, N.E., Fuller, G.N., Van Tassel, P., Maor, M.H., Sawaya, R.E., Levin, V.A., 2000. Malignant Gliomas: MR Imaging Spectrum of Radiation Therapy- and Chemotherapy-induced Necrosis of the Brain after Treatment. Radiology 217, 377–384.

Langen, K.-J., Galldiks, N., Hattingen, E., Shah, N.J., 2017. Advances in neuro-oncology imaging. Nat. Rev. Neurol. 13, 279–289.

Li, H., Li, J., Cheng, G., Zhang, J., Li, X., 2016. IDH mutation and MGMT promoter methylation are associated with the pseudoprogression and improved prognosis of glioblastoma multiforme patients who have undergone concurrent and adjuvant temozolomide-based chemoradiotherapy. Clin. Neurol. Neurosurg. 151, 31–36.

Loebel, F., Winter, S.F., Onken, J., Cahill, D., Koch, A., Dietrich, J., 2017. PATH-18. MOLECULAR AND GENETIC ANALYSIS IDENTIFIES IDH MUTATION AS A KEY FACTOR OF LONG-TERM SURVIVAL IN GLIOBLASTOMA PATIENTS. Neuro. Oncol. 19, vi174–vi174.

Lubelski, D., Abdullah, K.G., Weil, R.J., Marko, N.F., 2013. Bevacizumab for radiation necrosis following treatment of high grade glioma: a systematic review of the literature. J. Neurooncol. 115, 317–22.

McPherson, C.M., Warnick, R.E., 2004. Results of contemporary surgical management of radiation necrosis using frameless stereotaxis and intraoperative magnetic resonance imaging. J. Neurooncol. 68, 41–7.

Minniti, G., Clarke, E., Lanzetta, G., Osti, M., Trasimeni, G., Bozzao, A., Romano, A., Enrici, R., 2011. Stereotactic radiosurgery for brain metastases: analysis of outcome and risk of brain radionecrosis. Radiat. Oncol. 6, 48.

Motegi, H., Kamoshima, Y., Terasaka, S., Kobayashi, H., Yamaguchi, S., Tanino, M., Murata, J., Houkin, K., 2013. IDH1 mutation as a potential novel biomarker for distinguishing pseudoprogression from true progression in patients with glioblastoma treated with temozolomide and radiotherapy. Brain Tumor Pathol. 30, 67–72.

Nobusawa, S., Watanabe, T., Kleihues, P., Ohgaki, H., 2009. IDH1 mutations as molecular signature and predictive factor of secondary glioblastomas. Clin. Cancer Res. 15, 6002–6007.

Olsen, A.L., Miller, J.J., Bhattacharyya, S., Voinescu, P.E., Klein, J.P., 2016. Cerebral perfusion in stroke-like migraine attacks after radiation therapy syndrome. Neurology 86, 787–789.

Perry, A., Schmidt, R.E., 2006. Cancer therapy-associated CNS neuropathology: an update and review of the literature. Acta Neuropathol. 111, 197–212.

Rahmathulla, G., Marko, N.F., Weil, R.J., 2013. Cerebral radiation necrosis: A review of the pathobiology, diagnosis and management considerations. J. Clin. Neurosci. 20, 485–502.

Rivera, A.L., Pelloski, C.E., Gilbert, M.R., Colman, H., De La Cruz, C., Sulman, E.P., Bekele, B.N., Aldape, K.D., 2010. MGMT promoter methylation is predictive of response to radiotherapy and prognostic in the absence of adjuvant alkylating chemotherapy for glioblastoma. Neuro. Oncol.

Roongpiboonsopit, D., Kuijf, H.J., Charidimou, A., Xiong, L., Vashkevich, A., Martinez-Ramirez, S., Shih, H.A., Gill, C.M., Viswanathan, A., Dietrich, J., 2017. Evolution of cerebral microbleeds after cranial irradiation in medulloblastoma patients. Neurology 88, 789–796.

Sanghera, P., Rampling, R., Haylock, B., Jefferies, S., McBain, C., Rees, J.H., Soh, C., Whittle, I.R., 2012. The Concepts, Diagnosis and Management of Early Imaging Changes after Therapy for Glioblastomas. Clin. Oncol. 24, 216–227.

Sanson, M., Marie, Y., Paris, S., Idbaih, A., Laffaire, J., Ducray, F., Hallani, S. El, Boisselier, B., Mokhtari, K., Hoang-Xuan, K., Delattre, J.Y., 2009. Isocitrate dehydrogenase 1 codon 132 mutation is an important prognostic biomarker in gliomas. J. Clin. Oncol. 27, 4150–4154.

Santomasso, B.D., 2020. Anticancer Drugs and the Nervous System. Contin. Lifelong Learn.

Neurol. 26, 732–764.

Shaw, P.J., Bates, D., 1984. Conservative treatment of delayed cerebral radiation necrosis. J. Neurol. Neurosurg. Psychiatry 47, 1338–41.

Shuper, A., Packer, R.J., Vezina, L.G., Nicholson, H.S., Lafond, D., 1995. `complicated migraine-like episodes' in children following cranial irradiation and chemotherapy. Neurology 45, 1837–1840.

Stupp, R., Mason, W.P., van den Bent, M.J., Weller, M., Fisher, B., Taphoorn, M.J.B., Belanger, K., Brandes, A.A., Marosi, C., Bogdahn, U., Curschmann, J., Janzer, R.C., Ludwin, S.K., Gorlia, T., Allgeier, A., Lacombe, D., Cairncross, J.G., Eisenhauer, E., Mirimanoff, R.O., 2005. Radiotherapy plus Concomitant and Adjuvant Temozolomide for Glioblastoma. N. Engl. J. Med. 352, 987–996.

Taal, W., Brandsma, D., De Bruin, H.G., Bromberg, J.E., Swaak-Kragten, A.T., Sillevis Smitt, P.A.E., Van Es, C.A., Van Den Bent, M.J., 2008. Incidence of early pseudo-progression in a cohort of malignant glioma patients treated with chemoirradiation with temozolomide. Cancer 113, 405–410.

Thust, S.C., van den Bent, M.J., Smits, M., 2018. Pseudoprogression of brain tumors. J. Magn. Reson. Imaging 48, 571–589.

Tofilon, P.J., Fike, J.R., 2000. The radioresponse of the central nervous system: a dynamic process. Radiat. Res. 153, 357–70.

Vaios, E.J., Winter, S.F., Muzikansky, A., Nahed, B. V, Dietrich, J., 2020. Eosinophil and lymphocyte counts predict bevacizumab response and survival in recurrent glioblastoma. Neuro-Oncology Adv. 2, 1–11.

van West, S.E., de Bruin, H.G., van de Langerijt, B., Swaak-Kragten, A.T., van den Bent, M.J., Taal, W., 2017. Incidence of pseudoprogression in low-grade gliomas treated with radiotherapy. Neuro. Oncol. 19, 719–725.

Verma, N., Cowperthwaite, M.C., Burnett, M.G., Markey, M.K., 2013. Differentiating tumor recurrence from treatment necrosis: A review of neuro-oncologic imaging strategies. Neuro. Oncol.

Wick, W., Hertenstein, A., Platten, M., 2016. Neurological sequelae of cancer immunotherapies and targeted therapies. Lancet Oncol.

Wick, W., Meisner, C., Hentschel, B., Platten, M., Schilling, A., Wiestler, B., Sabel, M.C., Koeppen, S., Ketter, R., Weiler, M., Tabatabai, G., Von Deimling, A., Gramatzki, D., Westphal, M., Schackert, G., Loeffler, M., Simon, M., Reifenberger, G., Weller, M., 2013. Prognostic or predictive value of MGMT promoter methylation in gliomas depends on IDH1 mutation. Neurology.

Winter, S.F., Forst, D.A., Oakley, D.H., Batchelor, T.T., Dietrich, J., 2021a. Intracranial Foreign Body Granuloma Mimicking Brain Tumor Recurrence: A Case Series. Oncologist 26, e893–e897.

Winter, S.F., Klein, J.P., Vaios, E.J., Karschnia, P., Lee, E.Q., Shih, H.A., Loebel, F.,

Dietrich, J., 2021b. Clinical presentation and management of SMART syndrome. Neurology (in press), 10.1212/WNL.0000000000012150.

Winter, S.F., Loebel, F., Loeffler, J., Batchelor, T.T., Martinez-Lage, M., Vajkoczy, P., Dietrich, J., 2019. Treatment-induced brain tissue necrosis: A clinical challenge in neuro-oncology. Neuro. Oncol. 21.

Winter, S.F., Martinez-Lage, M., Clement, N.F., Hochberg, E.P., Dietrich, J., 2021c. Fatal neurotoxicity after chimeric antigen receptor T-cell therapy: An unexpected case of fludarabine-associated progressive leukoencephalopathy. Eur. J. Cancer 144, 178–181.

Winter, S.F., Vaios, E.J., Dietrich, J., 2020a. Central nervous system injury from novel cancer immunotherapies. Curr. Opin. Neurol.

Winter, S.F., Vaios, E.J., Muzikansky, A., Martinez-Lage, M., Bussière, M.R., Shih, H.A., Loeffler, J., Karschnia, P., Loebel, F., Vajkoczy, P., Dietrich, J., 2020b. Defining Treatment-Related Adverse Effects in Patients with Glioma: Distinctive Features of Pseudoprogression and Treatment-Induced Necrosis. Oncologist 25, e1221–e1232.

Yang, I., Aghi, M.K., 2009. New advances that enable identification of glioblastoma recurrence. Nat. Rev. Clin. Oncol. 6, 648–57.

II. Affidavit

1. Statutory Declaration

"I, **Sebastian Friedrich Winter**, by personally signing this document in lieu of an oath, hereby affirm that I prepared the submitted dissertation on the topic ***Characterization of cancer treatment-related neurotoxicity in patients with malignant glioma - Charakterisierung behandlungsbedingter Neurotoxizität bei Patienten mit malignen Gliomen***, independently and without the support of third parties, and that I used no other sources and aids than those stated.

All parts which are based on the publications or presentations of other authors, either in letter or in spirit, are specified as such in accordance with the citing guidelines. The sections on methodology (in particular regarding practical work, laboratory regulations, statistical processing) and results (in particular regarding figures, charts and tables) are exclusively my responsibility.

Furthermore, I declare that I have correctly marked all of the data, the analyses, and the conclusions generated from data obtained in collaboration with other persons, and that I have correctly marked my own contribution and the contributions of other persons (cf. declaration of contribution). I have correctly marked all texts or parts of texts that were generated in collaboration with other persons.

My contributions to any publications to this dissertation correspond to those stated in the below joint declaration made together with the supervisor. All publications created within the scope of the dissertation comply with the guidelines of the ICMJE (International Committee of Medical Journal Editors; www.icmje.org) on authorship. In addition, I declare that I shall comply with the regulations of Charité – Universitätsmedizin Berlin on ensuring good scientific practice.

I declare that I have not yet submitted this dissertation in identical or similar form to another Faculty.

The significance of this statutory declaration and the consequences of a false statutory declaration under criminal law (Sections 156, 161 of the German Criminal Code) are known to me."

Date Signature

2. Declaration of own contribution to the publications

As sole first author, Sebastian Friedrich Winter contributed the following to the below listed publications (**Publications 1 – 3**):

Publication 1:

Winter, S.F., Loebel, F., Loeffler, J., Batchelor, T.T., Martinez-Lage, M., Vajkoczy, P. and Dietrich, J. Treatment-induced brain tissue necrosis: a clinical challenge in neuro-oncology. ***Neuro-oncology***, **2019**; *21*(9), pp.1118-1130.
Impact factor 2019: ***10.247***
Awarded Editor's Choice, September 2019 Issue

Contribution:

Concept & design:
- Substantial involvement prior to and during conduction of research

Literature research & data collection:
- Conducted 100% of the literature research and selection of relevant studies
- Collected 100% of primary patient data presented in Figure 2 (patient case)

Analysis & interpretation of relevant literature:
- Majority contribution (>90%) to analysis, interpretation, and systematic review of all included studies
- Identification of existing knowledge gaps and conceptualization of proposed strategies to advance the field

Manuscript writing:
- Structure, outline, and first full draft of the manuscript
- Design and creation of all (100%) figures and tables
- Drafting the final version of the manuscript
- Submission to journal and completion of revisions following peer-review

Publication 2 (selected *Top-Journal Publication*):

Winter, S.F., Vaios, E.J., Muzikansky, A., Martinez-Lage, M., Bussière, M.R., Shih, H.A., Loeffler, J., Karschnia, P., Loebel, F., Vajkoczy, P. and Dietrich, J. Defining Treatment-Related Adverse Effects in Patients with Glioma: Distinctive Features of Pseudoprogression and Treatment-Induced Necrosis. ***The Oncologist***, **2020**; *25*(8): e1221–e1232.
Impact factor 2020: ***5.260***

Contribution:

Concept & design:
- Substantial involvement prior to and during conduction of research

Collection & assembly of data:
- Full (100%) collection of demographic, clinical, radiographic, radiotherapy-specific, and histopathological data in all (n=60) patients
- Full radiographic evaluation of all (100%) ROIs (n= 137)
- Design, assembly, curation, and encoding of primary dataset

Data analysis & interpretation:
- Majority (80%) contribution to analysis and interpretation of all collected demographic, clinical, imaging, radiotherapy-related, and histopathological data
- Substantial (>50%) contribution to statistical analysis and interpretation

Manuscript writing:
- Structure, outline, and first full draft of the manuscript
- Design and creation of all (100%) figures and tables
- Drafting the final version of the manuscript
- Submission to journal and completion of revisions following peer-review
- Author co-correspondence for publication

Publication 3:

Winter, S.F., Klein, J.P., Vaios, E.J., Karschnia, P., Lee, E.Q., Shih, H.A., Loebel, F., and Dietrich, J. Clinical presentation and management of SMART syndrome. ***Neurology*, 2021 (published ahead of print)**
Impact factor 2019: ***8.770***

Contribution:

Concept & design:
- Substantial involvement prior to and during conduction of research

Collection & assembly of data:
- Majority (90%) collection of demographic, clinical, radiographic, and treatment-related data based on chart review
- Full (100%) design, assembly, and curation of primary dataset

Data analysis & interpretation:
- Majority (80%) contribution to analysis (including descriptive statistics) and interpretation of all collected demographic, clinical, and imaging data
- Contextualization with the current state of research in the field

Manuscript writing:
- Structure, outline, and first full draft of the manuscript
- Design and creation of all (100%) figures and tables
- Drafting the final version of the manuscript
- Submission to journal and completion of revisions following peer-review
- Author co-correspondence for publication

Signature of doctoral candidate

III. Selected Publications

1. Publication 1 – Winter et al., 2019, Neuro-Oncology

Winter, S.F., Loebel, F., Loeffler, J., Batchelor, T.T., Martinez-Lage, M., Vajkoczy, P. and Dietrich, J., 2019. Treatment-induced brain tissue necrosis: a clinical challenge in neuro-oncology. ***Neuro-oncology***, *21*(9), pp.1118-1130.
Impact factor 2019: ***10.247***
Editor's Choice, September 2019 Issue

Journal Data Filtered By: **Selected JCR Year: 2019** Selected Editions: SCIE,SSCI
Selected Categories: **"CLINICAL NEUROLOGY"** Selected Category Scheme: WoS
Gesamtanzahl: 204 Journale

Rank	Full Journal Title	Total Cites	Journal Impact Factor	Eigenfactor Score
1	LANCET NEUROLOGY	33,050	30.039	0.062420
2	Nature Reviews Neurology	11,029	27.000	0.028770
3	Alzheimers & Dementia	16,289	17.127	0.042180
4	ACTA NEUROPATHOLOGICA	21,908	14.251	0.040740
5	JAMA Neurology	10,471	13.608	0.043110
6	BRAIN	53,282	11.337	0.067050
7	NEURO-ONCOLOGY	12,950	10.247	0.029050
8	SLEEP MEDICINE REVIEWS	8,077	9.613	0.013000
9	ANNALS OF NEUROLOGY	37,304	9.037	0.044120
10	NEUROLOGY	90,213	8.770	0.103530
11	MOVEMENT DISORDERS	27,638	8.679	0.031140
12	JOURNAL OF NEUROLOGY NEUROSURGERY AND PSYCHIATRY	30,621	8.234	0.028510
13	Neurology-Neuroimmunology & Neuroinflammation	2,232	7.724	0.008400
14	NEUROPATHOLOGY AND APPLIED NEUROBIOLOGY	3,992	7.500	0.005960
15	Journal of Stroke	1,247	7.470	0.004240
16	STROKE	66,466	7.190	0.078010
17	Brain Stimulation	6,537	6.565	0.015580
18	NEUROSCIENTIST	5,188	6.500	0.007220
19	Alzheimers Research & Therapy	3,876	6.116	0.011650
20	EPILEPSIA	26,560	6.040	0.029790

1118

Neuro-Oncology

21(9), 1118–1130, 2019 | doi:10.1093/neuonc/noz048 | Advance Access date 4 March 2019

Treatment-induced brain tissue necrosis: a clinical challenge in neuro-oncology

Sebastian F. Winter, Franziska Loebel, Jay Loeffler, Tracy T. Batchelor, Maria Martinez-Lage, Peter Vajkoczy, and Jorg Dietrich

MGH Cancer Center, Massachusetts General Hospital, Harvard Medical School, Boston, Massachusetts, USA (S.F.W., T.T.B., J.D.); Department of Neurology, Massachusetts General Hospital, Harvard Medical School, Boston, Massachusetts, USA (S.F.W., T.T.B., J.D.); Department of Neurosurgery, Charité–Universitätsmedizin Berlin, corporate member of Freie Universität Berlin, Humboldt-Universität zu Berlin, and Berlin Institute of Health, Berlin, Germany (S.F.W., F.L., P.V.); Department of Radiation Oncology, Massachusetts General Hospital, Harvard Medical School, Boston, Massachusetts, USA (J.L.); C S Kubik Laboratory for Neuropathology, Massachusetts General Hospital and Harvard Medical School, Boston, Massachusetts, USA (M.M-L.)

Corresponding Author: Jorg Dietrich, MD, PhD, Department of Neurology, Massachusetts General Hospital, Harvard Medical School, 55 Fruit Street, Yawkey 9E, Boston, MA 02114, USA (Dietrich.Jorg@mgh.harvard.edu).

Abstract

Cancer therapy-induced adverse effects on the brain are a major challenge in neuro-oncology. Brain tissue necrosis (treatment necrosis [TN]) as a consequence of brain directed cancer therapy remains an insufficiently characterized condition with diagnostic and therapeutic difficulties and is frequently associated with significant patient morbidity.

A better understanding of the underlying mechanisms, improvement of diagnostic tools, development of preventive strategies, and implementation of evidence-based therapeutic practices are pivotal to improve patient management. In this comprehensive review, we address existing challenges associated with current TN-related clinical and research practices and highlight unanswered questions and areas in need of further research with the ultimate goal to improve management of patients affected by this important neuro-oncological condition.

Keywords

complications | malignant glioma | radiation necrosis | treatment effects | treatment necrosis

Cancer treatment-related effects on the central nervous system remain a challenging issue in neuro-oncology.[1,2] Specifically, treatment-induced brain tissue necrosis (treatment necrosis [TN]), perhaps inappropriately referred to as "radiation necrosis," continues to be a challenge for clinical management and can be a significant cause of patient morbidity and even mortality.[3–6] Radiographic and clinical presentation of TN is usually indistinguishable from those of residual/recurrent tumor (progressive disease [PD]), causing a major dilemma in patient management. Establishing a reliable diagnosis based on clinical assessment and conventional MRI is difficult, frequently necessitating a surgical tissue biopsy.[1,2,5,7] The pathophysiology of TN is complex and incompletely understood.[8,9] Depending on the location and extent of the necrotic lesion and the degree of associated mass effect, the condition's clinical course may be heterogeneous and unpredictable.[5] To date, no standard of care (SOC) for TN exists and treatment is mostly directed at controlling associated neurological symptoms.[5] Experimental therapies have shown mixed efficacy and await robust evidence-based assessment[5,10]; a consensus regarding best practices for efficient preventative, diagnostic, and therapeutic measures to manage TN has not yet been established.[5,11]

This review discusses diagnostic and therapeutic strategies directed at management of patients with TN, focusing on clinical pitfalls and research barriers that have precluded advancement of this field. Of note, the term "treatment (-induced) necrosis (TN)"[12–14] (unlike the conventional clinical term "radiation necrosis") reflects emerging knowledge of the mechanisms driving this condition. Specifically, existing studies point to a contribution of chemotherapeutic agents such as temozolomide (TMZ)[13] or tyrosine kinase inhibitors[15] and pre-existing comorbidities to the development of TN.

Treatment-Induced Necrosis: A Clinical Challenge

Our observations and those of others[1,2,5,12–14,16–22] suggest that numerous clinical and systemic factors complicate the understanding and management of TN, as summarized in Fig. 1. Addressing these challenges is essential to define risk factors and preventative strategies, reliable diagnostic and monitoring algorithms, and effective patient management practices.

Incidence and Clinical Relevance

TN constitutes a serious and relatively common treatment-related adverse effect, particularly since combined chemotherapy and radiation therapy (RT) with concurrent and sequential TMZ[23] was established as the SOC treatment for glioblastoma (GBM).[13,14,17] The exact incidence and prevalence of TN remains unknown; depending on the type of neoplastic lesion, treatment regimen, and data acquisition parameters, TN incidence ranges from 3–24%[9,24] or 5–50%.[8,25] For high-grade glioma patients, Ruben et al reported a 4.9% incidence of TN following RT (± adjuvant chemotherapy).[24] However, this study was not fully biopsy-controlled and patient data derived from an era before standard chemo-RT[23] was implemented. Since then, Chamberlain et al[13] found a 14% incidence of biopsy-confirmed TN in TMZ-based chemo-RT treated GBM patients, supporting the notion that the incidence with combined chemo-RT may be higher. Any improvement of patient overall survival (OS) with use of novel anti-neoplastic treatments will likely be associated with an increase in TN manifestation.[4] Moreover, the incidence and severity of TN is influenced by the choice of treatment modality, including targeted therapies, immunotherapies, anti-angiogenic therapies, and concurrent steroid use. For instance, TN incidences may be higher in patients treated for brain metastasis with tyrosine kinase inhibitors[15] and lower in those concurrently treated with corticosteroids[26] and anti-angiogenic therapies.[27,28] Whether immune checkpoint inhibitors may increase the risk of TN in patients with metastatic brain cancer has been discussed controversially.[29,30]

Risk Factors and Prevention

Prevention of TN is limited by an incomplete understanding of risk factors and a lack of efficacious neuroprotective strategies. Apart from anti-neoplastic treatment parameters, such as RT type (eg, brachytherapy, stereotactic radiosurgery) and radiation modality (proton vs photon radiation), radiation dose, -volume, -fraction size and/or hyperfractionation regimen, and use of concurrent and/or adjuvant chemotherapy, other potential risk factors for TN include patient age, survival time, and vascular comorbidities.[7,10,14,24,31–34] However, poor predictability and heterogeneity of TN suggest that additional yet unidentified risk factors are implicated.[35]

Radiographic Appearance and Spatiotemporal Pattern

Lacking a distinctive radiographic signature, TN is mostly indistinguishable from PD on conventional structural MRI.[2,7,14] As such, TN commonly occurs in close proximity to the original tumor location, usually appearing as a focal (or multiple) contrast enhancing nodule(s) with associated T2/fluid attenuated inversion recovery signal hyperintensity consistent with perilesional vasogenic edema[1,2,7] (Fig. 2). While thought to occur most commonly at the site of maximum radiation exposure (ie, adjacent to the tumor or surgical resection cavity),[7,14,17] a detailed correlative analysis of the spatial pattern of TN with the radiation field has, to our knowledge, not yet been carried out. Interestingly, solitary or multiple de novo necrotic lesions can also occur more remotely, on ipsilateral or even contralateral cerebral hemispheres.[7]

The periventricular white matter is considered a predilection site for TN, likely due to its high susceptibility to radiation-induced microvascular injury.[7,14,36] Some have observed a high frequency of corpus callosum involvement and subependymal expansion with TN as opposed to PD,[16,37] although the opposite was observed by others.[38] Further distinct MRI features of radionecrotic lesions, such as a "Swiss cheese" or "soap bubble"–like interior enhancement,[7] a "spreading wavefront" pattern of the lesion,[38] or a radiographic lesion quotient,[39] have been put forward. Despite these efforts, authoritative diagnosis of the condition based solely on conventional MRI has remained largely elusive.[14] Lastly, the frequent presence of "mixed" brain lesions, consisting of both TN and residual and/or recurrent (necrotic) tumor,[7,38,39] causes additional ambiguity on conventional MRI, making it a poor diagnostic tool for TN.

The temporal manifestation pattern of TN is highly variable.[5] While late-delayed radiation injury—predominantly manifesting as TN—frequently occurs within 12 months post-RT,[5,17,40] TN may develop months to many years after treatment, occasionally occurring up to a decade later.[3,41] Recent findings point to an increasing appearance of "early necrosis" developing within the first 6 months post-RT in those patients with glioma who receive standard chemo-RT, suggesting that concurrent TMZ may act as a radiosensitizing agent.[13] In this context, it has been hypothesized that (early) TN manifestation might serve as a predictive biomarker for a more durable treatment response.[13,17] This assumption should be interpreted with caution, as survival analyses carried out in patients with treatment-related effects are inherently reflective of a selected patient population with an implicit time bias, which needs to be accounted for.[36]

Finally, the distinction between different types of treatment-related effects is the subject of active clinical debate.[5] Apart from TN, other less severe and usually more transient types of treatment-related effects include acute and early-delayed radiation injury,[3,8,41] as well as pseudoprogression (PP).[1,14] While these entities are primarily distinguished by differences in temporal and clinical patterns, they are somewhat arbitrarily defined and may occasionally overlap, creating diagnostic ambiguities (Fig. 3).[5] In particular, the delineation between PP and TN has been complicated by semantic inconsistencies regarding the meaning of the term "pseudoprogression." PP likely

Clinical factors	Identified core issues
Risk factor profile	• Insufficient characterization; likely complex dynamic interplay between unknown predisposing *intrinsic* factors (patient clinical status, inherent genetic susceptibility, tumor entity & molecular-genetic factors) and partly identified *extrinsic* factors (treatment regimen).
Complex pathomechanisms	• Incomplete understanding of causal sequence of events and key targetable pathways/molecules driving & sustaining TN.[8,9]
Spatio-temporal radiographic pattern	• Incoherent terminology /arbitrary temporal distinction between pseudoprogression (PP), vs early-delayed radiation injury vs "early necrosis" vs TN. • Lack of spatial analyses correlating anatomical location of TN lesions with therapeutic radiation dose distribution and respective Rx dose exposure.
Mixed lesions	• Frequent manifestation of lesions containing both TN and residual or recurrent tumor and/or tumor necrosis.[7,38] Inability to distinguish between mixed entities on conventional MRI → pitfall for identifying correct biopsy targets, affecting diagnostic yield.
Diagnostic ambiguity *Radiographic*	• Inability to distinguish TN from PD on conventional MRI → no optimal advanced imaging modality → lack of robust imaging biomarkers → no consensus on preferred non-invasive diagnostic algorithm.[2,5,7] • Concomitant treatment with glucocorticoids, anti-angiogenics, or immune/targeted therapies may further complicate image interpretation with conventional MRI.[10,21,42]
Clinical	• The clinical picture of TN frequently mimics that of PD.[5]
Histopathological	• No established histopathological classification criteria for TN or PP → final pathologic diagnosis largely depends on pathologist's experience and subjective impression. • Radiation induced cellular atypia in non-neoplastic cells may mimic intra-lesional infiltration by scattered tumor cells and these can be virtually indistinguishable.[6]
Clinical course	• Heterogenous, difficult to predict. • Symptomatic cases may further progress or deteriorate despite medical intervention, occasionally requiring surgeryto prevent fatal outcome.[2,5] • Lack of level I or II clinical evidence for currently available treatment options.
Systemic factors	**Identified core issues**
Prospective biopsy-controlled studies	• There is a paucity of both prospective and biopsy-controlled studies that assess the predictive value of advanced diagnostic imaging methods for TN.[19] • Conversely, routine biopsy of diagnostically ambiguous casescarries surgical risk, may curtail patients' quality of life (QoL), and is associated with increased costs.
Focused randomized controlled clinical trials (RCTs)	• Lack of RCTs with endpoints devoted to characterizing treatment effects. • Potential "treatment effect confounders" are insufficiently controlled for in past and ongoing clinical trials → pitfall to interpretation of efficacy of experimental anti-neoplastic agents.[13,21,22]
Functional imaging performance assessment	• Poor inter-study comparability of diagnostic performance of functional imaging modalities due to associated image-acquisition/processing standardization issues.[16]
Clinical feasibility of functional imaging	• No comprehensive availability of advanced imaging modalities in standard medical care facilities.[12] • Increased operating cost of scanners/equipment, lack of insurance coverage for advanced diagnostic procedures.[12] • Frequent diagnostic need to combine different modalities → increased cost and time
Response assessment criteria	• Insufficiency of current criteria in accounting for potential radiographic correlates of treatment effects in follow-up treatment response monitoring
Current diagnostic approach	• Risk of over-emphasis on radiologic findings → pitfall of excluding potentially important risk factors, antecedent events and clinical aspects that may corroborate or challenge a Dx of TN.

Fig. 1 Overview of clinical and systemic factors challenging the study and better understanding of TN. Dx = diagnosis; QoL = quality of life; Rx = radiation.

represents a unique, transient scenario in patients with high-grade glioma within the first 3 months of combined TMZ-based chemo-RT.[1] Recently, van West et al employed this term to describe late enhancing, treatment-related lesions (median onset 12 mo post-RT) they observed and characterized in patients with low-grade glioma.[36] Concluding that the delayed onset for these lesions differed clearly from the earlier timeframe for PP in patients with high-grade gliomas, the authors suggest that these lesions "could be small areas of radiation necrosis."[36]

Diagnostic Considerations

Defining a reliable diagnostic algorithm for accurate detection of TN has been hampered by its radiographic similarity to PD on conventional MRI[2,7] and frequent manifestation as a mixed pathology with recurrent or residual tumor.[7,39] Moreover, complex radiographic findings seen after combinatorial anti-angiogenic, cytotoxic, and immunotherapy regimens[21,42,43] compromise adequate MRI-based follow-up monitoring and characterization of treatment response with Macdonald and revised Response

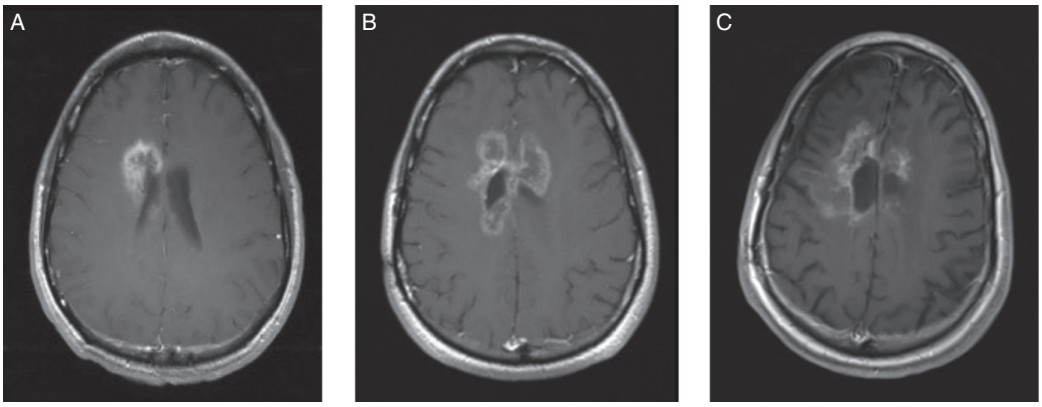

Fig. 2 Progressive treatment necrosis (A–C; T1-weighted gadolinium-enhanced axial MRI sequences). (A) A 35-year-old male with right frontal low-grade astrocytoma (World Health Organization grade II) underwent surgical resection followed by TMZ-based chemo-RT treatment. Eight months post-RT completion he developed headaches of increased frequency and was found to have a new nodular focus of enhancement in the right frontal lobe subjacent to the resection cavity, with periventricular and corpus callosum involvement, a biopsy of which revealed TN. (B) Sequential TMZ was resumed and completed over the next 6 months; however, the patient experienced worsening of his symptoms as the region of enhancement continued to expand. (C) Despite initiation of corticosteroid and bevacizumab treatment, he developed progressive left-sided hemiparesis and cognitive decline over the following 2 years, prompting a second biopsy of the continually enhancing lesion, which again confirmed TN. Therapeutic management of symptomatic TN was continued; however, the patient deteriorated further, necessitating a transfer to hospice care, where he eventually passed away 2 years after the second biopsy.

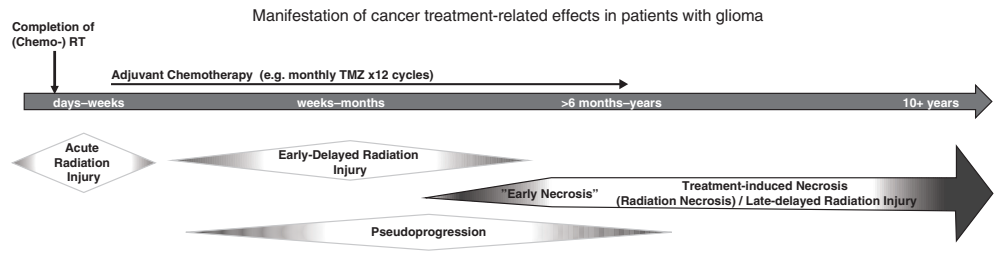

Fig. 3 Timeline schematic illustrating the temporal manifestation pattern and clinical course of cancer treatment–related effects. Acute and early-delayed types of radiation injury represent transient, reversible neurotoxic phenomena observed within days to weeks, and weeks to several months following chemo-RT.[41] By contrast, TN typically constitutes a late-delayed type of radiation injury observed >6 months post-RT with a frequently irreversible and progressive course[1]; however, concurrent TMZ-based chemo-RT may contribute to increasing incidences of "early necrosis."[13] Pseudoprogression (PP) likely represents a unique, transient, predominantly radiographic phenomenon encountered in patients with high-grade glioma within the first 3 months of combined TMZ-based chemo-RT.[1] Differentiation between these entities remains a clinical challenge.

Assessment in Neuro-Oncology (RANO) criteria.[44–46] While existing RANO criteria limit clinical trial enrollment to patients with radiographic PD in whom contrast enhancing lesions appear at or beyond 12 weeks post-RT,[46] treatment-related effects (especially TN) frequently manifest beyond this cutoff point (Fig. 3). Misdiagnosis of tumor progression could result in premature first-line treatment discontinuation and administration of a salvage treatment (which should have been withheld until true PD) or may delay a necessary treatment change in cases where treatment effects, such as PP or TN, are mistakenly assumed.[20,22,44] Furthermore, erroneous inclusion of misdiagnosed patients into clinical trials condones misinterpretation of the efficacy of any investigational agent.[13,21,22]

Beyond efforts to revise currently employed radiographic treatment response assessment criteria,[18,21] attempts to identify more accurate, clinically feasible diagnostic imaging biomarkers and, ultimately, enable a "virtual biopsy" of TN[1,12,17,40] have included the assessment of diffusion weighted[47] and diffusion tensor[48] MRI, MRI perfusion studies,[49–51] CT perfusion (CTP) studies,[52] MR spectroscopy (MRS),[53–55] positron emission tomography (PET),[56–59] single photon emission computed tomography (SPECT),[60] or combinations thereof.[55,61,62] Notwithstanding, histopathological evaluation remains the diagnostic gold standard,[5,11] albeit many of the aforementioned non-invasive technologies hold substantial additive value in complementing conventional MRI findings and improving diagnostic certainty in cases of suspected TN and when a surgical tissue biopsy is too risky or otherwise not feasible.[1,12,17,19,20,40] Further advantages include guidance for stereotactic biopsy procedures and more tailored, less neurotoxic radiation field mapping for radiotherapeutic interventions[16] (eg, via quantitative TN versus PD distinction within mixed lesions), identification of tumor "hot spots," and characterization of the degree of tumor infiltration into perilesional brain parenchyma. Techniques such as MRI-localized biopsies and radiographic-histopathological correlations (eg, via MR signal intensity to cell density correlation maps)[63] have addressed the challenges of tumor sampling resulting from the high degree of intratumoral heterogeneity and frequent presence of mixed pathology following anti-neoplastic treatment.

Several reviews have evaluated the growing body of literature on the role of advanced imaging in TN diagnosis.[12,16,19,20,40,64] Concluding that a preferred non-invasive diagnostic gold standard for TN is still lacking, several reports identify distinct strengths and weaknesses of various imaging modalities, and provide valuable recommendations for clinical practice and research design (Table 1). Methodological problems involve the lack of randomized controlled clinical trials, absence of histopathological verification of lesions identified by imaging, poorly matched patient groups, high variability in clinical practices at time of radiographic disease progression, and potential operator dependency in radiographic assessment.[12,19,20,64] Moreover, most studies investigate a single imaging modality, whereas combined use of multiple functional imaging modalities has become a common clinical reality with improved diagnostic accuracy.[12,20,55,62] Other difficulties relate to producing methodologically accurate meta-analyses of published data due to inconsistencies in defining TN[40] and unresolved standardization in image acquisition and processing.[16]

Most reviews emphasize a critical necessity for prospective, biopsy-controlled studies to improve the current body of evidence.[12,19,20,64] Moreover, widespread adoption of advanced imaging is difficult to achieve in clinical practice due to limited availability, high operational costs, and common lack of insurance coverage for such procedures.[12] Low spatial resolution of most techniques and limited utility for accurate longitudinal monitoring (due to standardization issues) are additional concerns.[16]

Recommendations on diagnostic imaging for TN versus PD distinction vary. Several groups endorse multivoxel MRS,[19,20,65] PET with novel amino acid based radiotracers,[19] (technetium-99) SPECT,[20,40] and CTP.[16,40] Conversely, routine diagnostic use of fluorodeoxyglucose (^{18}F-FDG) PET is discouraged due to its low specificity and poor signal-to-noise ratio.[20,40] Nevertheless, virtually all neuroimaging techniques were found to bear some specific disadvantages (see Table 1). Others have therefore advocated a multimodal diagnostic approach through the combined use of several techniques,[12] such as MRS with diffusion-weighted imaging (DWI),[55] or MRI combined with fluoro-ethyl-tyrosine (FET) PET and MRS.[62] The advent of hybrid PET-MRI[56] may facilitate such combinatorial approaches in becoming more clinically feasible and less time-consuming.[18] An interesting novel approach includes the use of delayed-contrast MRI to construct treatment response assessment maps (TRAMs) for differentiation of PD from treatment effects based on delayed contrast accumulation (nontumor tissues) versus contrast clearance (representing active tumor).[66] Histological validation demonstrated 100% sensitivity and 92% positive predictive value to active tumor of this approach, including adequate representation of tumor burden by TRAMs.

Blood-based biomarkers are increasingly explored for diagnosis and treatment response in neuro-oncology, including efforts to achieve liquid biopsy-based differentiation of treatment effects from PD, with technical limitations mainly pertaining to sensitivity issues.[67] One recent study investigated expression profile differences of myeloid-derived suppressor cells (MDSCs) as a potential biomarker for predicting recurrent GBM and differentiating it from TN.[68] While early results of this approach have been encouraging, potential diagnostic feasibility of the MDSC biomarker for lower-grade gliomas—where TN would be expected to occur even more frequently—remains to be established. The predictive value of this approach in the setting of "mixed lesions" remains unclear, as only TN lesions with <5% of active tumor were included.[68] Other previous efforts have investigated blood-derived microvesicles as a potential diagnostic biomarker for PD versus TN/PP differentiation in chemo-RT treated GBM patients with equivocal imaging findings.[69]

Finally, histopathological diagnosis and classification of biopsied lesions raises several challenges. Currently, no specific guidelines for histopathological characterization of treatment-induced brain tissue necrosis or other treatment-related effects exist; the final pathological diagnosis depends largely on the pathologist's professional

Table 1 Comprehensive overview of existing reviews assessing the diagnostic performance of different advanced imaging modalities for TN vs PD

Study/Type	No./Types of Studies Reviewed	Selected Notable Findings	Key Issues Identified	Overall Recommendations
Alexiou et al, (2009)[19] **- Systematic Review** **- Focus on value of MRI techniques, SPECT, PET to differentiate TN from glioma recurrence.**	46 clinical studies - 3 Class I, - 9 Class III, - and 34 Class IV evidence level studies	*DWI / MRS*: several Class III & IV studies. - 1 biopsy-controlled Class I study (Rock et al, 2004) showing MRS ratios (Cho/NAA, NAA/normal Cr and NAA/Cho) can reliably differentiate TN from PD. ADC values improved differentiation, but not in mixed lesions. *PET*: majority Class III & IV studies. - Accuracy of ^{18}F-FDG-PET hampered by high background signal; ranges of 62–100% sensitivity and 40–100% specificity in evaluated studies. - Novel PET tracers (^{11}C-MET, ^{18}F-FDOPA,[18] F-FET) with different advantage/disadvantage profiles, but potentially improved diagnostic sensitivity (75–100%) and specificity (75–100%). - 1 prospective biopsy-controlled study (Mehrkens et al, 2008) showed 84% pos. predictive value of ^{18}F-FET PET for detecting glioma recurrence.	- Majority of studies had ↓evidence levels - Many studies not biopsy-controlled - Mostly retrospective design - Unclear methodology in some studies	- Tentative recommendation to use multivoxel MRS and/or PET with newer radiotracers to detect true tumor recurrence - Recommendation to carry out prospective, biopsy-confirmed studies with higher evidence levels.
Jain et al, (2010)[16] **- Comprehensive Review** **- Discusses individual advantages, limitations, and clinical utility of functional neuro-imaging modalities in distinguishing between TN and PD.**	Unspecified number of key studies discussed: - Perfusion imaging studies - MRS studies - DWI/DTI studies - PET/SPECT studies	*Perfusion imaging*: limited performance in mixed lesions and in pat. receiving anti-angiogenic treatments. - Potential advantage of CTP over MR perfusion, due to relative ease to generate quantitative perfusion parametric maps through defined arterial input & venous output function. - CTP clinical utility limited by Rx exposure + iodinated contrast agent; MR perfusion easily obtainable as additional sequence to conventional Gd-MRI. - 1 biopsy-controlled CTP study showed 83.3% sensitivity / 100% specificity for TN vs PD detection (Jain et al, 2007) *MRS*: most studies lack biopsy-controls. - MRS metabolic ratios can reliably differentiate pure, but not mixed lesions with tissue heterogeneities below current spatial resolution (~1 cc). - Multivoxel > single voxel MRS for diagnostic performance (Chernov et al, 2005) - Longer scan times required to obtain reproducible data. *DWI*: Unresolved ongoing discussion on which lesion type (TN or PD) has higher ADC values. *PET / SPECT*: Overall more limited availability and ↓spatial resolution - ^{18}F-FDG-PET downsides: ↑background signal, potential false-negatives (LLGG appear hypometabolic) or false-positives (abscess or reactively inflamed TN lesions can appear hypermetabolic). - These challenges might be improved by employing novel amino acid tracers or combinations thereof with FDG, as well as co-registration of PET with structural MRI.	- Most techniques lack standardization of image acquisition & post-processing parameters → 1) difficulty to use as treatment response monitoring tool. 2) difficulty to conduct multicenter studies or compare different studies. - Most techniques have ↓resolution → difficulty for in vivo quantification of (particularly mixed) lesions.	- Advanced imaging can facilitate TN/PD distinction; however, clinical feasibility is still limited by several remaining issues. - Critical need for further development and greater clinical use of functional imaging biomarkers → conventional imaging is insufficient for radiographic characterization of effects produced by new and combinatorial treatment regimens
Caroline & Rosenthal (2012)[64] **- Systematic Review** **- Assesses efficacy of imaging modalities to distinguish between PP, TN, and PD (HGGs).**	26 clinical studies - 4 main groups of imaging modalities: MRI, PET, SPECT, and combinations thereof.	*MRI-based techniques*: - Conventional Gd-MRI and MRS appear to be more sensitive than specific. - MR perfusion using rCBF appears to be more specific than sensitive. - DWI and DTI appear to have similar accuracy (86.7% and 85.7%, respectively) in detecting PD *PET / SPECT*: - ^{201}Tl-SPECT may be more specific (100% specificity / 84–100% sensitivity range) than FDG or amino acid based PET tracers. - Combined MRI w/ ^{201}Tl-SPECT may have ↑sensitivity than combined MRI w/ ^{18}F-FDG-PET; using combinations of PET tracers may exceed the level of diagnostic accuracy reached by single tracers alone.	- Many included studies had small sample sizes or were not biopsy-controlled - Overall lack of prospective biopsy-controlled studies in the field	- No specific recommendations on preferred imaging techniques given - Advocated need for large, prospective, biopsy-controlled studies.

Table 1 *Continued*

Study/Type	No./Types of Studies Reviewed	Selected Notable Findings	Key Issues Identified	Overall Recommendations
Shah et al, (2013)[40] **- Systematic Review** **- Assesses case reports/ case series/prospective studies for efficacy of imaging modalities to distinguish TN from recurrent glioma.**	17 clinical studies - All selected studies included at least 1 case of histological confirmation.	- SPECT had the highest combined mean specificity (97.8%) out of the reviewed studies. Its mean sensitivity (87.6%) was comparable to that of conventional MRI, the most sensitive modality (88.9%) - MET-PET has ↑mean sensitivity and specificity (84.2% and 82.4%, respectively) than FDG-PET (70.1 and 64.8%, respectively). - CTP combined with a permeability surface air product (PS) yielded 100% sensitivity, 89% specificity in a biopsy-controlled cohort of 38 pat. (Jain et al, 2011)	*Limitations noted in own review:* - No differentiation between TN and PP made in analysis - Predominance of PD cases over TN cases → potential bias in sensitivity/ specificity values *Other identified issues:* - Potential operator dependency/ subjective bias in studies - Clinicians must ensure that technology is available and that neuroradiologists are familiar with it.	- SPECT, in particular Tc-99 SPECT, may be the modality of choice for diagnostic purposes. - CTP is recommended if maximal sensitivity for detection of PD is clinically desired. - MRI alone and ^{18}F-FDG-PET have low specificity and should be avoided.
Verma et al, (2013)[12] **- Comprehensive Review** **- Discusses efficacy and limitations of structural & functional imaging modalities in distinguishing TN from PD.**	Tabular analysis of: - 8 DWI /DTI studies (ADC and FA values) - 10 perfusion studies (MR or CT-based) - 14 MRS studies (MRS ratios) - 16 PET studies - 14 SPECT studies	*DWI/DTI:* Remains largely at exploratory stage, awaits thorough evaluation. - Measurements (esp. ADC values) affected by scanner type, magnetic field strength → difficult to establish standardized parameters and universal threshold values to differentiate TN from PD. - Effects of necrosis, gliosis, fibrous scar tissue, tissue granulation on ADC and FA values not well understood - Mean ADC and FA values easily skewed by mixed lesions. *Perfusion imaging:* Variable Pro/Con profile for each technique. DSC MR imaging potentially most clinically feasible. - DSC MRI: *Pros*- better SNR, shorter scan times, ease of use, better availability. *Cons*- prone to susceptibility artifacts → limited application in pat. w/ hemorrhages, calcifications, surgical clips. - DCE MRI: *Pros*- robust against susceptibility artefacts, ↑spatial resolution that better characterizes mixed lesions. *Cons*- complex/error prone hemodynamic parameter quantification → no FDA-approved standardized software exists. - CTP: *Pros*- technology widely available, no magnetic susceptibility artefacts, parameter quantification linear and less error prone. *Cons*- ↓clinical feasibility than MRI → toxicity (ionizing radiation, iodinated contrast agents), ↓resolution, image acquisition and processing less flexible. *MRS:* Multivoxel MR measuring abnormal spectra beyond the contrast-enhanced area could help detect extent of perilesional tumor infiltration → potential for improved radiation field mapping/ reduction of TN risk. - Frequent tissue necrosis in PD may metabolically mimic TN (↑lipid and ↑lactate levels) - Prone to ↑variability (low SNR, acquisition- and biological variability, inaccurate voxel relocalization during spectrum averaging) → ↓reproducibility of measurements - Limited clinical feasibility → long scan times, high cost, no insurance coverage, lack of universal consensus (↑metabolite ratio variability across studies) *Multimodal imaging:* - In a prospective, biopsy-controlled study, structural MRI when used in conjunction with FET-PET and MRS could boost accuracy of PD detection from 68% to 97% (Floeth et al, 2005)	Majority of studies focus on single imaging modalities only, have small sample sizes, lack biopsy-control Limited clinical utility: - ↓scanner availability - lack of insurance coverage - ↑operation costs - frequent diagnostic need for multiple combined imaging techniques further limits clinical feasibility	- Multiple combined imaging techniques should be used in case of mixed lesions to yield a) better physiological characterization of lesions and b) reduce misinterpretation of lesions. - Results from multimodal diagnostic imaging should be contextualized with info on patient demographics, therapeutic history, and primary tumor type. - Quantitative approaches using morphometric image feature analysis to detect fine-grained differences between TN and PD warrant further investigation.

Table 1 *Continued*

Study/Type	No./Types of Studies Reviewed	Selected Notable Findings	Key Issues Identified	Overall Recommendations
Ryken et al. (2014)[20] **-Systematic Review** **-Focus on which imaging techniques best differentiate PD from TN and PP in patients with previously diagnosed GBM.**	57 clinical studies, 46 focused on advanced imaging techniques -8 MRI perfusion studies -5 MRI diffusion studies -13 MRS studies -10 PET studies -10 SPECT studies	See detailed imaging recommendations with corresponding levels of evidence (Class I–III)[a]. *Multimodal imaging:* - Combined use of multiple imaging techniques and multi-parametric analyses are classified as class 3 data (lacking independent validation), but may offer greatly improved diagnostic accuracy - A 55 pat. cohort study (36 pat. w/ biopsy-confirmed diagnosis) showed a 96% diagnostic accuracy of MRS combined with DWI in detecting TN vs PD (Zeng 2007)	- Reviewed studies lack high levels of evidence due to: -poor study design -heterogeneity of pat. population -variability in practices at time of progression- MRS (*Level II*) or SPECT (*Level III*) - Paucity of prospectively collected data with as diagnostic methods for PD vs TN / PP differentiation. - Routine use of PET to identify PD is not recommended (*Level III*)	- MRI (w/ or w/o Gd.) as imaging surveillance method to detect progression of GBM (*Level II* evidence)

Abbreviations: ^{11}C-MET = (11)c-methionine; ^{18}F-FDG-PET = fluorodeoxyglucose; ^{18}F-FDOPA = fluorodopa; ^{18}F-FET = fluoro-ethyl-tyrosine; ^{201}Tl = (201)thallium; ADC = apparent diffusion coefficient; Cho = choline; Cr = creatine; CTP = computed tomography perfusion imaging; DCE = dynamic contrast-enhanced; DSC = dynamic susceptibility contrast; DTI = diffusion tensor imaging; DWI = diffusion weighted imaging; FA = fractional anisotropy; GBM = glioblastoma multiforme; Gd = gadolinium; HGG = high-grade glioma; LGG = low-grade glioma; MRI = magnetic resonance imaging; MRS = magnetic resonance spectroscopy; NAA = N-acetylaspartate; pat. = patients; PD = progressive disease; PET = positron emission tomography; PP = pseudoprogression; rCBF = regional cerebral blood flow; Rx = radiation; SNR = signal-to-noise ratio; SPECT = single-photon emission computed tomography; Tc-99 = technetium-99; TN = treatment necrosis; w/ = with; w/o = without

[a] Grading of evidence levels in this study was carried out according to "a three-tiered system for assessing studies addressing diagnostic testing as approved by the American Association of Neurological Surgeons (AANS)/Congress of Neurological Surgeons (CNS) Joint Committee on Guidelines criteria."

experience and personal judgment. As the histopathological distinction between TN and PP remains challenging, findings are often summarized under the umbrella term "treatment effect." Moreover, analyzed lesions frequently reveal "mixed results," consisting of necrosis with differing quantities of scattered atypical tumor cells and/or foci of solid tumor (representing PD), thus making re-initiation of anti-neoplastic treatment a judgment call. Occasionally, lesions may contain inflammatory components, such as lymphocytic infiltrates, rather than plain necrosis. While rare atypical cells are found in most TN specimens, radiation-induced cellular atypia in non-neoplastic cells is a known phenomenon that may cause further diagnostic ambiguity.[6]

Establishing treatment effect–specific quantitative and qualitative measures for (i) more accurate histopathological differentiation between distinct types of TN or other treatment-induced phenomena like PP, and (ii) precise determination of the amount of tumor versus treatment-related pathology within the specimen would improve diagnostic accuracy and aid further patient management decisions and prognostication. Such measures may be more conceivable for specimens resected in toto, as tissue samples obtained by stereotactic needle biopsy—depending on the amount of available tissue—carry a higher risk of sampling error and non-diagnostic yield.[70]

Therapeutic Considerations

The clinical course of patients diagnosed with TN is highly variable. Necrotic lesions may develop entirely without symptoms (identified by neuroimaging only), but approximately 42%[34] to 54%[15] of patients will demonstrate progressive cognitive decline, diffuse and/or focal neurological deficits, signs of increased intracranial pressure, and/or seizures[71] (ie, frequently mimicking the clinical picture of PD) (Fig. 1). While clinical symptoms may resolve gradually, some patients will get progressively worse, requiring medical and/or surgical therapeutic intervention to halt further neurological decline or, rarely, to prevent a fatal outcome.[72]The rather ill-defined heterogeneous clinical picture of TN along with aforementioned radiological difficulties pose a management challenge,[1] as therapeutic strategies for TN differ sharply from those for PD.[73]

No SOC treatment protocol for TN presently exists and the pathophysiology of the condition remains poorly understood. Histopathological correlates of TN commonly include thrombosis, hemorrhage, parenchymal necrosis, histiocytic infiltrates, gliosis, fibrinous exudates, and vascular abnormalities.[6] While thought to be driven by a combination of treatment-induced vascular endothelial injury, glial cell injury, hypoxic injury/vascular endothelial growth factor (VEGF) overexpression and (auto)immune-mediated responses,[6,8,9,17] the exact sequence of pathomechanisms and key targetable molecular drivers of TN remain uncertain.

Among numerous therapeutic strategies put forward for TN (see Supplementary Table 1 for a comprehensive

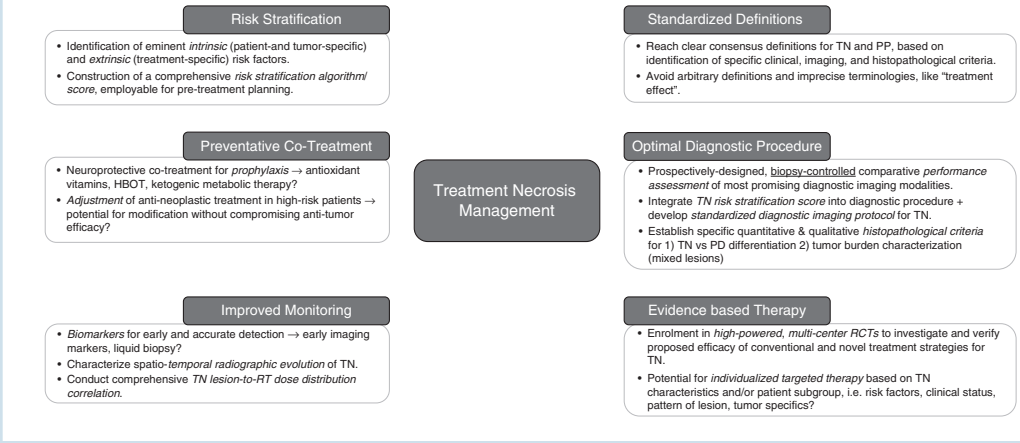

Fig. 4 Schematic illustrating 6 eminent, interdependent research pillars paramount to mapping the field of treatment necrosis management in neuro-oncology. Key research topics and unanswered questions are highlighted.

overview of relevant published studies), no causal therapy is presently available as existing interventions are mostly limited to management of TN-associated symptoms.[5] As such, vasogenic edema and associated mass effect, thought to be caused by radiation-induced blood–brain barrier disruption and inflammatory cytokine release,[9,74] are commonly managed with corticosteroids.[75] More recently, the VEGF-A monoclonal antibody bevacizumab (Avastin) has shown some promise in reversing neurological symptoms and radiographic changes in patients with TN.[27,76–80] However, the long-term therapeutic feasibility of both medications is limited by their side effect profiles[81] as well as treatment costs (in the case of bevacizumab).[79] Single case reports of patients with TN experiencing paradoxical neurological worsening under bevacizumab treatment[82] or developing acquired resistance to the drug[83] have been documented. Anti-coagulant/anti-platelet drugs with vitamin E,[84–86] hyperbaric oxygen therapy (HBOT),[87–89] intramuscular nerve growth factor,[90] and antibiotic applications[91] constitute other experimental strategies, although response rates have been mixed and associated studies were generally of insufficient levels of clinical evidence.[5,10] Minimally invasive techniques, such as laser interstitial thermal therapy (LITT),[92–94] are being increasingly explored to treat TN or PD lesions that are surgically inaccessible[94,95] and/or located in eloquent brain regions,[96] or when open surgical procedures are contraindicated. Evidence from 2 biopsy-controlled retrospective studies[95,97] and 1 multicenter prospective study has suggested clinical and radiographic improvement from LITT with minimal morbidity in patients with previously symptomatic TN lesions.[98] Finally, surgical resection carries an implicit advantage of yielding diagnostic histopathological information that may guide future patient management. While potentially a life-saving intervention in the management of acutely symptomatic, mass-effect producing TN lesions, surgical intervention may bear the risk of procedure-related complications and worse neurological outcome.[72] Delayed timing of surgery (usually after all conservative therapy has failed) may propel surgical risk, whereas more aggressive, early surgical intervention could potentially improve clinical outcome.[72]

Taken together, existing therapeutic options for patients with TN are limited. Most available treatment strategies lack sufficient clinical evidence to draw dependable conclusions on their possible therapeutic efficacy. Bevacizumab appears to have the most evidence to suggest favorable effects on both clinical and radiographic improvement as well as reducing steroid dependency, although the side effect profile and high treatment cost may preclude its long-term therapeutic feasibility.[27,77,79,80] Intra-arterial anti-VEGF therapy might potentially reduce bevacizumab-associated side effects[99,100]; however, its efficacy remains to be shown in glioma patients affected by TN. Intramuscular nerve growth factor treatment has shown some early promise in reversing cognitive deficits and radiographic findings without significant adverse effects in patients with temporal lobe necrosis, warranting further investigation.[90] Finally, the use of LITT to treat surgically inaccessible symptomatic TN lesions bears promise in alleviating neurological symptoms and reducing the need for steroids without the risk of conventional surgical approaches.[95,97,98]

Future Perspectives: Mapping the Field

Improvement in the management of TN faces a number of clinical and systemic challenges (Fig. 1 and Fig. 2).

While an array of advanced diagnostic imaging modalities and therapeutic strategies have been developed (Table 1 and Supplementary Table 1), no diagnostic or therapeutic consensus for TN presently exists. High-powered, prospective, and biopsy-controlled clinical studies may help to improve performance assessment of diagnostic neuroimaging and provide the basis to establish dependable, treatment-effect specific imaging criteria to supplement existing modified RANO criteria.[45] Moreover, sufficient availability of biopsy material would facilitate research to advance histopathological characterization for different types of treatment effects (Fig. 3).

In addition to defining an evidence-based diagnostic and therapeutic SOC, future work should address prevention strategies and improved patient monitoring (Fig. 4). The former will necessitate assessment of putative risk factors for TN and, optimally, the construction of a clinically employable risk stratification tool to identify "high risk patients." Adjustment of cancer therapy regimens and use of potential neuroprotective strategies, such as ketogenic metabolic therapy,[101] high-dose antioxidants,[86] or HBOT,[88] during and after chemo-RT treatment are possible areas of investigation. Here, clinical evaluation should ideally include a non-inferiority design, to ensure that tumor response is not adversely affected. Additional challenges to clinical trial design relate to patient selection criteria, that is, whether stratification of patients with TN based on the underlying condition (malignant glioma, brain metastases, or nasopharyngeal carcinoma) would be reasonable. Finally, greater emphasis on comprehensive evaluation of treatment-related effects across the entire neuro-oncological care trajectory would permit more integrated analysis of collected clinical data.

Conclusion

Progress in this complex field of TN is limited by several clinical and systemic factors. Critical questions pertaining to the true incidence and presentation of TN, risk factors, histopathological correlates, radiographic patterns, and the role of advanced functional imaging modalities remain to be addressed. Deriving conclusive answers from the current body of literature is chiefly precluded by the paucity of biopsy-controlled studies. A greater research focus on treatment-related effects through rigorous collection of clinical data and inclusion of relevant parameters as primary or secondary endpoints in multicenter randomized controlled trials would be of tremendous benefit to improve prevention, diagnosis, treatment response assessment, and therapeutic management of affected patients.

Supplementary Material

Supplementary data are available at *Neuro-Oncology* online.

Funding

This work was supported by the Charité Berlin/MDC joint Berlin Institute of Health (BIH) (MD Stipend Grant [S.F.W.]); the Rolf W. Günther Foundation of Radiological Sciences (*R.W.G. Stiftung für Radiologische Wissenschaften*) (S.F.W.); the German National Academic Foundation (*Studienstiftung des deutschen Volkes*) (S.F.W.); the American Brain Foundation (J.D.); the American Cancer Society (J.D.); and the Amy Gallagher Foundation (J.D.).

Conflict of interest statement. The authors declare no conflicts of interest.

References

1. Dietrich J, Winter SF, Klein JP. Neuroimaging of brain tumors: pseudoprogression, pseudoresponse, and delayed effects of chemotherapy and radiation. *Semin Neurol*. 2017;37(5):589–596.
2. Dietrich J, Klein JP. Imaging of cancer therapy-induced central nervous system toxicity. *Neurol Clin*. 2014;32(1):147–157.
3. Giglio P, Gilbert MR. Cerebral radiation necrosis. *Neurologist*. 2003;9(4):180–188.
4. Na A, Haghigi N, Drummond KJ. Cerebral radiation necrosis. *Asia Pac J Clin Oncol*. 2014;10(1):11–21.
5. Eisele SC, Dietrich J. Cerebral radiation necrosis: diagnostic challenge and clinical management. *Rev Neurol*. 2015;61(5):225–232.
6. Perry A, Schmidt RE. Cancer therapy-associated CNS neuropathology: an update and review of the literature. *Acta Neuropathol*. 2006;111(3):197–212.
7. Kumar AJ, Leeds NE, Fuller GN, et al. Malignant gliomas: MR imaging spectrum of radiation therapy- and chemotherapy-induced necrosis of the brain after treatment. *Radiology*. 2000;217(2):377–384.
8. Rahmathulla G, Marko NF, Weil RJ. Cerebral radiation necrosis: a review of the pathobiology, diagnosis and management considerations. *J Clin Neurosci*. 2013;20(4):485–502.
9. Furuse M, Nonoguchi N, Kawabata S, Miyatake S, Kuroiwa T. Delayed brain radiation necrosis: pathological review and new molecular targets for treatment. *Med Mol Morphol*. 2015;48(4):183–190.
10. Fink J, Born D, Chamberlain MC. Radiation necrosis: relevance with respect to treatment of primary and secondary brain tumors. *Curr Neurol Neurosci Rep*. 2012;12(3):276–285.
11. Parvez K, Parvez A, Zadeh G. The diagnosis and treatment of pseudoprogression, radiation necrosis and brain tumor recurrence. *Int J Mol Sci*. 2014;15(7):11832–11846.
12. Verma N, Cowperthwaite MC, Burnett MG, Markey MK. Differentiating tumor recurrence from treatment necrosis: a review of neuro-oncologic imaging strategies. *Neuro Oncol*. 2013;15(5):515–534.
13. Chamberlain MC, Glantz MJ, Chalmers L, Van Horn A, Sloan AE. Early necrosis following concurrent Temodar and radiotherapy in patients with glioblastoma. *J Neurooncol*. 2007;82(1):81–83.
14. Brandsma D, Stalpers L, Taal W, Sminia P, van den Bent MJ. Clinical features, mechanisms, and management of pseudoprogression in malignant gliomas. *Lancet Oncol*. 2008;9(5):453–461.

15. Kim JM, Miller JA, Kotecha R, et al. The risk of radiation necrosis following stereotactic radiosurgery with concurrent systemic therapies. *J Neurooncol*. 2017;133(2):357–368.
16. Jain R, Narang J, Sundgren PM, et al. Treatment induced necrosis versus recurrent/progressing brain tumor: going beyond the boundaries of conventional morphologic imaging. *J Neurooncol*. 2010;100(1):17–29.
17. Yang I, Aghi MK. New advances that enable identification of glioblastoma recurrence. *Nat Rev Clin Oncol*. 2009;6(11):648–657.
18. Langen KJ, Galldiks N, Hattingen E, Shah NJ. Advances in neuro-oncology imaging. *Nat Rev Neurol*. 2017;13(5):279–289.
19. Alexiou GA, Tsiouris S, Kyritsis AP, Voulgaris S, Argyropoulou MI, Fotopoulos AD. Glioma recurrence versus radiation necrosis: accuracy of current imaging modalities. *J Neurooncol*. 2009;95(1):1–11.
20. Ryken TC, Aygun N, Morris J, et al. The role of imaging in the management of progressive glioblastoma: a systematic review and evidence-based clinical practice guideline. *J Neurooncol*. 2014;118(3).
21. Huang RY, Neagu MR, Reardon DA, Wen PY. Pitfalls in the neuroimaging of glioblastoma in the era of antiangiogenic and immuno/targeted therapy—detecting illusive disease, defining response. *Front Neurol*. 2015;6:33.
22. Sanghera P, Rampling R, Haylock B, et al. The concepts, diagnosis and management of early imaging changes after therapy for glioblastomas. *Clin Oncol*. 2012;24(3):216–227.
23. Stupp R, Mason WP, van den Bent MJ, et al; European Organisation for Research and Treatment of Cancer Brain Tumor and Radiotherapy Groups; National Cancer Institute of Canada Clinical Trials Group. Radiotherapy plus concomitant and adjuvant temozolomide for glioblastoma. *N Engl J Med*. 2005;352(10):987–996.
24. Ruben JD, Dally M, Bailey M, Smith R, McLean CA, Fedele P. Cerebral radiation necrosis: incidence, outcomes, and risk factors with emphasis on radiation parameters and chemotherapy. *Int J Radiat Oncol Biol Phys*. 2006;65(2):499–508.
25. Mikhael M. Dosimetric considerations in the diagnosis of radiation necrosis of the brain. In: Gilbert H, Kagan A, eds. *Radiation Damage to the Nervous System*. New York: Raven Press; 1980:59–91.
26. Lam TC, Wong FC, Leung TW, Ng SH, Tung SY. Clinical outcomes of 174 nasopharyngeal carcinoma patients with radiation-induced temporal lobe necrosis. *Int J Radiat Oncol Biol Phys*. 2012;82(1):e57–e65.
27. Levin VA, Bidaut L, Hou P, et al. Randomized double-blind placebo-controlled trial of bevacizumab therapy for radiation necrosis of the central nervous system. *Int J Radiat Oncol Biol Phys*. 2011;79(5):1487–1495.
28. Clarke J, Neil E, Terziev R, et al. Multicenter, phase 1, dose escalation study of hypofractionated stereotactic radiation therapy with bevacizumab for recurrent glioblastoma and anaplastic astrocytoma. *Int J Radiat Oncol Biol Phys*. 2017;99(4):797–804.
29. Du Four S, Janssen Y, Michotte A, et al. Focal radiation necrosis of the brain in patients with melanoma brain metastases treated with pembrolizumab. *Cancer Med*. 2018;7(10):4870–4879.
30. Fang P, Jiang W, Allen P, et al. Radiation necrosis with stereotactic radiosurgery combined with CTLA-4 blockade and PD-1 inhibition for treatment of intracranial disease in metastatic melanoma. *J Neurooncol*. 2017;133(3):595–602.
31. Marks JE, Baglan RJ, Prassad SC, Blank WF. Cerebral radionecrosis: incidence and risk in relation to dose, time, fractionation and volume. *Int J Radiat Oncol Biol Phys*. 1981;7(2):243–252.
32. Blonigen BJ, Steinmetz RD, Levin L, Lamba MA, Warnick RE, Breneman JC. Irradiated volume as a predictor of brain radionecrosis after linear accelerator stereotactic radiosurgery. *Int J Radiat Oncol Biol Phys*. 2010;77(4):996–1001.
33. Lee AW, Foo W, Chappell R, et al. Effect of time, dose, and fractionation on temporal lobe necrosis following radiotherapy for nasopharyngeal carcinoma. *Int J Radiat Oncol Biol Phys*. 1998;40(1):35–42.
34. Minniti G, Clarke E, Lanzetta G, et al. Stereotactic radiosurgery for brain metastases: analysis of outcome and risk of brain radionecrosis. *Radiat Oncol*. 2011;6:48.
35. Brandes AA, Tosoni A, Spagnolli F, et al. Disease progression or pseudoprogression after concomitant radiochemotherapy treatment: pitfalls in neurooncology. *Neuro Oncol*. 2008;10(3):361–367.
36. van West SE, de Bruin HG, van de Langerijt B, Swaak-Kragten AT, van den Bent MJ, Taal W. Incidence of pseudoprogression in low-grade gliomas treated with radiotherapy. *Neuro Oncol*. 2017;19(5):719–725.
37. Rogers L, Scarpace L, Gutierrez J, Ryu S. Magnetic resonance imaging features of histologically documented cerebral radiation necrosis. *Neurology*. 2006;66(5):A398–A399.
38. Mullins ME, Barest GD, Schaefer PW, Hochberg FH, Gonzalez RG, Lev MH. Radiation necrosis versus glioma recurrence: conventional MR imaging clues to diagnosis. *AJNR Am J Neuroradiol*. 2005;26(8):1967–1972.
39. Dequesada IM, Quisling RG, Yachnis A, Friedman WA. Can standard magnetic resonance imaging reliably distinguish recurrent tumor from radiation necrosis after radiosurgery for brain metastases? A radiographic-pathological study. *Neurosurgery*. 2008;63(5):898–903; discussion 904.
40. Shah AH, Snelling B, Bregy A, et al. Discriminating radiation necrosis from tumor progression in gliomas: a systematic review what is the best imaging modality? *J Neurooncol*. 2013;112(2):141–152.
41. Tofilon PJ, Fike JR. The radioresponse of the central nervous system: a dynamic process. *Radiat Res*. 2000;153(4):357–370.
42. Ellingson BM, Chung C, Pope WB, Boxerman JL, Kaufmann TJ. Pseudoprogression, radionecrosis, inflammation or true tumor progression? challenges associated with glioblastoma response assessment in an evolving therapeutic landscape. *J Neurooncol*. 2017;134(3):495–504.
43. Tanaka S, Louis DN, Curry WT, Batchelor TT, Dietrich J. Diagnostic and therapeutic avenues for glioblastoma: no longer a dead end? *Nat Rev Clin Oncol*. 2013;10(1):14–26.
44. Eisele SC, Wen PY, Lee EQ. Assessment of brain tumor response: RANO and Its offspring. *Curr Treat Options Oncol*. 2016;17(7):35.
45. Ellingson BM, Wen PY, Cloughesy TF. Modified criteria for radiographic response assessment in glioblastoma clinical trials. *Neurotherapeutics*. 2017;14(2):307–320.
46. Wen PY, Chang SM, Van den Bent MJ, Vogelbaum MA, Macdonald DR, Lee EQ. Response assessment in neuro-oncology clinical trials. *J Clin Oncol*. 2017;35(21):2439–2449.
47. Hein PA, Eskey CJ, Dunn JF, Hug EB. Diffusion-weighted imaging in the follow-up of treated high-grade gliomas: tumor recurrence versus radiation injury. *AJNR Am J Neuroradiol*. 2004;25(2):201–209.
48. Sundgren PC, Fan X, Weybright P, et al. Differentiation of recurrent brain tumor versus radiation injury using diffusion tensor imaging in patients with new contrast-enhancing lesions. *Magn Reson Imaging*. 2006;24(9):1131–1142.
49. Larsen VA, Simonsen HJ, Law I, Larsson HB, Hansen AE. Evaluation of dynamic contrast-enhanced T1-weighted perfusion MRI in the differentiation of tumor recurrence from radiation necrosis. *Neuroradiology*. 2013;55(3):361–369.
50. Barajas RF Jr, Chang JS, Segal MR, et al. Differentiation of recurrent glioblastoma multiforme from radiation necrosis after external beam radiation therapy with dynamic susceptibility-weighted contrast-enhanced perfusion MR imaging. *Radiology*. 2009;253(2):486–496.
51. Mitsuya K, Nakasu Y, Horiguchi S, et al. Perfusion weighted magnetic resonance imaging to distinguish the recurrence of metastatic brain tumors from radiation necrosis after stereotactic radiosurgery. *J Neurooncol*. 2010;99(1):81–88.
52. Jain R, Narang J, Schultz L, et al. Permeability estimates in histopathology-proved treatment-induced necrosis using perfusion CT: can these

add to other perfusion parameters in differentiating from recurrent/progressive tumors? *AJNR Am J Neuroradiol.* 2011;32(4):658–663.

53. Plotkin M, Eisenacher J, Bruhn H, et al. 123I-IMT SPECT and 1H MR-spectroscopy at 3.0 T in the differential diagnosis of recurrent or residual gliomas: a comparative study. *J Neurooncol.* 2004;70(1):49–58.
54. Rock JP, Scarpace L, Hearshen D, et al. Associations among magnetic resonance spectroscopy, apparent diffusion coefficients, and image-guided histopathology with special attention to radiation necrosis. *Neurosurgery.* 2004;54(5):1111–7; discussion 1117.
55. Zeng QS, Li CF, Liu H, Zhen JH, Feng DC. Distinction between recurrent glioma and radiation injury using magnetic resonance spectroscopy in combination with diffusion-weighted imaging. *Int J Radiat Oncol Biol Phys.* 2007;68(1):151–158.
56. Jena A, Taneja S, Jha A, et al. Multiparametric evaluation in differentiating glioma recurrence from treatment-induced necrosis using simultaneous 18F-FDG-PET/MRI: a single-institution retrospective study. *AJNR Am J Neuroradiol.* 2017;38(5):899–907.
57. Chen W, Silverman DH, Delaloye S, et al. 18F-FDOPA PET imaging of brain tumors: comparison study with 18F-FDG PET and evaluation of diagnostic accuracy. *J Nucl Med.* 2006;47(6):904–911.
58. Takenaka S, Asano Y, Shinoda J, et al. Comparison of (11)C-methionine, (11)C-choline, and (18)F-fluorodeoxyglucose-PET for distinguishing glioma recurrence from radiation necrosis. *Neurol Med Chir (Tokyo).* 2014;54(4):280–289.
59. Kim YH, Oh SW, Lim YJ, et al. Differentiating radiation necrosis from tumor recurrence in high-grade gliomas: assessing the efficacy of 18F-FDG PET, 11C-methionine PET and perfusion MRI. *Clin Neurol Neurosurg.* 2010;112(9):758–765.
60. Zhang H, Ma L, Wu C, Xu BN. Performance of SPECT in the differential diagnosis of glioma recurrence from radiation necrosis. *J Clin Neurosci.* 2015;22(2):229–237.
61. Hatzoglou V, Yang TJ, Omuro A, et al. A prospective trial of dynamic contrast-enhanced MRI perfusion and fluorine-18 FDG PET-CT in differentiating brain tumor progression from radiation injury after cranial irradiation. *Neuro Oncol.* 2016;18(6):873–880.
62. Floeth FW, Pauleit D, Wittsack HJ, et al. Multimodal metabolic imaging of cerebral gliomas: positron emission tomography with [^{18}F]fluoro-ethyl-L-tyrosine and magnetic resonance spectroscopy. *J Neurosurg.* 2005;102(2):318–327.
63. Chang PD, Malone HR, Bowden SG, et al. A multiparametric model for mapping cellularity in glioblastoma using radiographically localized biopsies. *AJNR Am J Neuroradiol.* 2017;38(5):890–898.
64. Caroline I, Rosenthal MA. Imaging modalities in high-grade gliomas: pseudoprogression, recurrence, or necrosis? *J Clin Neurosci.* 2012;19(5):633–637.
65. Chernov M, Hayashi M, Izawa M, et al. Differentiation of the radiation-induced necrosis and tumor recurrence after gamma knife radiosurgery for brain metastases: importance of multi-voxel proton MRS. *Minim Invasive Neurosurg.* 2005;48(4):228–234.
66. Zach L, Guez D, Last D, et al. Delayed contrast extravasation MRI: a new paradigm in neuro-oncology. *Neuro Oncol.* 2015;17(3):457–465.
67. Zachariah MA, Oliveira-Costa JP, Carter BS, Stott SL, Nahed BV. Blood-based biomarkers for the diagnosis and monitoring of gliomas. *Neuro Oncol.* 2018;20(9):1155–1161.
68. Soler DC, Young AB, Cooper KD, et al. The ratio of HLA-DR and VNN2+ expression on CD14+ myeloid derived suppressor cells can distinguish glioblastoma from radiation necrosis patients. *J Neurooncol.* 2017;134(1):189–196.
69. Koch CJ, Lustig RA, Yang XY, et al. Microvesicles as a biomarker for tumor progression versus treatment effect in radiation/temozolomide-treated glioblastoma patients. *Transl Oncol.* 2014;7(6):752–758.
70. Jain D, Sharma MC, Sarkar C, Deb P, Gupta D, Mahapatra AK. Correlation of diagnostic yield of stereotactic brain biopsy with number of biopsy bits and site of the lesion. *Brain Tumor Pathol.* 2006;23(2):71–75.
71. Chi D, Behin A, Delattre J-Y. Neurologic complications of radiation therapy. In: Schiff D, Kesari S, Wen P, eds. *Cancer Neurology in Clinical Practice.* Totowa, NJ: Humana Press; 2008:259–286.
72. McPherson CM, Warnick RE. Results of contemporary surgical management of radiation necrosis using frameless stereotaxis and intraoperative magnetic resonance imaging. *J Neurooncol.* 2004;68(1):41–47.
73. Sheline GE, Wara WM, Smith V. Therapeutic irradiation and brain injury. *Int J Radiat Oncol Biol Phys.* 1980;6(9):1215–1228.
74. Brown WR, Thore CR, Moody DM, Robbins ME, Wheeler KT. Vascular damage after fractionated whole-brain irradiation in rats. *Radiat Res.* 2005;164(5):662–668.
75. Shaw PJ, Bates D. Conservative treatment of delayed cerebral radiation necrosis. *J Neurol Neurosurg Psychiatry.* 1984;47(12):1338–1341.
76. Torcuator R, Zuniga R, Mohan YS, et al. Initial experience with bevacizumab treatment for biopsy confirmed cerebral radiation necrosis. *J Neurooncol.* 2009;94(1):63–68.
77. Furuse M, Nonoguchi N, Kuroiwa T, et al. A prospective, multicentre, single-arm clinical trial of bevacizumab for patients with surgically untreatable, symptomatic brain radiation necrosis†. *Neurooncol Pract.* 2016;3(4):272–280.
78. Sadraei NH, Dahiya S, Chao ST, et al. Treatment of cerebral radiation necrosis with bevacizumab: the Cleveland clinic experience. *Am J Clin Oncol.* 2015;38(3):304–310.
79. Lubelski D, Abdullah KG, Weil RJ, Marko NF. Bevacizumab for radiation necrosis following treatment of high grade glioma: a systematic review of the literature. *J Neurooncol.* 2013;115(3):317–322.
80. Tye K, Engelhard HH, Slavin KV, et al. An analysis of radiation necrosis of the central nervous system treated with bevacizumab. *J Neurooncol.* 2014;117(2):321–327.
81. Dietrich J, Rao K, Pastorino S, Kesari S. Corticosteroids in brain cancer patients: benefits and pitfalls. *Expert Rev Clin Pharmacol.* 2011;4(2):233–242.
82. Jeyaretna DS, Curry WT Jr, Batchelor TT, Stemmer-Rachamimov A, Plotkin SR. Exacerbation of cerebral radiation necrosis by bevacizumab. *J Clin Oncol.* 2011;29(7):e159–e162.
83. Zhuang H, Yuan X, Sun D, et al. Acquired-resistance of bevacizumab treatment for radiation brain necrosis: a case report. *Oncotarget.* 2016;7(11):13265–13268.
84. Williamson R, Kondziolka D, Kanaan H, Lunsford LD, Flickinger JC. Adverse radiation effects after radiosurgery may benefit from oral vitamin E and pentoxifylline therapy: a pilot study. *Stereotact Funct Neurosurg.* 2008;86(6):359–366.
85. Glantz MJ, Burger PC, Friedman AH, Radtke RA, Massey EW, Schold SC Jr. Treatment of radiation-induced nervous system injury with heparin and warfarin. *Neurology.* 1994;44(11):2020–2027.
86. ClinicalTrials.gov [Internet]. Identifyer NCT01508221. *Evaluation of the Use of Trental and Vitamin E for Prophylaxis of Radiation Necrosis.* Bethesda, MD: National Library of Medicine (US); 2000.
87. Chuba PJ, Aronin P, Bhambhani K, et al. Hyperbaric oxygen therapy for radiation-induced brain injury in children. *Cancer.* 1997;80(10):2005–2012.
88. Ohguri T, Imada H, Kohshi K, et al. Effect of prophylactic hyperbaric oxygen treatment for radiation-induced brain injury after stereotactic radiosurgery of brain metastases. *Int J Radiat Oncol Biol Phys.* 2007;67(1):248–255.
89. Valadão J, Pearl J, Verma S, Helms A, Whelan H. Hyperbaric oxygen treatment for post-radiation central nervous system injury: a retrospective case series. *Undersea Hyperb Med.* 2014;41(2):87–96.

90. Wang XS, Ying HM, He XY, Zhou ZR, Wu YR, Hu CS. Treatment of cerebral radiation necrosis with nerve growth factor: a prospective, randomized, controlled phase II study. *Radiother Oncol.* 2016;120(1):69–75.
91. Feng Y, Chen X, Guo N, Gao X. Effects of antibiotics on CNS radiation necrosis. *J Clin Oncol.* 2015;33(15 SUPPL. 1). doi:10.1200/jco.2015.33.15_suppl.e17008
92. Murovic JA, Chang SD. The pathophysiology of cerebral radiation necrosis and the role of laser interstitial thermal therapy. *World Neurosurg.* 2015;83(1):23–26.
93. Sharma M, Balasubramanian S, Silva D, Barnett GH, Mohammadi AM. Laser interstitial thermal therapy in the management of brain metastasis and radiation necrosis after radiosurgery: an overview. *Expert Rev Neurother.* 2016;16(2):223–232.
94. Rahmathulla G, Recinos PF, Valerio JE, Chao S, Barnett GH. Laser interstitial thermal therapy for focal cerebral radiation necrosis: a case report and literature review. *Stereotact Funct Neurosurg.* 2012;90(3):192–200.
95. Torres-Reveron J, Tomasiewicz HC, Shetty A, Amankulor NM, Chiang VL. Stereotactic laser induced thermotherapy (LITT): a novel treatment for brain lesions regrowing after radiosurgery. *J Neurooncol.* 2013;113(3):495–503.
96. Iyer A, Halpern CH, Grant GA, Deb S, Li GH. Magnetic resonance-guided laser-induced thermal therapy for recurrent brain metastases in the motor strip after stereotactic radiosurgery. *Cureus.* 2016;8(12):e919.
97. Smith CJ, Myers CS, Chapple KM, Smith KA. Long-term follow-up of 25 cases of biopsy-proven radiation necrosis or post-radiation treatment effect treated with magnetic resonance-guided laser interstitial thermal therapy. *Neurosurgery.* 2016;79(Suppl 1):S59–S72.
98. Ahluwalia M, Barnett GH, Deng D, et al. Laser ablation after stereotactic radiosurgery: a multicenter prospective study in patients with metastatic brain tumors and radiation necrosis. *J Neurosurg.* 2018;130(3):804–811.
99. Dashti SR, Spalding A, Kadner RJ, et al. Targeted intraarterial anti-VEGF therapy for medically refractory radiation necrosis in the brain. *J Neurosurg Pediatr.* 2015;15(1):20–25.
100. ClinicalTrials.gov [Internet]. *Low-dose Intra-arterial Bevacizumab for Edema and Radiation Necrosis Therapeutic Intervention (LIBERTI).* Bethesda, MD: National Library of Medicine (US); 2000.
101. Winter SF, Loebel F, Dietrich J. Role of ketogenic metabolic therapy in malignant glioma: a systematic review. *Crit Rev Oncol Hematol.* 2017;112:41–58.

Supplementary Table S1, in Winter et al., 2019

Table S1. Overview of relevant published and clinical trial data on current therapeutic strategies for treatment necrosis.

Treatment Modality	Study Design	LOE	Regimen	Efficacy		Adverse Events	Critical Issues/Questions
				Clinical Improvement	*Radiographic Improvement*		
Medical Therapies							
Bevacizumab	Levin et al. (2011)[27] - Placebo-controlled randomized double-blind trial - 14 pat. w/ grade 2-3 primary brain neoplasm, meningioma, or head/neck cancer s/p RT ≥6mos before study entry - TN radiographically and/or Bx-proven	I	-Treatment group: IV bevacizumab at 7.5 mg/kg at 3-week intervals for 2 cycles - Control group: Placebo (IV saline) at 3-week intervals for 2 cycles - Control MRI 6wk post study entry → 2 more cycles of regimen in responders w/o adverse effects - Treatment failures had option to cross over at or before 6wk MRI scan	-All pat. in treatment arm w/ improvement vs 5/7 (71%) of placebo-treated pat. w/ worsening of neurological signs/ symptoms at 6wk clinic visit. - 4/5 bevacizumab treated pat. had ↓dexamethasone dose by 12wks post-treatment initiation. - Neurocognitive testing w/ mixed findings → trend towards improved learning/memory after 6 wks of bevacizumab therapy	-MRI responses (↓T1 contrast enhancement / ↓T2 FLAIR signal) observed in all pat. in treatment arm vs radiographic TN lesion progression observed in placebo cohort by 6 weeks (p = .0013). - 6 pat. who crossed over to treatment arm after progression of TN had subsequent ↓enhancement volume.	-Any grade: 6/11 (54.5%) bevacizumab treated pat. - Grade ≥3: 3/11 (27%) pat. (1 aspiration pneumonia; 1 PE secondary to DVT; 1 CVT)	- TN not Bx-proven in all cases - Questions related to optimal dosing and treatment length remain. -Significant side effect profile: ½ of pat. had some form of adverse event; ¼ had a serious adverse event
	Lubelski et al. (2013)[39] - Systematic review of 7 studies w/ 30 pat. total w/ HGG s/p mostly fractionated RT (mean total dose 58.4Gy) treated w/ bevacizumab for radiographically diagnosed and/or Bx-proven TN	II	-Bevacizumab, *"typically administered as infusions of 5–10 mg/kg every 2 weeks over an average of 4–8 weeks"*	-16/23 (70%) pat. had improved neurological signs/symptoms, 5/23 (22%) had partial improvement or mixed results, 2/23 (9%) remained at BL. - All pat. had ↓dexamethasone doses following treatment initiation	- All pat. had radiographic response to treatment, i.e. ↓gadolinium-enhanced T1 signal and ↓T2 FLAIR signal, mostly durable throughout the remainder of pat. F/U	- Reported in 5/7 studies (18/29 pat.; 62 %), included DVT, PE, ↓visual field, ↓hemiplegia, pneumonia, seizure, fatigue	- Limited data; primarily level III clinical evidence -Pat. QoL & cost/benefit profile are poorly assessed → authors suggest that to be cost effective this treatment would need to produce a *"2.4 month increase in survival, a 20 % improvement in a patient's quality-of-life, or some linear combination of the two"*

	Tye et al. (2014)[80] -Retrospective comprehensive analysis of 16 studies (from 2007-2012) w/ 71 pat. total w/ mostly primary or secondary brain neoplasms s/p mostly fractionated RT (median total dose 59.4 Gy) and radiographically diagnosed (78%) or Bx-proven (22%) TN	II	- 11mos median time from RT-completion to bevacizumab initiation - 8mos median F/U time post bevacizumab treatment -Regimen: median # of cycles 4 (range: 1–8 cycles); median dosage 7.5 mg/kg; median interval between cycles 2wks	-79 % of pat. had ↑KPS under treatment (median improvement 10; range: 0–40) - ↓steroid dose following bevacizumab treatment; median reduction 6 mg (range: 0–24 mg).	- 97 % of pat. had some form of radiographic post bevacizumab treatment - Median ↓T1 contrast enhancement 63 % (range: 0–100 %); median ↓T2/FLAIR signal abnormality 59 % (range: 0–81 %).	- Serious adverse events included 1 CVT, 1 aspiration pneumonia, 1 pneumonia w/ severe sepsis, 1 PE, 3 pat. w/ thrombosis induced ischemic changes	- Most studies reviewed were level III-IV clinical evidence - highly heterogenous pat. populations (different conditions, RT doses/modalities, F/U times) - only 22% had Bx-based TN diagnosis -Authors acknowledge risk of publication bias (under-reporting of bevacizumab non-responders)
	Furuse et al. (2016)[77] -Prospective multi-center single-arm trial - 41 pat. w/ brain or head/neck cancer s/p RT ≥3mos before study entry -Pat. had amino-acid PET based diagnosis of TN - Suspected TN lesions surgically untreatable, refractory to conventional (steroid, HBOT, anticoagulant) treatment, and symptomatic w/ peri-lesional edema	II	- IV bevacizumab at 5 mg/kg biweekly as a cycle, until completion of 6 cycles. - Control MRI after 3 cycles → if no negative change detected, regimen was continued.	-16/ 38 pat. (42.1%) reached transient 10-20%↑ in their KPS → decrease started 6mos post-treatment completion; at 12mos, ½ of pat. had KPS decrease below initial BL. -Average dexamethasone dose was 1.7 mg/day pre-intervention → reduced in 29/35 patients (76.3%) w/ 0.6 mg/day minimum reached at 6mos post-treatment. Final average dose (0.8 mg/day) was below initial BL.	-1º outcome measure: remission of peri-lesional edema on MRI → 30/38 pat. (78.9%) achieved remission at median time of 3mos - 27/38 pat. (71.1%) had post-treatment completion progression of edema (median: 9mos post-enrollment), however, this did not reach initial BL levels. - Minimum average volume of contrast-enhanced lesions (↓92.8% from BL) reached at last treatment → thereafter, ↑edema, but did not reach BL levels.	- Any grade: 36 pat. (87.8%) - Grade ≥3: 10 pat. (24.4%) - 3 pat. d/c'd regimen (2 grade 2 intracranial hemorrhages; 1 case of neurological deterioration)	- TN was not Bx-proven; short latency of TN onset (≥3mos) may have favored inclusion of pat. w/ PP -Observed incidence of adverse events (grade ≥3) in ca. ¼ of pat. remains a concern. -Despite a high radiographic response rate, clinical efficacy remained modest and transient. - Questions related to optimal dosing as well as safety & efficacy of bevacizumab re-induction for recurrent TN warrant further investigation.

Hyperbaric Oxygen Therapy (HBOT)	Chuba et al. (1997)[87] -Retrospective analysis - 10 pediatric pat. (9/10 ≤ 14 years; 9 w/ primary brain neoplasm; 1 w/ AVM) s/p external beam RT - 8 Bx-confirmed (6 w/ TN, 2 w/ mixed TN); 2 non-biopsied presumed TN	IV	- 20-30 sessions at 100% oxygen at 2.0-2.4 atmospheres, for 90min -2hrs	- All 10 pat. had initial improvement or stabilization - 6/10 pat. alive at F/U (3/36mos range) w/ durable neurological improvement	- 9/10 pat. had initial stabilization or improvement, which was durable in 6/10 pat. alive at F/U (3-36mos range)	-No severe HBOT toxicity observed (1 pat. w/ ear pain, requiring myringotomy tube placement)	- Pat. received steroid therapy before, during, and after HBOT - Pediatric pat. population
	Ohguri et al. (2007)[88] - Retrospective analysis - 32 pat. s/p SRS for brain met. given prophylactic HBOT (vs 46 non-HBOT controls) - TN not Bx-confirmed	III	-Treatment group received 20 HBOT sessions total (5x per week) for 60min at 100% oxygen at 2.5 atmospheres - HBOT initiated within 1wk post SRS	- White matter injury was not symptomatic in treatment group, but in 1/3 of cases in non-HBOT group.	- ↓incidence of radiation injury (TN or white-matter injury) in HBOT group: 11% vs 20% (non-treated) -Preventative effect of prophylactic HBOT mostly pronounced in white matter injury, not TN	- No serious adverse events - Small number of pat. w/ transient auditory problems (hearing difficulties, ear pain)	- Treatment group was intentionally selected according to predictors of longer survival (inactive extracranial tumors, younger age, higher KPS) → potential confounders - Radiation injury was merely diagnosed clinicoradiographically
	Valadão et al. (2014)[89] -Retrospective case series - 10 pat. w/ mostly secondary brain neoplasms -7/10 had presumed TN - TN not Bx-confirmed	IV	- 30 HBOT sessions total for 90min at 100% oxygen at 2.4 atmospheres - 7/10 pat. received concomitant steroid treatment	- 3/7 pat. w/ TN subjectively improved; the rest reported worsening symptoms.	- Of the pat. w/ presumed TN 2 improved, 2 had no change, 3 worsened radiographically.	-No information provided	- Many confounders → 5/10 pat had Hx of seizure disorder, 7/10 received steroid co-treatment and 5/10 received concomitant Ctx, which precludes adequate assessment of HBOT efficacy - TN was not Bx-confirmed
Anti-coagulant/platelet Drugs	Williamson et al. (2008)[84] -Retrospective case series - 11 pat. w/ mostly brain metastases s/p SRS treatment w/	IV	- Pentoxifylline 400 mg p.o. BID and Vitamin E 400 IU p.o. BID. - 10/11 pat. received initial and ad-hoc high-dose corticosteroid treatment for acute symptom management.	- Not an outcome measure	- Pre- to post-therapy average Δedema was –72.3 ml (less edema); 10/11 pat. had ↓edema (1 pat. w/ ↑edema turned out to have PD, not TN)	- 2 pat. discontinued Pentoxifylline treatment due to persistent nausea. - all pat. experienced intermittent nausea/abdominal discomfort	- ↑heterogenous pat. population (age range 9 – 70yrs), different conditions treated, different SRS doses received (some had 1-2 prior SRS treatments)

	clinicoradiographically suspected TN appearing 3 – 18mos post-SRS. - TN was <u>not</u> Bx-confirmed in 7/11 pat.; 4 pat. had Bx confirming TN (3) and PD (1).		- Treatment duration ranged from 1.2 to 13.1 months (mean= 6 months)				- initial + intermittent corticosteroid use as potential confounder
	NCT01508221 (2012 – ongoing)[86] - Phase 2 (recruiting, ca. 50 pat.) -Single-arm open-label intervention - Pat. w/ brain metastases scheduled to undergo SRS -1º Purpose: Prevention	II	-Pentoxifylline [Trental] 400 mg TID + Vitamin E 400IU BID starting the first day after the last radiosurgery treatment for prophylaxis of TN.	- 1º outcome measure: incidence of symptomatic TN.	N/A	N/A	-Pat. w/ Hx of (or anticipated need for) Avastin treatment are excluded → potential selection bias for a pat. population w/ less severe CNS disease burden and fewer anticipated complications (including TN)?
Nerve Growth Factor (NGF)	Wang et al. (2016)[90] - Prospective, randomized, placebo controlled phase II trial - 28 pat. w/ radiographically suspected, symptomatic, progressive temporal lobe necrosis s/p nasopharyngeal carcinoma treatment w/ one course of RT	I	-Treatment group (14 pat.): NGF dissolved in 2 mL saline injected intramuscularly at 18 micro g/time, daily for 2 months. Concomitant steroid use like control group. - Control group (14 pat.): steroid treatment "with gradually reduced dosage"	- Subjective evaluation of signs/symptoms (MMSE based) yielded sustained partial or complete recovery in the treatment group that became significant over control at 9mos post-intervention (13 versus 4, p = 0.001)	-Radiographic TN evaluation (via RECIST criteria) showed a higher response rate (PR or CR) in the treatment group at 3-4mos (10 versus 2, p = 0.006) and 6-8mos (12 versus 3, p = 0.002) post-NGF therapy.	- No serious adverse events reported - 3 pat. in treatment group complained of mild local pain at the injection site	- Does NGF (co-)treatment provide durable symptomatic relief by reversing TN? - Could NGF-induced reversal of TN relativize the contraindication for re-irradiation of pat. w/ TN that have tumor recurrence?
Interventional Therapies							
Intra-arterial anti-VEGF therapy	Dashti et al. (2015)[99] - Retrospective case series - 2 pediatric pat. (11 & 12yo) w/ cerebral AVMs s/p SRS w/ clinicoradiographically presumed TN	IV	- Single intraarterial infusion of 2.5 mg/kg bevacizumab in a volume of 100ml over 14min after hyperosmotic BBB disruption (using 37°C warm 25% mannitol)	-Durable clinical response at 8.5mos mean F/U duration -Both pat. experienced resolution of previously intractable H/A and cushingoid features (weaned off steroids)	-Durable radiographic response at 8.5mos mean F/U duration - >70% reduction of TN associated cerebral edema - TN lesions had 22% (at 5mos post-intervention; case 1) and 34% (at	-No procedure-related complications	- Feasibility of procedure remains to be assessed in pat. w/ malignant brain tumors.

				- 1 pat. regained significant motor function	3mos; case 2) ↓contrast enhancement		
	NCT02819479 / LIBERTI Trial (2016-ongoing)[100] - Phase 2 (recruiting, ca. 15 pat.) -Single-arm open-label intervention -Pat. w/ steroid refractory, symptomatic, and radiographically suspected TN	II	- Single intra-arterial dose of 2.5 mg/kg bevacizumab following hyperosmotic BBB disruption via intra-arterial 25% mannitol (at 4-12 ml/sec for 30 sec)	- 2º outcome measures: ↓steroid usage, improvement of H/A, H/A associated morbidity, neurocognitive function, neurological function, KPS, QoL	- 1º outcome measure: radiographic decrease in TN and cerebral edema; measured at Day 0, 3mos and 12 mos, via T1+Con and T2/FLAIR MRI volumetric analysis.	- 2º outcome measure: Adverse events, recorded at Day 0, 3mos and 12 mos.	- Pat. may continue previous prescribed regimens including steroids, vitamin E, pentoxiphylline, and HBOT → potential confounder? -Pat. w/ malignant brain tumors were excluded
Laser Interstitial Thermal Therapy (LITT)	Torres-Reveron et al. (2013)[95] -Retrospective case series -6 pat. w/ sympt. regrowth SRS-treated met. lesions -Bx-confirmed TN	IV	-Treatment dose: 7.5–12 W for 20–180 sec using a 15W 980nm diode laser (Visualase system) -Steroids at 10 mg q6 h immediately post-op, weaned within 2-6wks	-Durable neurological improvement until death in 4/6 cases -All pat. weaned off steroids 2mos post-LITT - 1 pat. had lesion regrowth at 3mos post-LITT, requiring steroids and surgical debulking	- Transient increase (2 wks post-LITT) in lesion size, thereafter constant decrease to new baseline by 4.5-6mos -Cont. FLAIR-signal decrease as early as 2 wks post-LITT -Radiographic resolution of lesions until death in 3/6 cases	- No procedure-related complications - All pat. d/c from hospital at 48h	- The clinical safety and feasibility of LITT as observed in this case series warrants larger prospective controlled studies to probe its potential therapeutic benefit for patients affected by TN.
	Smith et al. (2016)[97] -Retrospective design -25 pat. s/p extensive prior treatment of primary or secondary brain neoplasms -Bx-confirmed TN	III	-Used the Visualase/Medtronic system -treatment dose not specified - In all pat. ≥90% of planned ablation volume was shown to have been ablated on the postablation MRIs	-SF-36 indicated positive overall effects on mental health (P = .029) and vitality (P= .005) compared to pre-OP BL - Mean survival times post-LITT were 13.1 (WHO grade 4), 12.2 (WHO grade 3), and 19.2 mos (brain metastases).	- Mostly lesion volume increases by 2 & 6mos post-LITT; at 12mos roughly equal numbers of lesion increase vs decrease; at 2 years 5/6 of survivors had lesion volume reduction below pre-OP BL -Majority of cases had reduction in enhancement signal intensity over time	- No data on adverse events reported	- Lack of a control group precludes definite attribution of observed survival outcome and mental health improvements to the use of LITT; prospective studies / RCTs are warranted.
	Ahluwalia et al. (2018)[98]	II	- Used the NeuroBlate™ robotic laser thermotherapy	-31% of pat. could stop or reduce steroid usage at 12wks post-LITT	- PFS at 12 wks: 100% (n=11/11)	-Rate of neurol. complications was 12% overall (10.5% in TN	- Small sample size; high study drop-out rate post-LITT intervention

	- Prospective multi-center study -42 pat. w/ progressive brain met. s/p SRS (19 w/ TN, 20 w/ recurrent disease, both Bx-confirmed; 3 pat. not biopsied)		system	- no significant change in median KPS scores over 26wks post-LITT - OS of TN pat. 100% at 12wks and 82% at 26wks	- PFS at last F/U: 90.9 (n=10/11) - TN local lesion response at 12 wks: 100% CR following total ablation (n=4/4); 60% PR n=(3/5) and 40% SD (n=2/5) following subtotal ablation.	cohort); in 4/5 of these cases, LITT had been performed adjacent to eloquent brain areas w/ motor, sensory, and/or speech function.	- Limited data precludes robust conclusions regarding effects of LITT on steroid usage, QoL, cognition, and functional status
Surgical Resection	McPherson & Warnick (2004) [72] -Retrospective design -11 pat. w/ sympt. brain lesions and Hx of mostly primary brain neoplasms s/p at least one RT treatment (7 pat. had SRS) -TN clinicoradiographically suspected - post-Sx path. revealed 9 TN lesions, 2 mixed TN/PD lesions.	IV	- 9 pat. w/ failed prior high-dose steroid treatment -9 GTR, 2 STR (based on intra- or post-OP T1+Con MRI scans)	- ↓mean steroid dose at 3mos F/U (24mg/day pre-OP → 8mg/day post-OP) -KPS and neurological outcome: 4 pat. improved, 4 pat. at BL, 3 pat. worsened -No pat improved beyond 1 level in KPS	-N/A	-54% overall morbidity including both surgical complications & neurological deterioration	-Does the advantage of steroid dose reduction warrant a surgical intervention with >50% morbidity and mixed pat. outcome? -Timing of surgery for TN: Could early resection improve pat. outcome, or should surgery be reserved for cases in which conservative TN management has entirely failed (thereby accepting a likely much higher surgical risk)?

Abbreviations: AVM= arteriovenous malformation; BBB= blood brain barrier; BL= baseline; Bx= biopsy; CNS= central nervous system; CR= complete response; Ctx= chemotherapy; CVT= cerebral vein thrombosis; d/c= discharged; DVT= deep vein thrombosis; F/U= follow-up; GTR= gross total resection; H/A= headache; HBOT= hyperbaric oxygen therapy; HGG= high-grade glioma; Hx= history; KPS= Karnofsky Performance Score; LOE= level of evidence; MMSE= mini-mental state examination; mos= months; MRI= magnetic resonance imaging; pat.= patients; NGF= nerve growth factor; PD= progressive disease; PE= pulmonary embolism; PET= positron emission tomography; PR= partial response; QoL= quality of life; RT= radiotherapy; SF-36= 36-item short form survey; s/p= status post; SRS= stereotactic radiosurgery; STR= subtotal resection; Sx= surgery; TN= treatment necrosis; w/=with; wk= week; w/o= without

2. Publication 2 – Winter et al., 2020, Oncologist *(selected Top-Journal Publication)*

Winter, S.F., Vaios, E.J., Muzikansky, A., Martinez-Lage, M., Bussière, M.R., Shih, H.A., Loeffler, J., Karschnia, P., Loebel, F., Vajkoczy, P. and Dietrich, J. Defining Treatment-Related Adverse Effects in Patients with Glioma: Distinctive Features of Pseudoprogression and Treatment-Induced Necrosis. ***The Oncologist***, **2020**; *25*(8): e1221–e1232.
Impact factor 2020: ***5.260***

Journal Data Filtered By: **Selected JCR Year: 2018** Selected Editions: SCIE,SSCI
Selected Categories: **"ONCOLOGY"** Selected Category Scheme: WoS
Gesamtanzahl: 229 Journale

Rank	Full Journal Title	Total Cites	Journal Impact Factor	Eigenfactor Score
1	CA-A CANCER JOURNAL FOR CLINICIANS	32,410	223.679	0.077370
2	NATURE REVIEWS CANCER	50,529	51.848	0.074080
3	LANCET ONCOLOGY	48,822	35.386	0.146770
4	Nature Reviews Clinical Oncology	9,626	34.106	0.031890
5	JOURNAL OF CLINICAL ONCOLOGY	154,029	28.245	0.281750
6	Cancer Discovery	13,715	26.370	0.064810
7	CANCER CELL	36,056	23.916	0.091050
8	JAMA Oncology	9,488	22.416	0.048340
9	ANNALS OF ONCOLOGY	40,751	14.196	0.103620
10	Journal of Thoracic Oncology	16,601	12.460	0.038810
11	Molecular Cancer	11,626	10.679	0.021350
12	JNCI-Journal of the National Cancer Institute	36,790	10.211	0.051650
13	NEURO-ONCOLOGY	11,858	10.091	0.029150
14	LEUKEMIA	24,555	9.944	0.054750
15	SEMINARS IN CANCER BIOLOGY	6,992	9.658	0.010730
16	CLINICAL CANCER RESEARCH	78,171	8.911	0.134870
17	Trends in Cancer	1,420	8.884	0.006040
18	Journal of Hematology & Oncology	5,366	8.731	0.013620
19	Journal for ImmunoTherapy of Cancer	2,716	8.676	0.011350
20	Cancer Immunology Research	5,420	8.619	0.025380
21	CANCER RESEARCH	130,932	8.378	0.123870

Rank	Full Journal Title	Total Cites	Journal Impact Factor	Eigenfactor Score
22	CANCER TREATMENT REVIEWS	8,419	8.332	0.016930
23	Blood Cancer Journal	2,247	7.895	0.009060
24	Journal of the National Comprehensive Cancer Network	5,746	7.570	0.019940
25	BIOCHIMICA ET BIOPHYSICA ACTA-REVIEWS ON CANCER	5,226	6.887	0.008260
26	EUROPEAN JOURNAL OF CANCER	30,731	6.680	0.055220
27	CANCER AND METASTASIS REVIEWS	6,011	6.667	0.006220
28	ONCOGENE	63,249	6.634	0.074600
29	CANCER LETTERS	30,146	6.508	0.043780
30	INTERNATIONAL JOURNAL OF RADIATION ONCOLOGY BIOLOGY PHYSICS	45,833	6.203	0.046810
31	Cancers	5,196	6.162	0.011780
32	CANCER	67,408	6.102	0.071820
33	Oncogenesis	2,016	5.995	0.006360
34	Molecular Oncology	5,016	5.962	0.013590
35	Liver Cancer	769	5.944	0.002210
36	JOURNAL OF PATHOLOGY	15,994	5.942	0.021030
37	Molecular Therapy-Oncolytics	486	5.710	0.001990
38	BREAST CANCER RESEARCH	10,943	5.676	0.017310
39	Therapeutic Advances in Medical Oncology	1,377	5.670	0.003110
40	JOURNAL OF EXPERIMENTAL & CLINICAL CANCER RESEARCH	6,309	5.646	0.010260
41	STEM CELLS	21,467	5.614	0.030220
42	Gastric Cancer	4,454	5.554	0.008650
43	Clinical Epigenetics	2,900	5.496	0.009690

Rank	Full Journal Title	Total Cites	Journal Impact Factor	Eigenfactor Score
44	BRITISH JOURNAL OF CANCER	45,886	5.416	0.062950
45	OncoImmunology	7,790	5.333	0.025470
46	ONCOLOGIST	11,831	5.252	0.021610
46	RADIOTHERAPY AND ONCOLOGY	17,873	5.252	0.027470
48	CANCER EPIDEMIOLOGY BIOMARKERS & PREVENTION	19,542	5.057	0.031380
49	CELLULAR ONCOLOGY	1,382	5.020	0.001960
50	CRITICAL REVIEWS IN ONCOLOGY HEMATOLOGY	7,401	5.012	0.012890
51	INTERNATIONAL JOURNAL OF CANCER	50,955	4.982	0.072280
52	BIODRUGS	1,685	4.903	0.003370
53	CANCER IMMUNOLOGY IMMUNOTHERAPY	7,779	4.900	0.012870
54	MOLECULAR CANCER THERAPEUTICS	18,062	4.856	0.029010
55	Translational Lung Cancer Research	1,542	4.806	0.005080
56	ENDOCRINE-RELATED CANCER	6,958	4.774	0.012150
57	CANCER SCIENCE	12,382	4.751	0.016610
58	American Journal of Cancer Research	4,359	4.737	0.010100
59	CANCER GENE THERAPY	2,842	4.681	0.003200
60	BONE MARROW TRANSPLANTATION	12,031	4.674	0.020710
61	Advances in Cancer Research	2,355	4.667	0.003750
62	ONCOLOGY RESEARCH	2,368	4.634	0.003170
63	PROSTATE CANCER AND PROSTATIC DISEASES	2,144	4.600	0.005380
64	LUNG CANCER	11,738	4.599	0.020200
65	MOLECULAR CANCER RESEARCH	7,899	4.484	0.013800

The Oncologist®

Neuro-Oncology

Defining Treatment-Related Adverse Effects in Patients with Glioma: Distinctive Features of Pseudoprogression and Treatment-Induced Necrosis

Sebastian F. Winter,[a,b,f,g] Eugene J. Vaios,[a] Alona Muzikansky,[c] Maria Martinez-Lage,[d] Marc R. Bussière,[e] Helen A. Shih,[e] Jay Loeffler,[e] Philipp Karschnia,[a,h] Franziska Loebel,[f,g] Peter Vajkoczy,[f,g] Jorg Dietrich[a,b]

[a]Massachusetts General Hospital Cancer Center, [b]Department of Neurology, [c]Biostatistics Center, [d]CS Kubik Laboratory for Neuropathology, and [e]Department of Radiation Oncology, Massachusetts General Hospital and Harvard Medical School, Boston, Massachusetts, USA; [f]Department of Neurosurgery, Charité – Universitätsmedizin Berlin, corporate member of Freie Universität Berlin, Humboldt-Universität zu Berlin, Berlin, Germany; [g]Berlin Institute of Health, Berlin, Germany; [h]Department of Neurosurgery, Ludwig Maximilians University, Munich, Germany

Disclosures of potential conflicts of interest may be found at the end of this article.

Key Words. Tissue necrosis • Pseudoprogression • Treatment-related effects • Malignant glioma • Neurotoxicity

Abstract

Background. Pseudoprogression (PP) and treatment-induced brain tissue necrosis (TN) are challenging cancer treatment–related effects. Both phenomena remain insufficiently defined; differentiation from recurrent disease frequently necessitates tissue biopsy. We here characterize distinctive features of PP and TN to facilitate noninvasive diagnosis and clinical management.

Materials and Methods. Patients with glioma and confirmed PP (defined as appearance <5 months after radiotherapy [RT] completion) or TN (>5 months after RT) were retrospectively compared using clinical, radiographic, and histopathological data. Each imaging event/lesion (region of interest [ROI]) diagnosed as PP or TN was longitudinally evaluated by serial imaging.

Results. We identified 64 cases of mostly (80%) biopsy-confirmed PP (n = 27) and TN (n = 37), comprising 137 ROIs in total. Median time of onset for PP and TN was 1 and 11 months after RT, respectively. Clinically, PP occurred more frequently during active antineoplastic treatment, necessitated more steroid-based interventions, and was associated with glioblastoma (81 vs. 40%), fewer *IDH1* mutations, and shorter median overall survival. Radiographically, TN lesions often initially manifested periventricularly (n = 22/37; 60%), were more numerous (median, 2 vs. 1 ROIs), and contained fewer malignant elements upon biopsy. By contrast, PP predominantly developed around the tumor resection cavity as a non-nodular, ring-like enhancing structure. Both PP and TN lesions almost exclusively developed in the main prior radiation field. Presence of either condition appeared to be associated with above-average overall survival.

Conclusion. PP and TN occur in clinically distinct patient populations and exhibit differences in spatial radiographic pattern. Increased familiarity with both conditions and their unique features will improve patient management and may avoid unnecessary surgical procedures. ***The Oncologist*** 2020;25:1–12

Implications for Practice: Pseudoprogression (PP) and treatment-induced brain tissue necrosis (TN) are challenging treatment-related effects mimicking tumor progression in patients with brain cancer. Affected patients frequently require surgery to guide management. PP and TN remain arbitrarily defined and insufficiently characterized. Lack of clear diagnostic criteria compromises treatment and may adversely affect outcome interpretation in clinical trials. The present findings in a cohort of patients with glioma with PP/TN suggest that both phenomena exhibit unique clinical and imaging characteristics, manifest in different patient populations, and should be classified as distinct clinical conditions. Increased familiarity with

Correspondence: Sebastian F. Winter, B.Sc., Department of Neurosurgery, Charité – Universitätsmedizin Berlin, Charitéplatz 1, 10117 Berlin, Germany. Telephone: 49-17672807577; e-mail: sebastian-friedrich.winter@charite.de, sfwinter@mgh.harvard.edu; or Jorg Dietrich, M.D., Ph.D., Department of Neurology and Massachusetts General Hospital Cancer Center, Massachusetts General Hospital, Harvard Medical School, 55 Fruit St., Yawkey 9E, Boston, Massachusetts 02114, USA. Telephone: 617-643-6593; e-mail: Dietrich.Jorg@mgh.harvard.edu Received February 4, 2020; accepted for publication April 27, 2020. http://dx.doi.org/10.1634/theoncologist.2020-0085

PP and TN key features may guide clinicians toward timely noninvasive diagnosis, circumvent potentially unnecessary surgical procedures, and improve response assessment in neuro-oncology.

Introduction

Cancer treatment–related adverse effects on the brain are a major diagnostic and therapeutic challenge in neuro-oncology [1–3]. Pseudoprogression (PP) [4] and treatment-induced brain tissue necrosis (TN) [1] remain insufficiently characterized conditions increasingly encountered in patients with malignant glioma after standard-of-care chemoradiation (chemo-RT) treatment [4, 5]. Because PP and TN are frequently indistinguishable from recurrent disease on conventional imaging [6–9], many patients require tissue biopsy to guide further management, resulting in potentially unnecessary surgical interventions in a significant number of patients. Moreover, patients with treatment-related changes misclassified as progressive disease present a major challenge for appropriate clinical trial enrollment and can adversely affect outcome interpretation, especially in cases that manifest >12 weeks after radiotherapy (RT), that is, beyond the cutoff point currently stipulated in the Response Assessment in Neuro-Oncology (RANO) criteria [1, 10].

The pathology of PP and TN remains incompletely understood [11]. PP likely represents a unique clinical scenario encountered in patients with high-grade gliomas (HGGs; World Health Organization [WHO] grades III–IV) within the first few months of chemo-RT initiation [4, 12–14]. Conversely, TN commonly occurs 6 months to several years—sometimes up to a decade—after initiation of (chemo-)RT, may be irreversible and progressive, and can be associated with significant patient morbidity and mortality [1, 2, 5, 15, 16]. As both conditions are primarily distinguished based on their temporal manifestation, they are often arbitrarily defined and used interchangeably in the literature [17]. Reports of "early necrosis" (TN onset <5 months from RT completion) after temozolomide (TMZ)-based chemo-RT add further diagnostic ambiguity to this classification system in the absence of biopsy-proven features to accurately guide clinical diagnosis and management [18, 19]. Because histopathological criteria specific to each condition have not been established, histopathological findings are commonly summarized as "treatment effect." Efforts to improve noninvasive differentiation of both conditions from recurrent disease have focused on advanced functional imaging [20, 21]. Although positron emission tomography (PET) with novel amino acid tracers (e.g., fluoro-ethyl-tyrosine–PET), computed tomography perfusion studies, multivoxel magnetic resonance (MR) spectroscopy, and combined MR-PET have shown promise in augmenting diagnostic certainty, tissue biopsy remains the diagnostic gold standard [1, 11, 20]. Symptoms associated with PP and TN are commonly managed with steroids or surgical resection [4]. In addition, bevacizumab, anticoagulant drugs, and hyperbaric oxygen therapy have shown some benefit in select patients [1, 5]. Progress in the field has been limited because of a paucity of biopsy-controlled studies, the lack of high-powered prospective randomized controlled trials, and poor standardization across diagnostic imaging modalities used in studies [20, 22]. We here aim to characterize the key clinical and imaging features of PP and TN in patients with malignant glioma in an attempt to improve the current understanding of these conditions, facilitate noninvasive diagnosis of treatment-related adverse effects, and improve response assessment in neuro-oncology.

Materials and Methods

We conducted a retrospective analysis of demographic, clinical, radiographic, and histopathological data from 60 patients with brain tumors diagnosed with PP or TN after glioma therapy at the Massachusetts General Hospital (MGH) between 1997 and 2015. Patient data were obtained from an MGH institutional database. This study received institutional review board approval for all activities.

Eligibility

All 60 patients were treated at MGH and met the following eligibility criteria: (a) tissue-based diagnosis of glioma (WHO grades I–IV) between December 1997 and November 2015, (b) antineoplastic treatment (radiation with or without chemotherapy), and (c) biopsy-proven or clinico-radiographically established diagnosis of treatment-related effects based on serial imaging.

Classification of Treatment Effects

Individual treatment-related effects were primarily characterized based on the time of radiographic appearance of each lesion (hereinafter referred to as region of interest [ROI]) after RT. ROI appearance <5 months after completion of RT was defined as PP, whereas appearance ≥5 months was defined as TN, based on current consensus [1, 2, 5, 15, 16]. For comparative statistical analysis, patients were categorized accordingly and allocated to either PP or TN groups. Notably, 2 of 60 patients presented with lesions classified as "early TN" before the 5-month cutoff [18, 19]. Moreover, 4 of 60 patients presented with both biopsy-proven early PP and later TN and were therefore included in both groups. Accordingly, a total of 64 cases of treatment-related effects were identified and analyzed this cohort of 60 patients.

Variables

We collected demographic, clinical, therapeutic, and outcome parameters for each patient. Variables specific to the initial manifestation of treatment-related effects (first ROI) included characteristics of radiographic onset (time interval from RT completion; onset during active therapy vs. during surveillance), presence of new neurologic symptoms, type of treatment for PP/TN (if any), advanced diagnostic imaging results (if any), histopathological features (if biopsied), and overall number of ROIs developed throughout the condition.

Variables of interest collected for each individual ROI included time of onset after RT completion, duration until complete radiographic resolution (whenever traceable), anatomical aspects (lobar vs. deep-seated [corpus callosum, cingulate gyrus, basal ganglia, thalamus, brainstem,

Table 1. Summary of patient characteristics, treatment specifics, and clinical outcome

Patient characteristics	Total cohort	PP group	TN group	*p* value[a]
Demographics				
Sex ratio (m/f), %	56/44	67/33	49/51	.29456
Median age at diagnosis, years	53	55	47	.08752
Tumor specifics				
Tumor burden, %				.33091
Single lesion	75	67	81	
Multifocal disease	25	33	19	
Intercranial location, %				.05799
Left	42	59	30	
Central	50	41	57	
Mixed	8	0	13	
WHO grade, % (*n*)				.02750
I	1.5 (1)	0 (0)	2.7 (1)	
II	10.9 (7)	0 (0)	18.9 (7)	
III	29.7 (19)	18.5 (5)	37.8 (14)	
IV	57.8 (37)	81.5 (22)	40.5 (15)	
Molecular-genetic profile, % (*n*)				
IDH1 mutated	41.5 (17/41)	11.1 (2/18)	65.2 (15/23)	.00548
MGMT methylated	58.8 (20/34)	52.6 (10/19)	66.6 (10/15)	.61115
Clinical status, %				
With cardiovascular comorbidities	64.1	70.4	59.5	.56611
Earliest KPS (median) after initial surgery	90	90	90	.87992
Treatment specifics				
Extent of surgical resection, *n*				.64589
GTR	18	8	10	
NTR	11	6	5	
STR	20	9	11	
PR	6	4	2	
Biopsy only	5	0	5	
Regimen				
Proton/photon RT, *n*	5/59	1/26	4/33	—
With (modified) TMZ-based standard chemo-RT, % (*n*)	68.8	88.9	54.1	.01534
With concurrent Ctx, % (*n*)	76.6	92.6	64.9	.04579
Steroid use, % (*n*)	70.1 (44/62)	81.5 (22/27)	62.9 (22/35)	.24848
Bevacizumab use, % (*n*)	58.1 (36/62)	63 (17/27)	54.3 (19/35)	.67511
Clinical outcome				
OS, median (95% CI), years	6.25 (0.94–11.56)	3.0 (2.08–3.92)	Not reached[b]	<.0001
With recurrence, % (*n*)	59.6 (34/57)	83.3 (20/24)	42.4 (14/33)	.03062

[a]For difference between groups; false discovery rate–adjusted for multiple hypothesis testing.
[b]Last observation censored at 24.9 years (OS estimate at 62%).
Abbreviations: chemo-RT, chemoradiation; CI, confidence interval; Ctx, chemotherapy; f, female; GTR, gross-total resection; KPS, Karnofsky performance status; m, male; NTR, near-total resection; OS, overall survival; PP, pseudoprogression; PR, partial resection; RT, radiotherapy; TMZ, temozolomide; TN, treatment-induced brain tissue necrosis; STR, subtotal resection; WHO, World Health Organization.

cerebellum, and all periventricular locations] location; periventricular involvement; non-nodular enhancement within or around the resection cavity margins), maximum size, shortest distance from the tumor resection cavity margin, degree of radiation dose exposure, and histopathological characteristics (distinction between pure treatment effect, treatment effect with rare atypical cells, or mostly treatment effect mixed with foci of solid tumor).

Radiographic Analysis

Radiographic analysis of T1-weighted gadolinium enhanced MR imaging (MRI) sequences was carried out with each

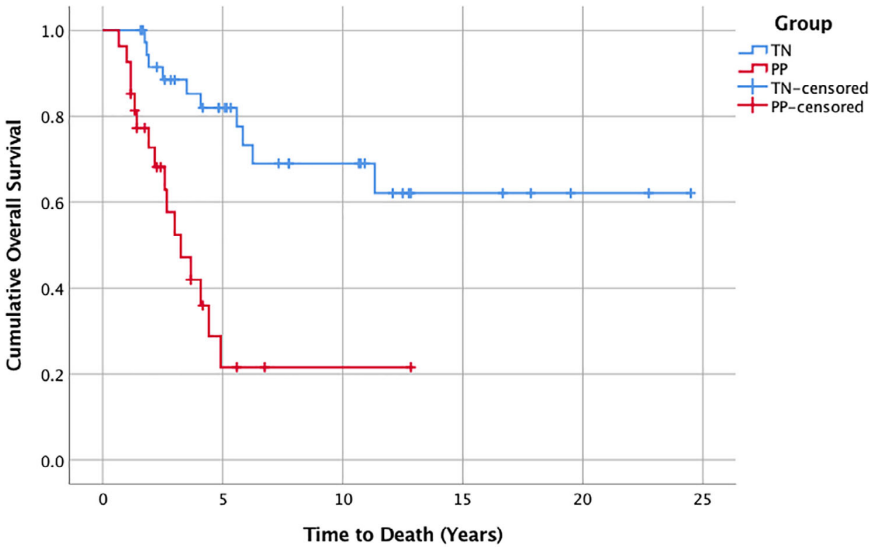

Figure 1. Kaplan-Meier survival analysis depicting PP and TN groups. PP group (red line): 16 progression events; 11 censored. Median overall survival was 3.25 years (95% confidence interval, 2.16–4.9). TN group (blue line): 10 progression events; 27 censored. Median overall survival was not reached. Last observation was censored at 24.5 years, with an overall survival estimate of 62%. For comparison, $p < .0001$.
Abbreviations: PP, pseudoprogression; TN, treatment-induced brain tissue necrosis.

patient using standard clinical imaging software. The date of appearance of diagnosed treatment-related effects was determined retrospectively and defined as the date of the first MRI demonstrating de novo contrast enhancement (T1-gadolinium sequence) in the respective anatomical location of the ROI.

Depending on sufficient availability of follow-up MRI scans, the spatiotemporal pattern of each ROI was traced longitudinally over time. Radiographic measurements of ROI area were carried out for each available MRI scan. ROIs displaying a non-nodular, circumferential enhancement pattern around the tumor resection cavity margin were excluded from size measurements.

The radiographic duration of treatment-related effects was defined for each ROI as the time of first radiographic appearance on MRI until complete radiographic resolution or last available MRI. Reasons for discontinuation of measurements included treatment (surgical resection of ROI or systemic treatment with bevacizumab) or tumor recurrence at the same ROI. The shortest ROI-to-resection cavity margin distance (mm) was measured in axial, coronal, or sagittal planes using the MRI of first radiographic appearance for each ROI. Whenever available, the patient's RT dose distribution was correlated to the anatomical location of each ROI as a proxy for the extent of radiation dose exposure (below, at, or above maximal therapeutic target value; in Gy) received. Diagnostic results from MR perfusion (MRP) and diffusion weighted imaging (DWI) studies, if available, were interpreted with respect to the patients' ROIs and included in the analysis.

Statistical Analysis

Descriptive statistics were used to analyze clinical and radiographic features for both groups. For associations between groups, p values were determined using chi-square and Fisher's exact tests for categorical variables and a Wilcoxon rank-sum test for continuous variables. All reported p values were adjusted for multiple hypothesis testing by false discovery rate; statistical significance was considered as $p < .05$. The Kaplan-Meier (KM) method was used to calculate median overall survival (OS); median follow-up time was calculated based on the reverse KM estimator approach.

In order to statistically compare radiographic and histopathological features of individual ROIs between patient groups, a logistic regression analysis using a univariate generalized estimating equation (GEE) model, predicting affiliation with TN group as the function of the tested variable and adjusting for repeated observations within a patient, was used. GEE-based analysis was purposefully limited to eight preselected variables of interest and statistical significance was reported using p values and parameter estimates for directionality.

Results

A total of 64 cases of treatment-related effects, classified as either PP ($n = 27$) or TN ($n = 37$), were identified and analyzed. Diagnosis of treatment-related effects was mostly secured by tissue biopsy; the remainder of cases (20%) were confirmed through longitudinal clinico-radiographic follow-up. All patients had previously undergone RT (most with concurrent and sequential chemotherapy), predominantly for HGG diagnosis (87.5%). Baseline patient performance status at time of diagnosis was generally high (median Karnofsky performance status [KPS] after initial surgery, 90/100); cardiovascular comorbidities were present in almost two-thirds of patients. Incidence of recurrence was 60%, and median

Table 2. Characteristics of first ROI identified as treatment effect

Characteristics of first ROI	Total cohort	PP group	TN group	*p* value[a]
Spatiotemporal radiographic features				
Onset after RT completion, median (range), months	6.5 (0–239)	1.0 (0–4)	11.0 (3–239)	<.00001
Periventricular location, %	48.4	33.3	59.5	.09098
Ring-like enhancement around RC, %	37.5	70.4	13.5	.00009
Functional imaging features, % (*n*)				
With functional imaging	77.4 (48/62)	92.0 (23/25)	67.6 (25/37)	.07587
Elevated rCBV in MRP	75.0 (30/40)	88.8 (16/18)	63.6 (14/22)	.19976
Restricted diffusion in DWI	54.1 (20/37)	57.7 (8/14)	52.2 (12/23)	.75603
Clinical features				
Onset during active treatment, %	54.7	85.2	32.4	.00044
Amount of Ctx received prior to onset, median (IQR), months	3.0 (1–9)	1.0 (1–3)	7.5 (2–12)	.00574
With concurrent new symptoms, % (*n*)	65.6 (40/61)	69.2 (18/26)	62.9 (22/35)	.82835
Symptoms related to ROI, % (*n*)	60.0 (24/40)	59.1 (13/22)	61.1 (11/18)	.61115
Receiving any treatment for ROI, %	78.1	88.9	70.2	.20967
Receiving steroids, %	54.7	74.1	40.5	.03592
Receiving bevacizumab, %	18.8	11.1	24.3	.29698
Receiving surgical debulking, %	35.9	51.9	24.3	.07991
Histopathological features, % (*n*)				.03592
Treatment effect only	16.0 (8/50)	0.0 (0/24)	30.8 (8/26)	
Treatment effect with rare atypical cells	62.0 (31/50)	70.8 (17/24)	53.8 (14/26)	
Treatment effect with foci of solid tumor	22.0 (11/50)	29.2 (7/24)	15.4 (4/26)	

[a]For difference between groups; false discovery rate–adjusted for multiple hypothesis testing.
Abbreviations: Ctx, chemotherapy; DWI, diffusion weighted imaging; IQR, interquartile range; MRP, magnetic resonance perfusion; PP, pseudoprogression; RC, resection cavity; rCBV, relative cerebral blood volume; ROI, region of interest; RT, radiotherapy; TN, treatment-induced brain tissue necrosis.

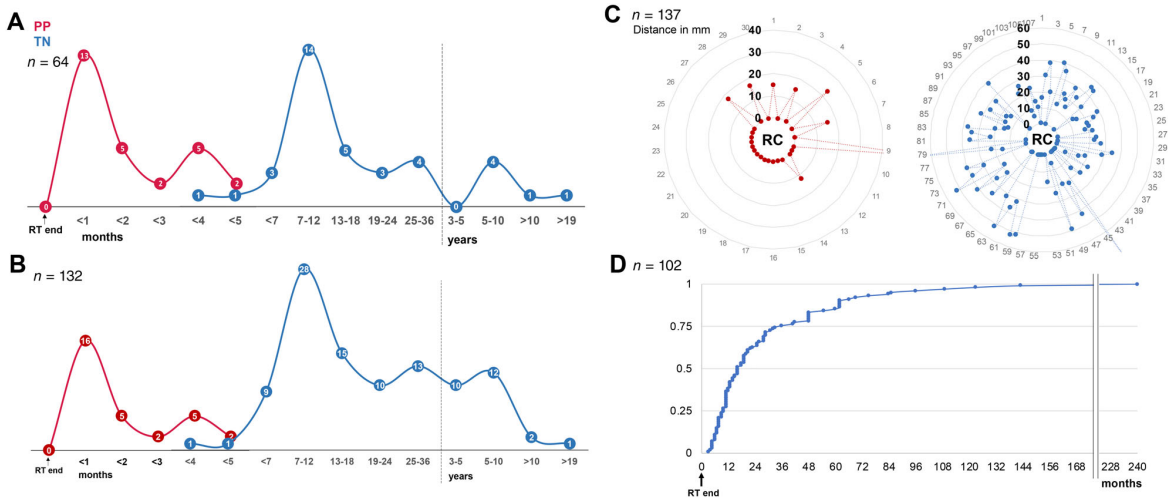

Figure 2. Spatiotemporal radiographic pattern of PP and TN lesions. **(A):** Temporal distribution of first region of interest (ROI) manifestation on magnetic resonance imaging (MRI) after RT completion. **(B):** Temporal distribution of overall ROI manifestation on MRI after RT completion. **(C):** Spatial distribution of ROIs relative to the tumor resection cavity (RC), illustrating shortest ROI-to-RC distances for each ROI. **(D):** Cumulative frequency of TN group ROI onset latency from RT completion.
Abbreviations: PP, pseudoprogression; RT, radiotherapy; TN, treatment-induced brain tissue necrosis.

OS was 6.25 (95% confidence interval, 0.94–11.56) years (Table 1). To characterize putative differences in clinical and spatiotemporal radiographic features between both types of treatment-related effects, an in-depth comparative analysis between patients with PP versus those with TN was carried out.

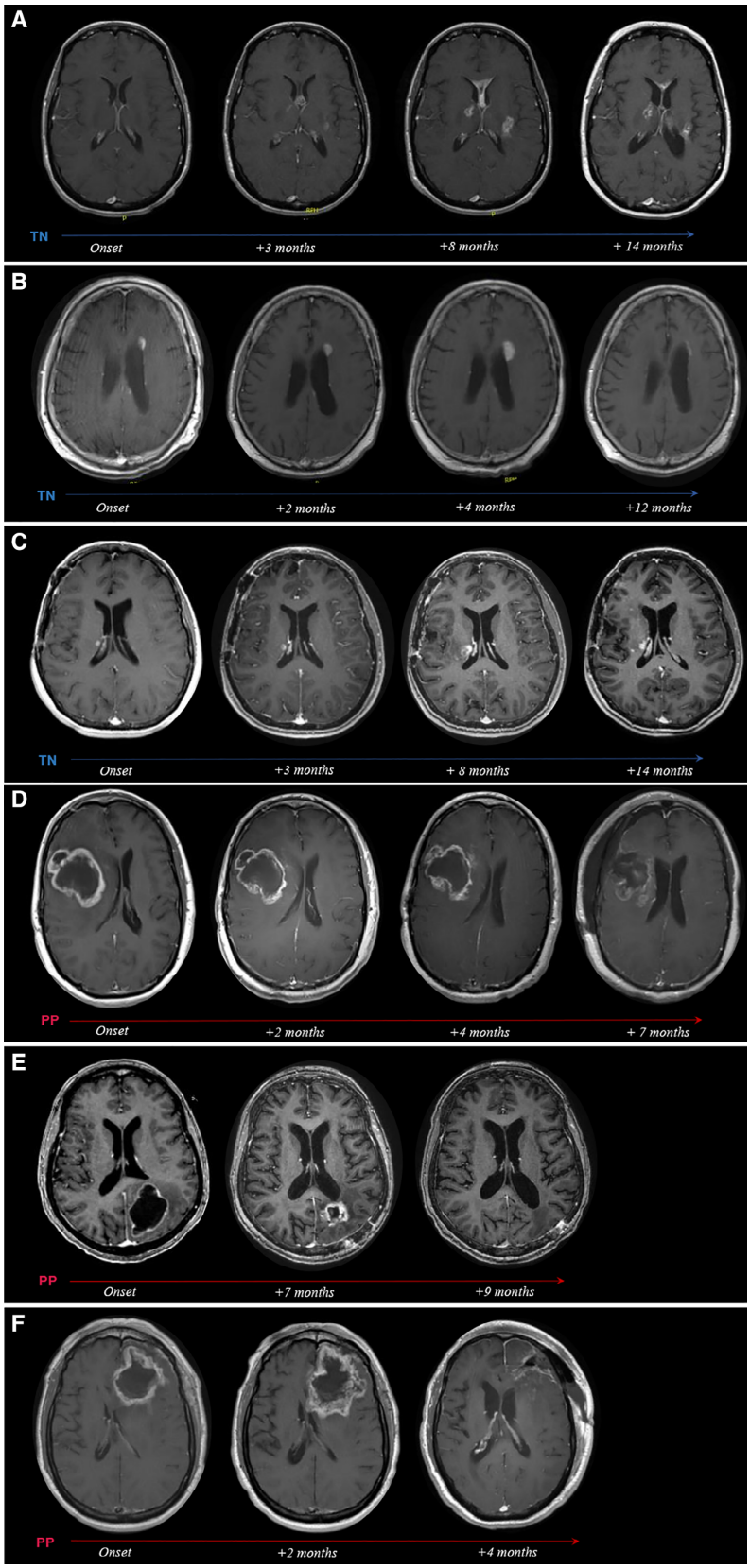

Differences in Patient Characteristics, Treatment Specifics, and Clinical Outcome

Age, gender, and KPS did not significantly differ between patients with PP and TN, although the former group was older (median age at time of diagnosis, 55 vs. 47 years) and had a slightly higher incidence of cardiovascular comorbidities (70.4 vs. 59.5%). The PP group had a significantly larger proportion of glioblastoma cases (81.5 vs. 40.5%; $p < .002$), with a higher fraction of tumors localized to left cerebral hemispheres that trended toward significance (59 vs. 30%; $p = .058$). Analysis of associated tumor molecular-genetic profiles in this group revealed considerably fewer *IDH1* mutations (11.1 vs. 65.2%; $p < .006$) and a slightly lower incidence of *MGMT* promoter methylation (52.6 vs. 66.6%), as compared with the TN group (Table 1).

Most cases in both groups were treated with open surgical resection followed by standard chemo-RT treatment. In line with the high incidence of glioblastoma multiforme (GBM; 81.5%) observed in patients with PP, concurrent chemotherapy ($p < .05$) and TMZ-based standard chemo-RT regimens ($p = .015$) were more frequently administered in this group. In addition, steroid-based interventions and bevacizumab use were slightly more pronounced. Median follow-up times for PP and TN groups were 5.6 and 10.7 years, respectively. Compared with the TN group, the rate of disease recurrence in patients with PP was nearly twice as high ($p = .03$; Table 1). The median OS on Kaplan-Meier survival analysis was 3.25 years for patients with PP. Patients in the TN group survived substantially longer (median OS not reached; 62% survival estimate, last observation censored at 24.5 years; $p < .0001$; Fig. 1). The 5-year survival rates for PP and TN groups were 26% and 82%, respectively.

Differences in Initial Clinico-Radiographic Presentation

Analysis of both spatiotemporal radiographic pattern and biopsy features of patients' first appearing lesion ("first ROI") revealed significant differences between PP and TN groups (Table 2).

Although group allocation per se was based on temporal stratification (5-month cutoff point), both PP and TN were found to exhibit specific temporal incidence peaks. As such, most PP lesions developed within weeks after RT completion (median onset, 1 month), thus more often manifesting during active antineoplastic treatment (85 vs. 32%; $p < .0005$). Conversely, TN incidence peaked between 7 and 12 (median, 11) months after RT, mostly in periods of imaging surveillance. In several patients ($n = 6$), TN first manifested in a late-delayed manner at >5 years, including two cases at 11.9 and 19.9 years, after RT (Fig. 2A).

Radiographically and anatomically, PP predominantly developed around the tumor resection cavity (RC) as a single, nonnodular, ring-like enhancing structure (70.4 vs. 13.5%; $p < .0001$; Fig. 3D–F), whereas TN typically first presented as one or multiple small nodular lesions located at a distance from the RC (Fig. 3A–C) and with greater preference for the periventricular white matter (59.5 vs. 33.3%; $p = .09$; Table 2). Although approximately 60% of patients in both groups developed new ROI-associated neurological symptoms, patients with PP were significantly more likely to receive steroid-based treatment (74.1 vs. 40.5%; $p < .04$) and underwent therapeutic surgical debulking twice as often (51.9 vs. 24.3%). In addition, this group was more likely to receive advanced diagnostic imaging, including MRP and DWI (92.0 vs. 67.6%) to assess radiographically suspicious ROIs, prior to biopsy. Interestingly, in both groups, results from advanced imaging were often suggestive of disease progression rather than treatment-related effects (Table 2). Histopathological analysis of initial ROIs revealed that PP specimens were significantly more likely to contain malignant elements (i.e., treatment effect mixed "with rare atypical cells" or "with foci of solid tumor") than biopsied TN lesions ($p < .04$; Table 2).

Differences in Spatiotemporal Radiographic Lesion Pattern

Longitudinal radiographic evaluation of the 64 PP and TN cases identified a total of 137 individual ROIs ($n = 62$ biopsied; $n = 75$ clinico-radiographic diagnosis). Intergroup

Figure 3. Radiographic evolution of TN and PP over time. T1+ contrast axial magnetic resonance imaging scans from representative patients with TN **(A–C)** and PP **(D–F)** depicting radiographic evolution of treatment-related changes over time. **(A):** Woman aged 37 years with anaplastic oligoastrocytoma status post (s/p) chemoradiation. Onset of biopsy-confirmed TN at 13 months after radiotherapy (RT), presenting as multiple contrast-enhancing lesions (seven total) associated with new neurological symptoms. Gradual regression of lesions under bevacizumab treatment. **(B):** Man aged 64 years with anaplastic astrocytoma s/p RT. At 28 months after RT, onset of multiple periventricularly located, contrast-enhancing lesions (four total) was noted. Follow-up by imaging surveillance showed near total radiographic resolution of all lesions within 1 year of onset without treatment. The dominant left periventricular enhancing lesion is highlighted in the serial scans. **(C):** Woman aged 43 years with anaplastic astrocytoma s/p chemoradiation. Onset of biopsy-confirmed TN at 11 months after chemoradiation (chemo-RT), presenting as multiple contrast-enhancing lesions (nine total) associated with new neurological symptoms, managed with steroids. Eight of nine lesions radiographically resolved within 6 to 26 months of onset. The dominant right periventricular lesion is shown. **(D):** Man aged 39 years with glioblastoma multiforme (GBM) s/p chemoradiation. Increased contrast enhancement around the resection cavity (RC) noted at 3 months after chemo-RT during active antineoplastic treatment. The lesion was associated with new neurological symptoms and was managed with steroids and surgical debulking at 7 months after onset, revealing extensive tissue necrosis. **(E):** Woman aged 65 years with GBM s/p chemoradiation. Increased contrast enhancement around the RC noted at 1 month after chemo-RT during active antineoplastic treatment. The lesion was associated with new neurological symptoms, managed with steroids, partially debulked (4 months after onset), and resolved at 9 months after onset. Histopathology revealed predominant tissue necrosis with few and scattered residual tumor cells. **(F):** Man aged 66 years with GBM s/p chemoradiation. Increased contrast enhancement around the RC noted at 1 month after chemo-RT during active antineoplastic treatment. The lesion was associated with new neurological symptoms, managed with steroids, and fully resected at 4 months after onset, revealing extensive tissue necrosis.
Abbreviations: PP, pseudoprogression; TN, treatment-induced brain tissue necrosis.

Table 3. ROI spatiotemporal radiographic and histopathological characteristics

ROI characteristics	Total cohort	PP group	TN group	*p* value (estimate)[a]
ROI characteristics				
Analyzed ROIs, *n*	137	30	107	
Biopsied, *n*	62	26	36	
Type of biopsy, %				.3580 (−0.7338)
Needle biopsy	40.3	19.2	55.6	
Open resection	53.2	80.8	33.3	
Autopsy	7.7	0.0	11.1	
Not biopsied, but spatiotemporal radiographic pattern similar to a biopsied ROI in same patient, *n*	45	1	44	
Clinico-radiographic diagnosis only, *n*	30	3	27	
Spatiotemporal radiographic features				
Onset after RT completion, median (IQR), months	11 (5–28)	0 (0–2)	16 (10–36)	.0010 (2.4756)
Locations, %				.0001 (−1.4993)
Deep-seated	33.6	6.7	41.1	
Lobar	57.7	73.3	53.3	
Both	8.8	20.0	5.6	
Periventricular location, %	40.2	30.0	43.0	.2600 (0.5651)
Ring-like enhancement around RC, %	18.3	63.3	5.6	<.0001 (−3.3699)
Max. size, median (IQR), cm^2	0.99 (0.16–4.42)	3.70 (1.08–7.50)	0.55 (0.15–3.36)	.1672 (−0.0341)
Shortest distance from RC, median (IQR), mm	16.5 (0.0–27.0)	0.0 (0.0–12.0)	21.5 (10.0–31.0)	.0011 (0.0902)
Correlation to RT dose distribution, %				
Located in main radiation field	98.9 (87/88)	100 (25/25)	98.4 (62/63)	
Radiation dose received, %				
Less than max. therapeutic dose	11.5	8.3	13.0	
Equal to max. therapeutic dose	42.3	29.2	48.1	
More than max. therapeutic dose	46.2	62.5	38.9	
Histopathological features, % (*n*)				.0084 (−1.4779)
Treatment effect only	24.2 (15/62)	0.0 (0/26)	41.7 (15/36)	
Treatment effect with rare atypical cells	56.5 (35/62)	73.1 (19/26)	44.4 (16/36)	
Treatment effect with foci of solid tumor	19.4 (12/62)	26.9 (7/26)	13.9 (5/36)	

[a]Based on a generalized estimating equation model, adjusted for multiple observations per patient, and applied to eight preselected variables of interest.

Abbreviations: IQR, interquartile range; PP, pseudoprogression; RC, resection cavity; ROI, region of interest; RT, radiotherapy; TN, treatment-induced brain tissue necrosis.

comparison at the level of individual ROIs (Table 3) revealed significant differences in both spatial and temporal radiographic lesion pattern. ROIs in the PP group (n = 30) predominantly appeared as unifocal lesions (81.4%), exhibiting a non-nodular, ring-like enhancement pattern at the tumor RC margin with greater frequency than ROIs in patients with TN (63.3 vs. 5.6%; $p < .0001$; Fig. 2C). By contrast, TN-related ROIs (n = 107) were typically nodular, located in deep-seated brain regions ($p = .0001$) at a variable distance from the tumor RC (median, 21.5 mm; range, 0–78 mm; Fig. 2C), and more numerous (median, 2 vs. 1 ROIs; $p = .01$; Table 3). Accordingly, most patients with TN developed multiple nodular ROIs over time (interquartile range, 1–4; max, 12), with approximately one-fourth of ROIs manifesting beyond 3 years after RT completion (Fig. 2B, D).

Whenever possible, individual ROIs were traced longitudinally from time of onset until full radiographic resolution or last available MRI scan (as shown in Fig. 3). For PP-related ROIs, this measurement was mostly precluded as 80% (n = 24/30) of PP lesions were removed surgically and/or treated with antiangiogenics after a median of 4 months after lesion onset. By comparison, only 35% (n = 35/100) of ROIs in the TN group received treatment, after a median of 8 months. The remainder either fully resolved radiographically (36%; median interval, 11.5 months) or persisted until the last available MRI scan (29%; median interval, 15 months).

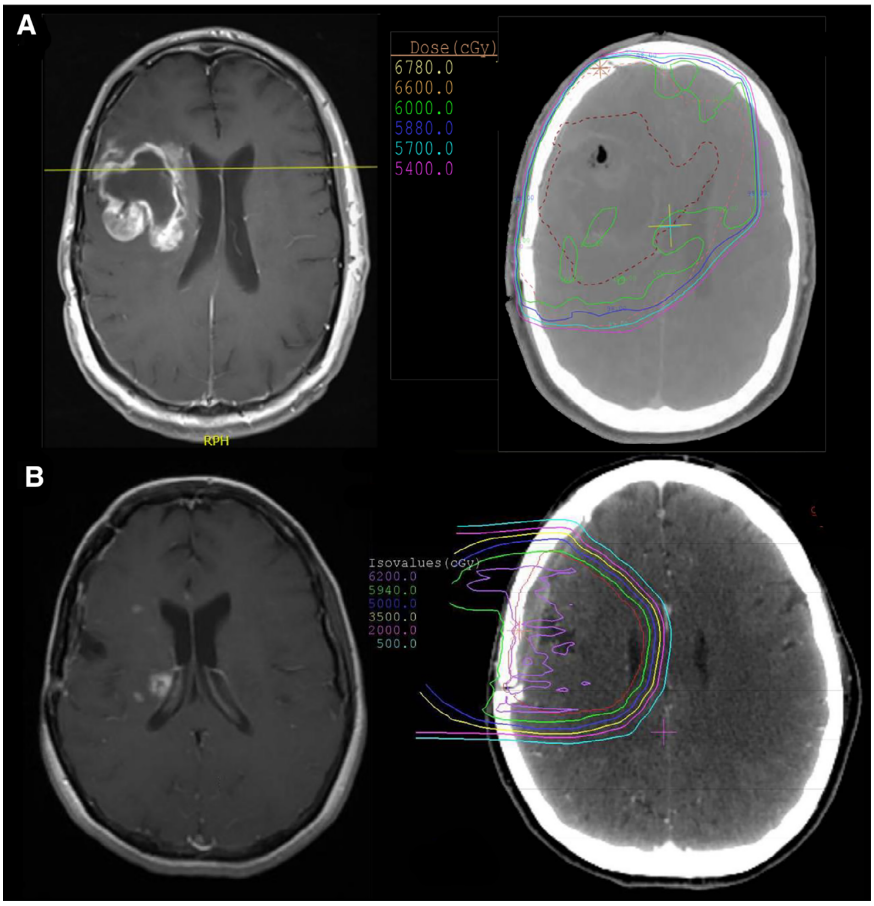

Figure 4. Typical observed radiographic features of treatment-induced brain tissue necrosis (TN) and pseudoprogression (PP). **(A):** Axial T1+ contrast magnetic resonance imaging (MRI) (left) showing a non-nodular focus of enhancement around the tumor resection cavity (RC) in the right frontal lobe, first manifesting at 3 months after radiotherapy (RT), consistent with PP. Corresponding radiotherapy dose distribution overlay on axial computed tomography (right) demonstrates the main radiation field encompassing the RC and surrounding brain parenchyma (60 Gy; green line). **(B):** T1+ contrast MRI (left) showing multiple small nodular foci of enhancement located medially to the RC in the right frontal region with involvement of the periventricular white matter, manifesting at 11 months after RT, consistent with TN. RT dose distribution overlay on axial computed tomography (right) demonstrates prior exposure of these regions of interest to the main radiation field (59.4 Gy; green line).

A correlative analysis between ROI anatomical location and available RT dose distribution curves (as shown in Fig. 4) revealed that 98.9% (n = 87/88) of ROIs were located within the main radiation field, with 46% of ROIs correlating spatially to areas of supratherapeutic radiation maxima (Table 3). Finally, among biopsied ROIs (PP, n = 26; TN, n = 36), TN lesions were found to contain fewer malignant elements (p = .008). Moreover, over one-third of patients with TN underwent a secondary biopsy of the same or a different ROI at a later time point, reconfirming treatment effects.

Discussion

Therapeutic management of patients with brain tumors is frequently complicated by PP and TN. However, diagnostic imaging criteria (including RANO) and clinical guidelines for adequate management remain insufficient. Long-term outcome data represent another area of uncertainty. With this study, we characterize 60 patients with glioma who developed PP or TN as a consequence of brain tumor therapy. Consistent with the clinical literature, we found that treatment-related effects occurred predominantly in patients with HGG after treatment with (TMZ-based) chemo-RT [4, 18, 23]; presented with either early or late radiographic onset (classified here as PP and TN) [2, 15, 16]; were frequently associated with new neurological symptoms [24, 25]; and were treated primarily with steroids, surgical debulking, and/or antiangiogenics [1, 26–28]. Nearly two-thirds of patients had underlying cardiovascular comorbidities, a potential risk factor for treatment-related effects [1]. Presence of either PP or TN appeared to be associated with above-average overall survival.

Comparative analysis by temporal stratification of treatment-related effects suggests that PP and TN are distinct conditions with unique features. Accordingly, we

found that both conditions exhibit significant differences in clinical course and spatiotemporal radiographic pattern and appear to affect distinct patient populations. As such, PP predominantly occurred in patients with GBM, during active antineoplastic treatment in the weeks to few months after chemo-RT, and typically presented on MRI as a unifocal, non-nodular, contrast-enhancing lesion around the RC margin. Affected patients frequently required steroids and surgical debulking and had a worse clinical outcome compared with those with TN. These findings corroborate previous descriptions of PP [4, 14] and support the notion that, rather than merely denoting a radiographic phenomenon, PP should be classified as a distinct clinical condition in neuro-oncology that requires timely diagnosis and appropriate clinical management [2]. Although PP is reportedly enriched in patients with *MGMT* promoter methylated tumors [29, 30], we found that *MGMT* promoter methylation was present in just over half of analyzed tumors in the PP group. Both presence of PP and *MGMT* promoter methylation have been proposed as potential prognostic markers for improved clinical outcome [12, 14, 29, 31, 32]. The observed median OS of 3.25 years in the PP group (81.5% GBM fraction) compares favorably with that historically reported for patients with GBM (approximately 15 months after surgery and chemoradiation) [33], which may support this assumption. Whether and how *IDH1* mutational status affects incidence of PP has been discussed controversially, with some reports suggesting that presence of IHD1 mutation could serve as a possible biomarker for PP [34, 35]. In our cohort, only 11% of patients with PP were found to have *IDH1*-mutated tumors. Our observations are in line with a recent study by Mohammadi et al., who found lower absolute rates of PP expression in patients with GBM with *IDH1*-mutated tumors [36].

Characteristically, TN was enriched in patients with grade III and IV gliomas (mostly *IDH1* mutated and *MGMT* promoter methylated), typically with onset between 7 and 12 months after RT [1], that is, during periods of imaging surveillance. We found that a number of patients presented with either "early necrosis" (n = 2; onset <5 months after RT) [18] or late-delayed TN (n = 6; onset >5 years after RT) [15, 16]. Although the former is most likely a consequence of the increased use of TMZ-based chemo-RT regimens and their radiosensitizing properties [18], the latter may represent a separate form of TN, with distinct pathophysiology, encountered in long-term survivors [1]. Some studies suggest that early TN may predict more durable treatment response and thus potentially improve clinical outcome [18, 21, 37]. We found that the majority of patients with TN were long-term survivors. The comparatively better clinical outcome in this group might be attributed to significant differences in primary diagnosis (GBM fraction 40.5% vs. 81.5%) and incidence rates of tumor *IDH1* mutational status (65 vs. 11%). Moreover, an implicit time bias from including a number of long-term survivors who presented with late-delayed TN is likely a contributing factor, although the vast majority (86%) of TN cases developed relatively early, that is, within 3 years after RT. Although *IDH1* mutation has been identified as an independent positive prognostic biomarker for survival in patients with glioma [38, 39], the relationship between *IDH1* mutational status and development of TN, as with PP, remains understudied. Whether presence of *IDH1* mutation constitutes a direct causal risk factor for TN development or, rather, indirectly increases the probability for TN development by contributing to prolonged OS is unclear.

Radiographically, the manifestation of TN differed from that of PP. TN characteristically presented as multiple small nodular contrast-enhancing lesions, frequently located in the periventricular white matter and/or in other deep-seated brain regions at varying distances from the RC. This corroborates the hypothesis that the delicately vascularized periventricular white matter may serve as a predilection site for TN [4, 6, 37]. Our longitudinal analysis at the level of individual ROIs suggests that some TN lesions persist in a progressive, potentially irreversible manner that may require therapeutic intervention, whereas other lesions are transient and could be sufficiently managed by imaging surveillance. Our findings are in line with recent observations by Van West et al. [37], who analyzed treatment-related effects in patients with low-grade glioma (LGG). In this study, onset of what the authors referred to as "pseudoprogression" occurred in 20% of patients with LGG and after a median of 12 months after RT, presented as asymptomatic, small nodular lesions with frequent location in the ventricle wall, with an average duration of 6 months until radiographic resolution [37]. Concluding that this clinico-radiographic picture differs from what has been described for early pseudoprogression in patients with HGG, the authors reasonably speculated that the observed lesions "could be small areas of radiation necrosis" [37].

Our correlative spatial analysis using RT dose distribution curves revealed that PP and TN lesions almost exclusively developed in the main prior radiation field, that is, those areas previously exposed to therapeutic radiation maxima (42.3%) or supratherapeutic radiation "hot spots" (46.2%). This finding underscores the diagnostic utility of RT dose distribution curves in guiding management of patients with glioma with suspicious, newly enhancing lesions on MRI. It also confirms the central role of RT in the development of treatment-related effects and highlights a clear need for improved protective strategies directed at sparing healthy brain parenchyma from radiation-induced neurotoxicity.

Of note, analysis of TN and PP lesions by MRP and DWI was frequently suggestive of disease progression. Although this finding may highlight the limitations of current advanced imaging modalities in reliably differentiating these conditions from recurrent disease [1, 20], we used a rather conservative binary approach to interpret MRP and DWI imaging reports in this study. Accordingly, evidence of elevated relative cerebral blood volume (or restricted DWI) at individual ROIs—whether mild or substantial—was classified as suggestive of progressive disease. Nonetheless, most patients in our cohort eventually underwent tissue biopsy in order to resolve diagnostic ambiguities on functional imaging. Of note, 25% of biopsy-confirmed PP lesions contained ROIs with "mixed pathology," defined as treatment-related changes with small foci of residual tumor on histopathological analysis [1, 21]. This comparatively higher

incidence of residual malignant elements in PP lesions is likely the result of (a) their direct proximity to the tumor RC margin and (b) their earlier manifestation, that is, during ongoing antineoplastic treatment.

One limitation of this study is that histopathological findings from biopsied lesions were commonly summarized as "treatment effect." Histopathological diagnosis and classification have been limited because of a lack of standardized criteria or guidelines to qualitatively assess and describe different types of treatment-related effects [1]. The distinct clinico-radiographic features of PP and TN strongly suggest that these entities differ in their underlying pathophysiology. For instance, local tissue inflammation and vascular changes produced by surgery-related parenchymal injury could be implicated as plausible mechanisms that drive frequent PP development around the RC margin. Additionally, treatment-induced apoptosis of seeded residual, nonenhancing tumor foci around the RC may fuel the inflammatory environment (with secondary edema and abnormal vessel permeability) thought to contribute to the development of PP [4]. By contrast, the mechanisms driving TN development and their dynamics are likely quite different, as TN lesions mostly occurred during periods of surveillance and in areas previously considered healthy brain parenchyma. The proposed pathological changes implicated in TN—parenchymal necrosis, gliosis, cellular infiltrates, vascular abnormalities, and fibrinous exudates—develop over longer periods of time and are likely more permanent [11]. Robust characterization of putative histopathological differences (e.g., tissue architecture, vascular pathology, cellular inflammatory profile, presence of malignant elements) between PP and TN is warranted and could yield new insights about the pathomechanisms of either condition, with potentially important therapeutic implications.

Our study has several strengths and limitations. Patient selection and data collection were carried out retrospectively, with a focus on patients with glioma with biopsy-confirmed treatment-related effects. Based on the typical manifestation ranges described for both conditions [1, 2, 4, 5, 15, 16], a temporal cutoff point was defined and used as a proxy for patient stratification into PP and TN diagnosis groups. Although we cannot rule out the possibility of diagnostic inaccuracies caused by this strategy, the diagnosis allocated to each patient was carefully reviewed, contextualized with available clinical and radiographic information, and corrected in two instances classified as "early necrosis." Despite the fact that tissue biopsy remains the diagnostic gold standard for PP and TN, there remains a lack of biopsy-confirmed studies in which patients were radiographically diagnosed with treatment-related effects [1]. To our knowledge, our study is the first in which a majority (80%) of cases of treatment-related effects were confirmed by tissue biopsy. Thus, the observed unique characteristics of PP and TN offer insight into their typical clinical course and radiographic spatiotemporal pattern in affected neuro-oncological patients. Moreover, our finding that both conditions preferentially occur in distinct patient populations (i.e., in specific clinical settings) may improve clinician awareness of these distinct conditions and guide patient management. Additionally, our findings suggest that RT dose distribution curves, which correlate with PP and TN, can serve as an important diagnostic tool for the interpretation of suspicious, newly enhancing lesions. Finally, our survival data may support previous studies suggesting that development of treatment-related effects could indicate a more durable treatment response and improved clinical outcome. A comparative analysis with matched controls is warranted to assess whether presence of PP or early TN could indeed serve as an independent positive prognostic biomarker in patients with glioma.

Conclusion

PP and TN appear to occur in clinically distinct patient populations that differ in tumor characteristics, treatment regimen, and clinical outcome. Both conditions exhibit unique features with respect to both clinical course and spatiotemporal radiographic pattern. Use of RT dose distribution curves for delineation of the prior radiation field may serve as an important diagnostic tool to differentiate these conditions from recurrent disease. In line with previous reports, the presence of either PP or TN may be associated with improved overall survival. Increased clinician familiarity with these distinct brain cancer treatment–related conditions and their unique features will improve early detection and diagnosis as well as patient management and thus may circumvent unnecessary surgical procedures.

Acknowledgments

The authors wish to thank Mia S. Bertalan for valuable technical assistance with accessing the Massachusetts General Hospital institutional database used for this study. Portions of this manuscript were presented by S.FW. at the 2018 Society for Neuro-Oncology Scientific Meeting in New Orleans, LA, and the 2019 American Academy of Neurology Annual Meeting in Philadelphia, PA.

Author Contributions

Sebastian F. Winter, Eugene J. Vaios, Alona Muzikansky, Maria Martinez-Lage, Marc R. Bussière, Helen A. Shih, Jay Loeffler, Philipp Karschnia, Franziska Loebel, Peter Vajkoczy, Jorg Dietrich

Conception/design: Sebastian F. Winter, Jorg Dietrich

Provision of study material or patients: Marc R. Bussière, Helen A. Shih, Jay Loeffler, Jorg Dietrich

Collection and/or assembly of data: Sebastian F. Winter

Data analysis and interpretation: Sebastian F. Winter, Eugene J. Vaios, Alona Muzikansky, Maria Martinez-Lage, Marc R. Bussière, Helen A. Shih, Jay Loeffler, Philipp Karschnia, Franziska Loebel, Peter Vajkoczy, Jorg Dietrich

Manuscript writing: Sebastian F. Winter, Eugene J. Vaios, Alona Muzikansky, Maria Martinez-Lage, Marc R. Bussière, Helen A. Shih, Jay Loeffler, Philipp Karschnia, Franziska Loebel, Peter Vajkoczy, Jorg Dietrich

Final approval of manuscript: Sebastian F. Winter, Eugene J. Vaios, Alona Muzikansky, Maria Martinez-Lage, Marc R. Bussière, Helen A. Shih, Jay Loeffler, Philipp Karschnia, Franziska Loebel, Peter Vajkoczy, Jorg Dietrich

Disclosures

The authors indicated no financial relationships.

References

1. Winter SF, Loebel F, Loeffler J et al. Treatment-induced brain tissue necrosis: A clinical challenge in neuro-oncology. Neuro Oncol 2019 [Epub ahead of print].

2. Dietrich J, Winter S, Klein J. Neuroimaging of brain tumors: Pseudoprogression, pseudoresponse, and delayed effects of chemotherapy and radiation. Semin Neurol 2017;37:589–596.

3. Karschnia P, Parsons MW, Dietrich J. Pharmacologic management of cognitive impairment induced by cancer therapy. Lancet Oncol 2019; 20:e92–e102.

4. Brandsma D, Stalpers L, Taal W et al. Clinical features, mechanisms, and management of pseudoprogression in malignant gliomas. Lancet Oncol 2008;9:453–461.

5. Eisele SC, Dietrich J. Cerebral radiation necrosis: Diagnostic challenge and clinical management. Rev Neurol 2015;61:225–232.

6. Kumar AJ, Leeds NE, Fuller GN et al. Malignant gliomas: MR imaging spectrum of radiation therapy- and chemotherapy-induced necrosis of the brain after treatment. Radiology 2000;217: 377–384.

7. Mullins ME, Barest GD, Schaefer PW et al. Radiation necrosis versus glioma recurrence: Conventional MR Imaging clues to diagnosis. AJNR Am J Neuroradiol 2005;26:1967–1972.

8. Dequesada IM, Quisling RG, Yachnis A et al. Can standard magnetic resonance imaging reliably distinguish recurrent tumor from radiation necrosis after radiosurgery for brain metastases? A radiographic-pathological study. Neurosurgery 2008;63:898–904.

9. Ellingson BM, Chung C, Pope WB et al. Pseudoprogression, radionecrosis, inflammation or true tumor progression? Challenges associated with glioblastoma response assessment in an evolving therapeutic landscape. J Neurooncol 2017;134:495–504.

10. Wen PY, Chang SM, Van den Bent MJ et al. Response assessment in neuro-oncology clinical trials. J Clin Oncol 2017;35:2439–2449.

11. Perry A, Schmidt RE. Cancer therapy-associated CNS neuropathology: An update and review of the literature. Acta Neuropathol 2006; 111:197–212.

12. Kucharczyk MJ, Parpia S, Whitton A et al. Evaluation of pseudoprogression in patients with glioblastoma. Neuro-Oncology Pract 2016;4: npw021.

13. Parvez K, Parvez A, Zadeh G. The diagnosis and treatment of pseudoprogression, radiation necrosis and brain tumor recurrence. Int J Mol Sci 2014;15:11832–11846.

14. Taal W, Brandsma D, De Bruin HG et al. Incidence of early pseudo-progression in a cohort of malignant glioma patients treated with chemoirradiation with temozolomide. Cancer 2008;113:405–410.

15. Tofilon PJ, Fike JR. The radioresponse of the central nervous system: A dynamic process. Radiat Res 2000;153:357–370.

16. Giglio P, Gilbert MR. Cerebral radiation necrosis. Neurologist 2003;9:180–188.

17. Kruser TJ, Mehta MP, Robins HI. Pseudoprogression after glioma therapy: A comprehensive review. Expert Rev Neurother 2013; 13:389–403.

18. Chamberlain MC, Glantz MJ, Chalmers L et al. Early necrosis following concurrent Temodar and radiotherapy in patients with glioblastoma. J Neurooncol 2007;82:81–83.

19. Peca C, Pacelli R, Elefante A et al. Early clinical and neuroradiological worsening after radiotherapy and concomitant temozolomide in patients with glioblastoma: Tumour progression or radionecrosis? Clin Neurol Neurosurg 2009; 111:331–334.

20. Verma N, Cowperthwaite MC, Burnett MG et al. Differentiating tumor recurrence from treatment necrosis: A review of neuro-oncologic imaging strategies. Neuro Oncol 2013;15: 515–534.

21. Yang I, Aghi MK. New advances that enable identification of glioblastoma recurrence. Nat Rev Clin Oncol 2009;6:648–657.

22. Jain R, Narang J, Sundgren PM et al. Treatment induced necrosis versus recurrent/progressing brain tumor: Going beyond the boundaries of conventional morphologic imaging. J Neurooncol 2010;100:17–29.

23. Ruben JD, Dally M, Bailey M et al. Cerebral radiation necrosis: Incidence, outcomes, and risk factors with emphasis on radiation parameters and chemotherapy. Int J Radiat Oncol 2006;65: 499–508.

24. Chi D, Béhin A, Delattre JY. Neurologic complications of radiation therapy. In: Schiff D, Kesari S, Wen P et al., eds. Cancer Neurology in Clinical Practice: Neurologic Complications of Cancer and Its Treatment. Totowa, NJ: Humana Press, 2008:259–286.

25. Minniti G, Clarke E, Lanzetta G et al. Stereotactic radiosurgery for brain metastases: analysis of outcome and risk of brain radionecrosis. Radiat Oncol 2011;6:48.

26. Shaw PJ, Bates D. Conservative treatment of delayed cerebral radiation necrosis. J Neurol Neurosurg Psychiatry 1984;47:1338–1341.

27. McPherson CM, Warnick RE. Results of contemporary surgical management of radiation necrosis using frameless stereotaxis and intraoperative magnetic resonance imaging. J Neurooncol 2004;68:41–47.

28. Lubelski D, Abdullah KG, Weil RJ et al. Bevacizumab for radiation necrosis following treatment of high grade glioma: A systematic review of the literature. J Neurooncol 2013;115: 317–322.

29. Brandes AA, Franceschi E, Tosoni A et al. MGMT promoter methylation status can predict the incidence and outcome of pseudoprogression after concomitant radiochemotherapy in newly diagnosed glioblastoma patients. J Clin Oncol 2008;26:2192–2197.

30. Yoon RG, Kim HS, Paik W et al. Different diagnostic values of imaging parameters to predict pseudoprogression in glioblastoma subgroups stratified by MGMT promoter methylation. Eur Radiol 2017;27:255–266.

31. Dworkin M, Mehan W, Niemierko A et al. Increase of pseudoprogression and other treatment related effects in low-grade glioma patients treated with proton radiation and temozolomide. J Neurooncol 2019;142:69–77.

32. Gerstner ER, McNamara MB, Norden AD et al. Effect of adding temozolomide to radiation therapy on the incidence of pseudo-progression. J Neurooncol 2009;94:97–101.

33. Stupp R, Mason WP, van den Bent MJ et al. Radiotherapy plus concomitant and adjuvant temozolomide for glioblastoma. N Engl J Med 2005;352:987–996.

34. Motegi H, Kamoshima Y, Terasaka S et al. IDH1 mutation as a potential novel biomarker for distinguishing pseudoprogression from true progression in patients with glioblastoma treated with temozolomide and radiotherapy. Brain Tumor Pathol 2013;30:67–72.

35. Li H, Li J, Cheng G et al. IDH mutation and MGMT promoter methylation are associated with the pseudoprogression and improved prognosis of glioblastoma multiforme patients who have undergone concurrent and adjuvant temozolomide-based chemoradiotherapy. Clin Neurol Neurosurg 2016;151:31–36.

36. Mohammadi H, Shiue K, Grass GD et al. Isocitrate dehydrogenase 1 mutant glioblastomas demonstrate a decreased rate of pseudoprogression: A multi-institutional experience. Neurooncol Pract 2019;7:185–195.

37. van West SE, de Bruin HG, van de Langerijt B et al. Incidence of pseudoprogression in low-grade gliomas treated with radiotherapy. Neuro Oncol 2017;19:719–725.

38. Nobusawa S, Watanabe T, Kleihues P et al. IDH1 mutations as molecular signature and predictive factor of secondary glioblastomas. Clin Cancer Res 2009;15:6002–6007.

39. Sanson M, Marie Y, Paris S et al. Isocitrate dehydrogenase 1 codon 132 mutation is an important prognostic biomarker in gliomas. J Clin Oncol 2009;27:4150–4154.

3. Publication 3 – Winter et al., 2021, Neurology

Winter, S.F., Klein, J.P., Vaios, E.J., Karschnia, P., Lee, E.Q., Shih, H.A., Loebel, F., and Dietrich, J. Clinical presentation and management of SMART syndrome. ***Neurology,*** **2021 (published ahead of print)**
Impact factor 2019: ***8.770***

Journal Data Filtered By: **Selected JCR Year: 2019** Selected Editions: SCIE,SSCI
Selected Categories: **"CLINICAL NEUROLOGY"** Selected Category Scheme: WoS
Gesamtanzahl: 204 Journale

Rank	Full Journal Title	Total Cites	Journal Impact Factor	Eigenfactor Score
1	LANCET NEUROLOGY	33,050	30.039	0.062420
2	Nature Reviews Neurology	11,029	27.000	0.028770
3	Alzheimers & Dementia	16,289	17.127	0.042180
4	ACTA NEUROPATHOLOGICA	21,908	14.251	0.040740
5	JAMA Neurology	10,471	13.608	0.043110
6	BRAIN	53,282	11.337	0.067050
7	NEURO-ONCOLOGY	12,950	10.247	0.029050
8	SLEEP MEDICINE REVIEWS	8,077	9.613	0.013000
9	ANNALS OF NEUROLOGY	37,304	9.037	0.044120
10	NEUROLOGY	90,213	8.770	0.103530
11	MOVEMENT DISORDERS	27,638	8.679	0.031140
12	JOURNAL OF NEUROLOGY NEUROSURGERY AND PSYCHIATRY	30,621	8.234	0.028510
13	Neurology-Neuroimmunology & Neuroinflammation	2,232	7.724	0.008400
14	NEUROPATHOLOGY AND APPLIED NEUROBIOLOGY	3,992	7.500	0.005960
15	Journal of Stroke	1,247	7.470	0.004240
16	STROKE	66,466	7.190	0.078010
17	Brain Stimulation	6,537	6.565	0.015580
18	NEUROSCIENTIST	5,188	6.500	0.007220
19	Alzheimers Research & Therapy	3,876	6.116	0.011650
20	EPILEPSIA	26,560	6.040	0.029790

This is a non-final version of an article published in final form in Winter, S.F., Klein, J.P., Vaios, E.J., Karschnia, P., Lee, E.Q., Shih, H.A., Loebel, F. and Dietrich, J., 2021. Clinical presentation and management of SMART syndrome. *Neurology*, *97*(3), pp.118-120.
DOI: https://doi.org/10.1212/WNL.0000000000012150

Published Ahead of Print on May 4, 2021 as 10.1212/WNL.0000000000012150

Neurology®
The most widely read and highly cited peer-reviewed neurology journal
The Official Journal of the American Academy of Neurology

AMERICAN ACADEMY OF NEUROLOGY®

Neurology Publish Ahead of Print
DOI: 10.1212/WNL.0000000000012150

Clinical Presentation and Management of SMART Syndrome

Author(s):
Sebastian F. Winter, MD[1, 2, 3]; Joshua P. Klein, MD PhD[4]; Eugene J. Vaios, MD MBA[1, 2, 5]; Philipp Karschnia, MD DSc[1, 2, 6]; Eudocia Q. Lee, MD MPH[7]; Helen A. Shih, MD MPH[8]; Franziska Loebel, MD DSc[3]; Jorg Dietrich, MD PhD[1, 2]

Equal Author Contributions:
N/A. Special designations: S.F.W. and J.D. serve as co-corresponding authors for this manuscript.

Corresponding Author:
Jorg Dietrich
dietrich.jorg@mgh.harvard.edu

Affiliation Information for All Authors: 1. Massachusetts General Hospital Cancer Center, Harvard Medical School, Boston, MA, USA; 2. Division of Neuro-Oncology, Department of Neurology, Massachusetts General Hospital and Harvard Medical School, Boston, MA, USA; 3. Department of Neurosurgery, Charité - Universitätsmedizin Berlin, corporate member of Freie Universität Berlin, Humboldt-Universität zu Berlin, and Berlin Institute of Health, Berlin, Germany; 4. Departments of Neurology and Radiology, Brigham and Women's Hospital and Harvard Medical School, MA, USA; 5. Department of Radiation Oncology, Duke Cancer Institute, Durham, North Carolina, USA; 6. Department of Neurosurgery, Ludwig Maximilians University, Munich, Germany; 7. Center for Neuro-Oncology, Dana-Farber Cancer Institute, Harvard Medical School, Boston, MA, USA; 8. Department of Radiation Oncology, Massachusetts General Hospital and Harvard Medical School, Boston, MA, USA

Contributions:
Sebastian F. Winter: Drafting/revision of the manuscript for content, including medical writing for content; Major role in the acquisition of data; Study concept or design; Analysis or interpretation of data
Joshua P. Klein: Drafting/revision of the manuscript for content, including medical writing for content; Major role in the acquisition of data; Analysis or interpretation of data
Eugene J. Vaios: Drafting/revision of the manuscript for content, including medical writing for content; Analysis or interpretation of data
Philipp Karschnia: Drafting/revision of the manuscript for content, including medical writing for content; Analysis or interpretation of data
Eudocia Q. Lee: Drafting/revision of the manuscript for content, including medical writing for content; Analysis or interpretation of data
Helen A. Shih: Drafting/revision of the manuscript for content, including medical writing for content; Analysis or interpretation of data
Franziska Loebel: Drafting/revision of the manuscript for content, including medical writing for content; Analysis or interpretation of data
Jorg Dietrich: Drafting/revision of the manuscript for content, including medical writing for content; Major role in the acquisition of data; Study concept or design; Analysis or interpretation of data

Number of characters in title: 54

Abstract Word count:

Word count of main text: 750

References: 7

Figures: 1

Tables: 0

Supplemental: STROBE Checklist

Search Terms: [72] Functional neuroimaging, [120] MRI, [219] Radiation therapy-tumor

Study Funding: This work was supported by the German Academic Scholarship Foundation [Studienstiftung des Deutschen Volkes] (S.F.W.), the Charité & MDC Berlin Institute of Health (MD Stipend Grant) (S.F.W.), the American Cancer Society (J.D.), the American Academy of Neurology (J.D.), the Amy Gallagher Foundation (J.D.), and the Derrick Wong family foundation (J.D.).

Disclosures: The authors report no disclosures relevant to the manuscript.

Introduction

Stroke-like migraine attacks after radiation therapy (SMART) syndrome represents a rare but serious condition manifesting years after cranial radiation therapy (RT).[1] Characterized by migraine-type headaches, stroke-like deficits, seizures and MR imaging abnormalities, including cortical gyriform enhancement in irradiated brain regions, SMART remains diagnostically and therapeutically challenging.[2–6] Distinction from tumor progression is difficult and treatment options are limited.[2] Although frequently reversible,[5] SMART episodes can recur[6] and effectuate persistent neurologic and/or imaging sequelae.[3]

Methods

This retrospective multicenter study presents 7 patients diagnosed with SMART at MGH, BWH, and DFCI between 2013–20. Patient data were obtained from institutional databases and include portions of two previously published cases.[6] Institutional review board approval was granted. Clinico-radiographic features, treatment strategies, and potential pathomechanisms of SMART are discussed.

Data Availability

Anonymized data are shared upon request from any qualified investigator.

Case series

All 7 patients (6 males, 1 female, aged 49 – 68 [mean, 58] years) had received partial (71%) or whole-brain RT (29%) for different indications, including primary (n=4) and secondary (n=2) intracranial malignancies and small-cell lung cancer (n=1). Relevant comorbidities included vascular risk factors (57%) and migraine (29%). SMART onset post-RT ranged between 1.5 – 28 (mean, 11.8) years. Most (57%) patients experienced multiple (range, 2 – 4) ipsilateral SMART episodes. In one case, episodes alternated between hemispheres, given bihemispheric radiation exposure. All patients presented with either migraine headaches (71%), seizures (57%), or both (29%), frequently accompanied by aphasia (71%) and/or confusion (43%). Data available from Dryad (**Table 1**): https://doi.org/10.5061/dryad.sn02v6x3j.

MR imaging universally demonstrated pathognomonic cortical gyriform enhancement with corresponding T2/FLAIR hyperintensity (86%) and inconsistent diffusion restriction (43%) (**figure**). Identified abnormalities were strictly unilateral, unconfined to cerebrovascular territories and affected previously irradiated, predominantly left parieto-occipital brain regions. In 2 patients, repeat MRI after 3 days demonstrated full cortical hemispheric expansion of abnormalities (**figure, E & F**). All available MR perfusion studies revealed regional hyperperfusion (n=3/3), with elevated cerebral blood flow (CBF) and/or -volume (CBV) indicating abnormal vascular reactivity (**figure, E**). Radiographic resolution occurred over 1 – 10 months (**figure, A – D, F & G**), except for Patient 4, where fluctuating imaging changes persisted over 5 years. Data available from Dryad (**Table 2**): https://doi.org/10.5061/dryad.sn02v6x3j.

All patients received supportive therapy, under which 71% had a full clinical recovery, in

alignment with radiographic improvement. Patients 5 and 7 (**figure, H**), who both had a complex migraine history (onset 7 years pre-RT and 4 years post-RT, respectively), experienced a protracted clinical course with incomplete neurologic recovery.

Discussion

Our findings support previous reports[2–5] and offer several new insights. Interestingly, left hemispheres were universally affected. Whether right-hemispheric involvement is clinically less pronounced remains unknown. While SMART typically occurs many years to decades post-RT,[3,4] two of our patients who received proton RT presented relatively early (within 4 years and 14 months, respectively) post-RT. Beyond radiation dose,[5] specific radiation modalities, like proton RT, may constitute unique risk factors of SMART. Both radiation-induced vascular dysfunction and neuronal hyperexcitability are implicated in SMART pathogenesis.[4,6,7] Many (57%) of our patients experienced clinical seizures and most (86%) received antiepileptics for seizure control and/or prophylaxis. Notably, Patient 3 (**figure, E**) was EEG-monitored from admission, but only developed seizures at hospital day 4, suggesting that seizure activity is an epiphenomenon rather than the cause of cortical signal abnormalities.[6] Instead, vascular dysfunction with resultant regional hyperperfusion (observed by us and others)[6,7] may effectuate the pathognomonic MR findings in SMART and provide a rationale for co-treatment with anti-platelet agents, verapamil, and anti-migraine medications.[3] Additionally, MR perfusion may offer diagnostic clues when SMART is suspected, including differentiation from conditions with overlapping radiographic spectra but presumably inverse perfusion patterns, like posterior reversible encephalopathy syndrome (PRES).[6]

It remains unclear why some SMART patients develop persistent neurologic deficits.[3,4] The imaging abnormalities we observed in two patients with "complicated SMART" did not differ from those identified in fully reversible SMART. Interestingly, seizure activity was not a feature of complicated SMART. Instead, headache and aphasia were cardinal symptoms in the setting of

a prior migraine history, raising the question whether migraine and/or underlying vascular abnormalities may predispose to complicated SMART.

This study is limited by its descriptive and retrospective nature. Because SMART is a diagnosis of exclusion and tissue biopsy is not required nor recommended,[2,3] excluding differentials like tumor progression, leptomeningeal disease, infection, and ischemic events is paramount. As SMART is mostly transient, allocating sufficient time for observation prior to considering aggressive antineoplastic treatment is advisable. Finally, greater familiarity with the clinico-radiographic presentation of SMART, routine use of MR perfusion imaging, and identification of unique risk factors are essential for improved management of affected patients.

Appendix 1 – Authors

Name	Location	Contribution
Sebastian F. Winter	Charité – Universitätsmedizin Berlin, Berlin, Germany.	Conception/design of study; data collection and assembly; data analysis and interpretation; manuscript writing/revision; final approval of manuscript
Joshua P. Klein	Brigham and Women's Hospital/Harvard Medical School, MA, USA.	Provision of patients; data analysis and interpretation; manuscript writing/revision; final approval of manuscript
Eugene J. Vaios	Duke Cancer Institute, Durham, North Carolina, USA	Data analysis and interpretation; manuscript writing/revision; final approval of manuscript
Philipp Karschnia	Ludwig Maximilians University, Munich, Germany	Data analysis and interpretation; manuscript writing/revision; final approval of manuscript
Eudocia Q. Lee	Dana-Farber Cancer Institute/Harvard Medical School, Boston, MA, USA	Provision of patients; data analysis and interpretation; manuscript writing/revision; final approval of manuscript
Helen A. Shih	Massachusetts General Hospital/Harvard Medical School, Boston, MA, USA.	Data analysis and interpretation; manuscript writing/revision; final approval of manuscript
Franziska Loebel	Charité – Universitätsmedizin Berlin, Berlin, Germany.	Data analysis and interpretation; manuscript writing/revision; final approval of manuscript
Jorg Dietrich	Massachusetts General Hospital Cancer Center/Harvard Medical School, Boston, MA, USA.	Conception/design of study; provision of patients; data collection; data analysis and interpretation; manuscript writing/revision; final approval of manuscript

References

1. Shuper A, Packer RJ, Vezina LG, Nicholson HS, Lafond D. `complicated migraine-like episodes' in children following cranial irradiation and chemotherapy. Neurology. Wolters Kluwer Health, Inc. on behalf of the American Academy of Neurology; 1995;45:1837–1840.
2. Black DF, Bartleson JD, Bell ML, Lachance DH. SMART: Stroke-like migraine attacks after radiation therapy. Cephalalgia. SAGE PublicationsSage UK: London, England; 2006;26:1137–1142.
3. Black DF, Morris JM, Lindell EP, et al. Stroke-like migraine attacks after radiation therapy (SMART) syndrome is not always completely reversible: A case series. Am J Neuroradiol. AJNR Am J Neuroradiol; 2013;34:2298–2303.
4. Fan EP, Heiber G, Gerard EE, Schuele S. Stroke-like migraine attacks after radiation therapy: A misnomer? Epilepsia. Blackwell Publishing Inc.; 2018;59:259–268.
5. Kerklaan JP, Lycklama Á Nijeholt GJ, Wiggenraad RGJ, Berghuis B, Postma TJ, Taphoorn MJB. SMART syndrome: A late reversible complication after radiation therapy for brain tumours. J Neurol. J Neurol; 2011;258:1098–1104.
6. Olsen AL, Miller JJ, Bhattacharyya S, Voinescu PE, Klein JP. Cerebral perfusion in stroke-like migraine attacks after radiation therapy syndrome. Neurology. Lippincott Williams and Wilkins; 2016;86:787–789.
7. Biju RD, Dower A, Moon BG, Gan P. Smart (Stroke-like migraine attacks after radiation therapy) syndrome: A case study with imaging supporting the theory of vascular dysfunction. Am J Case Rep. International Scientific Information, Inc.; 2020;21:e921795-1.

Figure. Examples of imaging characteristics identified in patients with SMART syndrome.

(A & B) Patient 1. Brain MRI, taken on hospital day 6 shortly after an episode of non-convulsive status epilepticus, in a patient who presented with aphasia, confusion, and headache 16 years post-WBRT. Findings demonstrate new cortical gyriform enhancement in the left temporo-parieto-occipital region with associated T2/FLAIR signal hyperintensity, in addition to extensive post-radiation white matter changes which are unchanged from previous scans ***(A)***. Follow-up MRI from 3 weeks later shows interval resolution of cortical enhancement with persistent but decreased T2 hyperintense gyral swelling ***(B)***.

(C & D) Patient 2. Brain MRI on admission, in a patient who presented with progressive headaches, right visual oscillations, and abnormal awake EEG 14 months after proton RT (59.4Gy), suggestive of early onset SMART syndrome. There is pachymeningeal and nodular leptomeningeal enhancement within the area of prior radiation, including the left occipital and to a lesser extent the parietal region with associated T2/FLAIR signal hyperintensity, gyral expansion, and foci of restricted diffusion ***(C)***. Follow-up MRI from 10 months later demonstrates near-total resolution of abnormal imaging findings within the left occipital region ***(D)***.

(E) Patient 3. Brain MRI, taken on hospital day 4 following seizure development in a patient who presented with sudden right hemiparesis and aphasia 28 years after prophylactic WBRT (36Gy). MRI findings demonstrate extensive cortical gyriform enhancement with associated diffuse T2/FLAIR signal hyperintensity involving large portions of the left cerebral hemisphere; there are corresponding regional elevations in cerebral blood volume (CBV) and -flow (CBF) on perfusion MRI.

(F & G) Patient 6. Brain MRI, taken on hospital day 5 following seizure development in a

patient who presented with aphasia, right facial droop, right-sided weakness, and fever (but negative infectious work-up) 10 years after chemo-RT. MRI findings demonstrate extensive cortical edema and enhancement involving the entirety of the left cerebral hemisphere, without associated T2/FLAIR signal hyperintensity. Extensive periventricular white matter abnormalities appear unchanged from prior scans ***(F)***. Follow-up MRI from 4 weeks later demonstrates full resolution of abnormal cortical enhancement ***(G)***.

(H) Patient 7. Brain MRI on admission, in a patient with recurrent episodes of migraine headaches and aphasia over a period of 6 months, 9 years after RT (60Gy). There is extensive cortical gyriform enhancement and edema with associated T2/FLAIR signal hyperintensity and low diffusivity (DWI & ADC) within the area of prior radiation in the left parieto-occipital lobe.

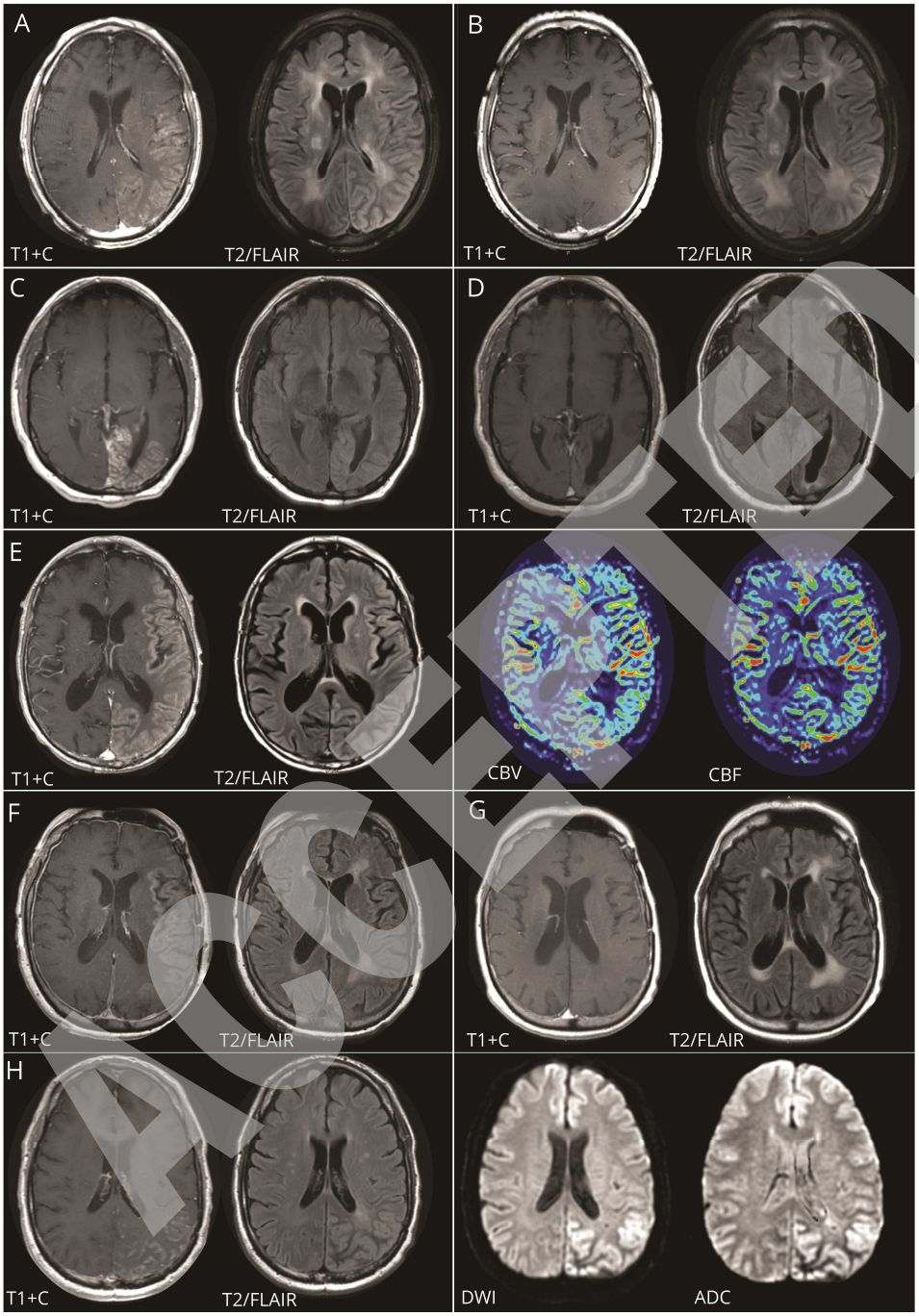

Figure.

Neurology®

Clinical Presentation and Management of SMART Syndrome

Sebastian F. Winter, Joshua P. Klein, Eugene J. Vaios, et al.

Neurology published online May 4, 2021
DOI 10.1212/WNL.0000000000012150

Table 1.

Patient	Gender	Age, y	RT indication	RT type (dose)	Interval from RT, y	Migraine history	Clinical symptoms				Recurrent episodes	Clinical Mx	Time to full clinical recovery
							Seizures	Headache	Aphasia	Other			
1	M	49	Secondary CNS lymphoma	WBRT	16	-	+	+	+	AMS	-	Levetiracetam, Lacosamide	1mo
2	M	55	AA (left occipital)	Protons (59.4Gy(RBE))	<1.5	-	- (abnormal EEG)	+	-	Visual oscillations	-	Levetiracetam, ASA	10mo
3	M	68	SCLC (prophylactic)	WBRT (36Gy)	28	-	+	-	+	Hemiparesis	+	Levetiracetam, Lacosamide, Magnesium	1mo
4	F	59	Osteosarcoma affecting the skull base	EBRT	14	-	+	+	-	Hemiparesis and visual field deficits	+	AED, Methylprednisolone	1mo
5	M	62	AOD (left temporo-parietal)	Protons (59.4 Gy(RBE))	4	+	-	+	+	AMS	+	Levetiracetam, Lacosamide, ASA, Atorvastatin	Partial recovery; >3y of fluctuating neurologic sx
6	M	59	GBM (left temporal)	Photons (60Gy)	10	-	+	-	+	Hemiparesis and AMS, fever	-	Levetiracetam, Dexamethasone, Prednisone, ASA	1mo
7	M	56	GBM (left occipital)	Photons (60Gy)	9	+	-	+	+	-	+	Methylprednisolone, Verapamil, Fioricet, Galcanezumab, Celecoxib	Partial recovery; episode ongoing

Abbreviations: AA= anaplastic astrocytoma (WHO III); AED= antiepileptic drugs; AOD= anaplastic oligodendroglioma (WHO III); AMS= altered mental status; ASA= acetylsalicylic acid; Dx= diagnosis; EBRT= external beam radiation therapy; F= female; GBM= glioblastoma multiforme (WHO IV); Gy= gray; M= male; mo= months; Mx= management; RBE= relative biological effectiveness; RT= radiation therapy; SCLC= small cell lung cancer; Sx= symptoms; WBRT= whole brain radiation therapy; y= years

Table 1. Demographic, clinical, and management characteristics identified in patients diagnosed with SMART syndrome.

Table 2.

Patient	Laterality (L/R)	In radiation field	Cortical gyriform enhancement (location)	T2/FLAIR signal hyperintensity	DWI diffusion restriction	MR perfusion	Time to radiographic improvement
1	L	+	Temporal, parietal, occipital	+	+ (mild)	↑CBF	<1mo
2	L	+	Occipital, parietal	+	+ (foci)	N/A	10mo
3	L	+	Entire hemisphere	+	-	↑CBF, ↑CBV	1mo
4	L	+	Occipital, parietal	+	-	↑CBV	>5y (gradual resolution w/ intermittent worsening)
5	L	+	Temporal	+	-	N/A	3mo
6	L	+	Entire hemisphere	-	-	N/A	1mo
7	L	+	Parietal, occipital	+	+	N/A	N/A; episode ongoing

Abbreviations: CBF= cerebral blood flow; CBV= cerebral blood volume; DWI= diffusion-weighted imaging; L= left; mo= months; N/A= not applicable; R= right; w/= with; y= years

Table 2. MR imaging characteristics identified in patients diagnosed with SMART syndrome.

IV. Curriculum Vitae

Mein Lebenslauf wird aus datenschutzrechtlichen Gründen in der elektronischen Version meiner Arbeit nicht veröffentlicht.

V. Complete List of Publications

1. Original Articles

Winter, S.F., Klein, J.P., Vaios, E.J., Karschnia, P., Lee, E.Q., Shih, H.A., Loebel, F., and Dietrich, J., 2021. Clinical presentation and management of SMART syndrome. ***Neurology*** *(published ahead of print)*
Impact factor 2019: 8.770

Winter, S.F., Forst, D.A., Oakley, D.H., Batchelor, T.T., Dietrich, J., 2021. Intracranial foreign body granuloma mimicking brain tumor recurrence: a case series. ***The Oncologist****, May;26(5):e893-e897.*
Impact factor 2020: 5.260

Winter, S.F., Martinez-Lage, M., Clement, N.F., Hochberg, E.P., Dietrich, J., 2021. Fatal neurotoxicity after chimeric antigen receptor T-cell therapy: An unexpected case of fludarabine-associated progressive leukoencephalopathy. ***European Journal of Cancer***, 144, 178–181.
Impact factor 2019: 7.275

Winter, S.F., Vaios, E.J., Muzikansky, A., Martinez-Lage, M., Bussière, M.R., Shih, H.A., Loeffler, J., Karschnia, P., Loebel, F., Vajkoczy, P. and Dietrich, J., 2020. Defining Treatment-Related Adverse Effects in Patients with Glioma: Distinctive Features of Pseudoprogression and Treatment-Induced Necrosis. ***The Oncologist***, *25*(8): e1221–e1232.
Impact factor 2020: 5.260

Vaios, E.J., **Winter, S.F.**, Muzikansky, A., Nahed, B.V. and Dietrich, J., 2020. Eosinophil and lymphocyte counts predict bevacizumab response and survival in recurrent glioblastoma. ***Neuro-Oncology Advances***, *2*(1), p.vdaa031.
Impact factor: N/A (new journal).

Karschnia, P., Batchelor, T.T., Jordan, J.T., Shaw, B., **Winter, S.F.**, Barbiero, F.J., Kaulen, L.D., Thon, N., Tonn, J.C., Huttner, A.J. and Fulbright, R.K., 2020. Primary dural lymphomas: Clinical presentation, management, and outcome. ***Cancer***, *126*(12):2811-2820.
Impact factor 2019: 5.742

Winter, S.F. and Winter, S.F., 2018. Human dignity as leading principle in public health ethics: a multi-case analysis of 21st century German health policy decisions. ***International journal of health policy and management***, *7*(3), p.210.
Impact factor 2018: 4.485

2. Review Articles

Winter, S.F., Vaios, E.J. and Dietrich, J., 2020. Central nervous system injury from novel cancer immunotherapies. ***Current Opinion in Neurology***, *33*(6), pp.723-735.
Impact factor 2020: 4.207

Winter, S.F., Loebel, F., Loeffler, J., Batchelor, T.T., Martinez-Lage, M., Vajkoczy, P. and Dietrich, J., 2019. Treatment-induced brain tissue necrosis: a clinical challenge in neuro-oncology. ***Neuro-oncology***, *21*(9), pp.1118-1130.
Impact factor 2019: 10.247
Editor's Choice, September 2019 Issue

Dietrich, J., **Winter, S.F.** and Klein, J.P., 2017, October. Neuroimaging of brain tumors: pseudoprogression, pseudoresponse, and delayed effects of chemotherapy and radiation. In ***Seminars in neurology*** (Vol. 37, No. 05, pp. 589-596). Thieme Medical Publishers.
Impact factor 2019: 2.034

Winter, S.F., Loebel, F. and Dietrich, J., 2017. Role of ketogenic metabolic therapy in malignant glioma: a systematic review. ***Critical reviews in oncology/hematology***, *112*, pp.41-58.
Impact factor 2019: 5.833

Winter, S.F., Santaguida, C., Wong, J. and Fehlings, M.G., 2016. Systemic and topical use of tranexamic acid in spinal surgery: a systematic review. ***Global Spine Journal***, *6*(3), pp.284-295.
Impact factor 2019: 2.683

3. Book Chapters

Dietrich, J., **Winter, S.F.** and Parsons, M.W., 2019. Delayed Neurologic Complications of Brain Tumor Therapy. In ***Oncology of CNS Tumors*** (pp. 751-767). Springer, Cham.

4. Policy Papers

The Division of Health Systems and Public Health, WHO Europe, 2015. Ambulatory care sensitive conditions in Germany. ***Copenhagen: WHO Regional Office for Europe***; December 2015.

5. Selected Citable Abstracts

Winter, S.F., Klein, J.P., Vaios, E.J., Loebel, F., and Dietrich, J., 2021. Stroke-Like Migraine Attacks After Radiation Therapy (SMART) Syndrome: A Case Series (4314). In *AAN 2021 Annual Meeting. **Neurology.*** 96 (15 Supplement)

Winter, S.F., Vaios, E., Muzikansky, A., Bussière, M.R., Shih, H.A., Martinez-Lage, M., Loebel, F., Vajkoczy, P. and Dietrich, J., 2019. Treatment-related adverse effects in patients with brain cancer: identification of distinctive features for pseudoprogression and treatment-induced necrosis. (S30. 003). In *AAN 2019 Annual Meeting. **Neurology.*** 92 (15 Supplement)

Vaios, E., **Winter, S.F.**, Muzikansky, A., Nahed, B. and Dietrich, J., 2018. Circulating blood cell counts as potential biomarkers of outcomes in recurrent glioblastoma patients treated with bevacizumab: hout-15. ***Neuro-Oncology***, *20*.

Winter, S.F., Vaios, E.J., Muzikansky, A., Bussière, M.R., Shih, H.A., Martinez-Lage, M., Loebel, F., Vajkoczy, P. and Dietrich, J., 2018. P01. 105 Clinical and imaging features of pseudoprogression in malignant glioma. ***Neuro-Oncology***, *20*(suppl_3), pp.iii255-iii255.

Winter, S.F., Löbel, F., Vaios, E.J., Bertalan, M.S., Bussière, M., Shih, H.A., Muzikansky, A., Martinez-Lage, M., Vajkoczy, P., Dietrich, J., 2018. Clinicoradiographic key features of biopsy-proven treatment-induced necrosis in patients with malignant glioma. (P057). In ***DGNC 2018 Annual Meeting***.

Loebel, F., **Winter, S.F.**, Onken, J., Cahill, D., Koch, A. and Dietrich, J., 2017, November. Molecular and genetic analysis identifies idh mutation as a key factor of long-term survival in glioblastoma patients. In *SNO 2017 Annual Meeting*. ***Neuro-Oncology***, Volume 19, Issue suppl_6.

Wefelmeyer, W., Barnes, S., **Winter, S.F.**, Burrone, J., Keller, G., Keck T., (2013). Exploring experience-dependent intrinsic and synaptic plasticity in the adult visual cortex. In ***BNA 2013 Festival of Neuroscience***.

VI. Acknowledgements

It is my distinct pleasure to acknowledge the following individuals, without whom the completion of this thesis would not have been possible:

I wish to thank my doctoral co-supervisors at the Department of Neurosurgery at Charité – Universitätsmedizin Berlin, Professor Dr. med. Peter Vajkoczy and Dr. med. Franziska Löbel, for their guidance as well as academic and administrative support throughout my doctoral studies. I am especially grateful and indebted to my academic advisor and doctoral co-supervisor at the Massachusetts General Hospital Cancer Center at Harvard Medical School, Professor Dr. Jorg Dietrich, for his dedicated mentorship, guidance, wisdom, and friendship.

Moreover, I wish to thank our co-authors and collaborators at the Charité Berlin and Harvard Medical School communities for their tremendous support, including Eugene J. Vaios, MD, Alona Muzikansky, MA, Maria Martinez-Lage, MD, Marc R. Bussière, MA, Helen A. Shih, MD, Jay Loeffler, MD, Philipp Karschnia, MD, Joshua P. Klein, MD, PhD, Eudocia Q. Lee, MD, and Tracy T. Batchelor, MD.

Furthermore, I wish to thank the academic assessors of this dissertation.

I am grateful to my academic advisors of the German Academic Scholarship Foundation (Studienstiftung des Deutschen Volkes), Professor Dr. med. Seija Lehnardt, Dr. Lars Peters, and Dr. Thomas Schopp, for their invaluable support and mentorship throughout my medical studies.

I am forever indebted to my parents, Dr. med. Heidi Winter and Professor Dr. med. Stefan F. Winter, and my sisters, Helen Winter, LLM, and Hannah Winter, MPhil, for their unconditional love, support, and encouragement throughout and beyond my academic career. I also wish to thank my dear friends for stimulating discussions, continuous encouragement, and great memories along the way.

Last but not least, I wish to thank our patients and their families.

The presented work was generously funded and supported by the Berlin Institute of Health of Charité Berlin & MDC (BIH MD Stipend Grant), the German Academic Scholarship Foundation, the Rolf W. Günther Foundation (Travel Grant), and the Massachusetts General Hospital Graduate Student Division (MGH GSD Travel Award).